






Applications of Microwaves in Medicine

J.-C. CHIAO ¹ (Fellow, IEEE), CHANGZHI LI ² (Senior Member, IEEE), JENSHAN LIN ³ (Fellow, IEEE),
ROBERT H. CAVERLY ⁴ (Life Fellow, IEEE), JAMES C. M. HWANG ⁵ (Life Fellow, IEEE), HAREL ROSEN⁶,
AND ARYE ROSEN⁷ (Life Fellow, IEEE)

(Invited Paper)

¹Electrical and Computer Engineering, Southern Methodist University, Dallas, TX 75050 USA

²Electrical and Computer Engineering, Texas Tech University, Lubbock, TX 79409 USA

³University of Florida, Gainesville, FL 32611 USA

⁴Electrical and Computer Engineering, Villanova University, Villanova, PA 19085 USA

⁵Materials Science and Engineering, Cornell University, Ithaca, NY 14853 USA

⁶Onsite Neonatal Partners, Inc., Voorhees, NJ 08043 USA

⁷Electrical and Computer Engineering, Drexel University, Philadelphia, PA 19104 USA

CORRESPONDING AUTHOR: J.-C. Chiao (e-mail: jchiao@smu.edu).

This work did not involve human subjects or animals in its research.

ABSTRACT Advances and updates in medical applications utilizing microwave techniques and technologies are reviewed in this paper. The article aims to provide an overview of enablers for microwave medical applications and their recent progress. The emphasis focuses on the applications of microwaves, in the following order, for 1) signal and data communication for implants and wearables through the human body, 2) electromagnetic energy transfer through tissues, 3) noninvasive, remote or *in situ* physical and biochemical sensing, and 4) therapeutic purposes by changing tissue properties with controlled thermal effects. For signal and data communication and wireless power transfer, implant and wearable applications are discussed in the categories of pacemakers, endoscopic capsules, brain interfaces, intraocular, cardiac and intracranial pressure sensors, neurostimulators, endoluminal implants, artificial retina, smart lenses, and cochlear implants. For noninvasive sensing, remote vital sign radar, biological cell probing, magnetic resonance and microwave imaging, biochemical, blood glucose, hydration and biomarker sensing applications are introduced. For therapeutic uses, the developments of microwave ablation, balloon angioplasty, and hyperthermia applications are reviewed. The scopes of this article mainly concentrate on the research and development efforts in the past 20 years. Recent review articles on specific topics are cited with accomplishment highlights and trends deliberated. At the end of this article, a brief history of the IEEE Microwave Theory and Techniques Society (MTT-S) Biological Effects and Medical Applications committee and the contributions by its members to the promotion and advancement of microwave technologies in medical fields are chronicled.

INDEX TERMS MTT 70th Anniversary Special Issue, microwave medical application, wireless implant, physiological signal communication, wireless power transfer, vital sign radar, cell probing, ablation, hyperthermia.

I. INTRODUCTION

Uses of electromagnetic waves for biological and medical applications have been advanced at a fast speed in both research and commercial sectors. Many clinical tools and systems have been FDA (Food and Drug Administration) approved and implemented for diagnosis and treatment options. Investigations into principles of biological, biochemical and physiological effects have yielded new knowledge and

created potential applications in the future. The spectrum of the electromagnetic waves for such applications can span from very low RFs (radio frequencies) to the frequency ranges of IR (infrared), UV (ultraviolet), visible light, and X-ray. In this article, the specific range for electromagnetic waves is limited to RF, microwaves, and millimeter waves in frequencies from kHz to THz. The features of electromagnetic waves are used for signal transduction and data communication, energy

transfer and delivery, noninvasive interrogation and probing, and modification of tissue properties. With the advances in new materials, high-speed electronics, miniature antennas, flexible and deformable substrates, system-on-chip integration, and multi-physics modeling techniques, these features find their novel uses in more biomedical applications with different forms such as wearables, integrated components in smartphones, and microfluidic systems, and other purposes including senior care, agriculture, sports, and biospecimen screening.

A. ABOUT THIS ARTICLE

The progress in technology development and applications of radio frequency (RF) and microwaves in medicine has been obvious and far-reaching. To celebrate the 50th anniversary of the IEEE Microwave Theory and Techniques Society (MTT-S), A. Rosen, M.A. Stuchly and A. Vander Vorst, members of the MTT technical committee of Biological Effects and Medical Applications TC-10, coauthored a review article “Applications of RF/Microwaves in Medicine,” published in March 2002 highlighting the biological effects such as energy absorption in human bodies, wave interaction with the nervous system, safety and exposure, diagnostic applications with microwave tomography and tumor detection, and therapeutic applications such as treatments of cardiac arrhythmias and noninvasive removal of tumors by ablation [1]. To celebrate the 70th anniversary of MTT-S, this article aims to review a limited portion of new research and developments of RF and microwave techniques in biomedical applications in the past 20 years. The article is divided into four main sections with topics of using electromagnetic waves and fields for communication, power transfer, sensing, and therapeutic uses. The purpose of this article is to provide brief information and synopsis about the medical applications of RF and microwave techniques to readers who plan to pursue deeper details in case of interest instead of explaining the basic principles or giving complete specifics. Published review articles about specific categories are cited for further exploration and understanding of the topics and knowledge.

II. SIGNAL TRANSDUCTION AND DATA COMMUNICATION

Signal and data communication through the body between implants and wearables or portable electronics can be categorized as near-field, mid-field and far-field applications. The tissue thickness for transcutaneous implant communication is usually a few millimeters. The dielectric properties are likely fixed and predictable in and near the implant region. Many commercial systems have been developed and they are reliably used for wireless data acquisition, implant dosage setting control, and charging. For implants deeper in the body, the wave propagation and scattering encounter complex dielectric properties due to individuals’ physical and time-variant physiological condition variations. The mid-field applications usually refer to a transceiver placed on or near the skin in order to communicate with an implant several centimeters deep inside the body or an endoscopy capsule moving through

the gastrointestinal (GI) tract. Far-field communication refers to a transceiver that has a distance in the air from the body and communicates with an implant. For mid-/far-field communication, because the field coverage areas and power required are larger, exposure to RF energy needs to be addressed and limited [2], [3]. Absorption limits per unit weight of body tissues are defined by specific absorption rate (SAR) and specific absorption to prevent thermal damage. IEEE C95.1 Standard limits the 10-g averaged SAR and specific absorption for a 6-min time period to 1.6 W/kg and 576 J/kg, respectively [2]. International Commission on Non-Ionizing Radiation Protection (ICNIRP) Guidelines limit the 10-g averaged SAR of the head to 2W/kg below 10 GHz and 2-mJ/kg averaged specific absorption for a single pulse [3]. The modulation theme is determined by the data type, rate, amount, error tolerance, and power consumption. A higher carrier frequency provides a wider bandwidth for a higher data transmission rate, however, encounters power attenuation issues in tissues.

A. PACEMAKER

A cardiac pacemaker is used to treat abnormal heart rhythms such as bradycardia (too slow) and tachycardia (too fast). Conventional cardiac pacemakers and newly-developed leadless cardiac pacemakers, which are U.S. FDA approved and commercially available, have implemented bi-directional data telemetry with on-off keying (OOK), frequency-shift keying (FSK), and Gaussian frequency-shift keying (GFSK) modulation themes [4]. Similarly, an implantable cardioverter defibrillator (ICD) monitors heart rates and delivers high-voltage electrical pulses when irregular heartbeats (called arrhythmias) are detected in order to restore the heartbeat back to normal [5]. Recorded *in-situ* electrocardiogram (ECG) data and control commands are transmitted by data packets via coupling of implant and transceiver loop antennas at frequencies in the Industrial, Scientific and Medical (ISM) band [6].

Reviews in medical societies have concluded that monitoring of vital signs through data telemetry provides safety, convenience and reassurance for patients, and enables a capability for clinicians to monitor diseases closely for quick and critical responses [7]. A conventional pacemaker is implanted under the skin below the collarbone on the left side of the chest. The leads and wires from the pacemaker are guided along the vein into the targeted chamber of the heart for attachment. Signals are coupled between the antenna placed on the skin and the one in the transcutaneous implant. The cross-sections of both antennas are similar and the thin skin tissues allow high-efficiency near-field coupling. Leadless cardiac pacemakers however encounter more challenges in coupling signals because the devices, in the shape of a capsule, are much smaller and implanted inside the chamber of the heart [8], [9], [10], [11]. The device does not have leads, which eliminates unwanted external electromagnetic energy coupling by the conductive wires into the leads causing signal interference, and reduces mechanical complications inside the body. The depth of signal propagation across multiple layers

of skin and heart tissues, and the smaller cross-section of the coil antenna inside the capsule present power budget issues in communication. Conformal antenna architectures and higher ISM-band frequencies have been proposed to achieve better efficiencies while the pacemaker remains a small form factor. Fractal-shaped antennas at 915 MHz, 2.4 GHz and 5.8 GHz with circular polarizations to deal with antenna misalignment issues have been proposed [12]. Circularly polarized antennas tolerated the uncertain polarization received inside the heart. Miniaturized meandered-line antennas on high dielectric constant substrates with a size of $3 \times 4 \times 0.5 \text{ mm}^3$ have been demonstrated at 2.4 GHz. It could communicate within a distance of 2 m from the external device to the implant antenna placed inside a body-mimicking solution while the power remained within 1 W [13] in order to be compliant with the safety guidelines [2], [3]. With the intention to achieve the ultra-wideband (UWB) feature while maintaining a miniature antenna size, a loop radiator above a meandered ground plane achieved a bandwidth of 3.04 GHz between 790 MHz and 3.83 GHz, which covered the ISM bands and Wireless Medical Telemetry Service (WMTS) (1395–1400 MHz), and the midfield (1.45–1.6 GHz) bands [14].

B. CAPSULE ENDOSCOPY

Capsule endoscopy was first introduced in 2001 for the visual evaluation of small bowel diseases. In 2009, it was approved by the FDA. Over the years, its safety and effectiveness have been investigated extensively [15], [16], [17]. Wireless capsule endoscopy eliminates the need of using optical fibers or a CMOS camera via a tethered endoscope, which is bulky and often requires general anesthesia to examine the gastrointestinal (GI) tract. A pill-like swallowable capsule consisting of cameras, batteries, lighting LEDs, microprocessors, and RF telemetry takes photos along the GI tract as it travels by peristalsis. The image data are transmitted wirelessly to a wearable reader on the body [18], [19], [20], [21]. Multiple commercial endoscopic capsules are available to image the esophagus, stomach, small intestine, and colon for diagnosis of gastroesophageal reflux disease, obscure GI bleeding, and Crohn's Disease. They are also used for the surveillance of polyps and tumors [22]. Capsule sizes depend on applications, integration of imaging chips and additional sensors (such as pH and temperature sensors), and battery capacity requirements. Typically, a cylindrical capsule has a diameter of less than 11 mm and a length of less than 3 cm because the diameters of the adult esophagus and small intestine are about 2.5 cm.

The electromagnetic characteristics are complex in the GI tract environment, even after the tract is clean with procedural preparation. The capsule is deep inside the body so signals encounter multiple layers of tissues with diverse anatomic shapes. The dielectric constants and conductivities of the human gastrointestinal tract tissues (stomach, small and large intestines) are roughly 62–67.2 and $0.87\text{--}1.01 \text{ S}\cdot\text{m}^{-1}$ at 434 MHz. Typical dielectric constants and conductivities for skin, muscle, fat, and bone are 46.1 and $0.7 \text{ S}\cdot\text{m}^{-1}$, 56.9 and

$0.81 \text{ S}\cdot\text{m}^{-1}$, 11.6 and $0.08 \text{ S}\cdot\text{m}^{-1}$, 13.1 and $0.09 \text{ S}\cdot\text{m}^{-1}$, respectively [23]. Adding the factor of wave scattering in 3-dimensional structures with layers of different types of tissues and individuals' physical differences, the signal multi-path propagation and attenuation parameters are difficult to estimate. Thus, the worst scenario is often considered for telemetry designs including the antenna impedance, resonant frequency, dispersion and power budget.

Existing commercial capsules mostly operate at 434 MHz [23]. The carrier frequencies utilized for the wireless capsule applications in the literature range from 20 MHz to 6 GHz covering several ISM, WMTS, and Medical Implants Communications Services (MICS) bands [24]. Generally speaking, a higher carrier frequency allows a wider bandwidth for high-speed data transmissions. Different bands require antenna redesigns. For example, the typical dielectric constants and conductivities for skin, muscle, fat, and bone at 2.4 GHz become 38.1 and $1.44 \text{ S}\cdot\text{m}^{-1}$, 52.8 and $1.71 \text{ S}\cdot\text{m}^{-1}$, 10.8 and $0.26 \text{ S}\cdot\text{m}^{-1}$, and 11.4 and $0.39 \text{ S}\cdot\text{m}^{-1}$, respectively [23]. The dielectric constants are dramatically different for the skin and conductivities increase more than twice for all tissue types, compared to those at 434 MHz.

Due to the dimension constraints, different antenna designs have been investigated including loop, dipole, folded dipole, helical, planar inverted-F antenna (PIFA), slot PIFA, microstrip, slot loop, patch antennas, and their combinations. The antennas are located at one end of the capsule or conformed to the inner or outer walls of the capsule [24], [25], [26], [27], [28], [29], [30]. Electrically small fractal antennas [31], [32] provide miniaturization and wideband characteristics have also been demonstrated in research [33], [34], [35]. A summary of the antenna designs, their key features and performance are listed in Table 1 of [24]. Besides the impedance and operating frequency, antenna radiation patterns that should be closer to omni-directional in order to accommodate capsule orientation variations during travel; a sufficient bandwidth to alleviate impedance detuning as waves pass different parts of the body when the capsule changes locations; and a limit on the SAR should all be considered carefully. Commercial capsules typically have $256 \times 256\text{--}320 \times 320$ image resolutions and transmit 2–6 or 28–35 frames per second. Modulations and protocols including ZigBee and Bluetooth Lower Energy (BLE) are utilized to transmit large amounts of image data, depending on the power budget and bandwidth needs.

Additional sensing functions have been considered in the capsule endoscopy with parameters such as pH [36], [37], [38], [39], body core temperature [40], [41], pressure [42], [43], [44], and concentrations of specific gases [45], [46]. These sensing modalities produce discrete values so they do not occupy much bandwidth in the telemetry. The GI tract changes its pH levels in different sections. The esophagus has a pH level of 5–6, the stomach has a pH of 1.2–3.5, the small intestine has a pH of 4.6–7.6, and the large intestine has a pH of 7.5–8. The pressure sensing provides motility information

in the GI tract. Gas sensing obtains hydrogen, oxygen, carbon dioxide, and methane data to assess gut microbiome activities [47]. Recently, capsules are also proposed for the treatment of chronic idiopathic constipation by on-demand mechanical vibrations to simulate intestinal peristalsis [48], [49], [50]. The remotely-control commands to vary vibration frequencies do not require much bandwidth either.

C. BRAIN INTERFACE

Brain-computer interfaces (BCI) are of great interest to record *in vivo* neural signals from the brain for diagnosis of neural disorders, such as epilepsy [51], [52], and control of prosthetic devices, such as robotic limbs, with signals from the motor cortex [53], [54]. BCI can be used to stimulate the brain or nervous systems to manage symptoms [55] including Parkinson's disease [56], [57], seizures [58], dystonia [59], [60], tremors [61], tinnitus [62], [63], Tourette syndrome [64], [65], and pain [66], [67], [68], [69], [70]. Research projects for neural recording and stimulation are currently conducted for memory loss, depression, schizophrenia, addiction, anxiety, obsessive-compulsive disorder, and more [70], [71], [72], [73], [74], [75], [76], [77], [78], [79].

One example is an implantable 64-channel wireless neural recording system, demonstrated with a micro-machined electrode array implanted on the cortex surface [80]. It detected and recognized neural action potentials and transmitted spike trains to an external recorder outside the skull. Loop antennas inductively coupled fields with a distance of 1 cm across the skull. Carrier frequencies of 4 and 8 MHz provided energy to the circuits and transmitted data with FSK to the implant. Reverse telemetry from the implant to the receiver at a programmed carrier frequency of 174–216 MHz encoded a bit stream of spikes with OOK at 2 Mbps. Another batteryless neural interface for 16-channel recording and 8-channel stimulation was demonstrated in [81]. The data stream was at 6.78 Mbps with the on-off keying pulse-position (OOK-PPM) modulation by a carrier frequency of 434 MHz. A monopole antenna was used to transmit data to a recorder allowing the test animal to move freely. Inductive coupling from multiple coils in the animal cage to the coil in the device at 13.56 MHz powered the interface implant.

Advances in amplifiers, noise reduction, analog-to-digital converters, and data compression techniques specific to neural signals [54] have increased the channel and electrode counts significantly [82], [83]. Higher electrode counts give better spatial resolutions for mapping the neural signals in the brain and in return provide finer motion controls in robotic limbs or a better understanding of the neural pathways. Higher carrier frequency provides a wider bandwidth and a higher transmission rate of spikes, however, it means that signal processing and communication circuits consume higher powers and produce more heat. Two factors for designs need to be considered. The US FDA requires an implant not to exceed a temperature increase of 0.5 °C in the brain, and US Federal Communications Commission (FCC) limits SAR of the RF signals to

less than 1.6 W/kg. A review of different electrode scales, device architectures, and related system blocks for electronics is provided in [84].

Closed-loop systems have been proposed to better achieve neural stimulation outcomes. Choosing neuro-stimulation parameters based on electrical signals recorded on related neurons can provide real-time feedback to manage neural activities and thus symptoms. Wireless systems for feedback-based pain management have been proposed in freely behaving animal models [85], [86], [87], [88]. Research advances have been greatly achieved since the demonstration. A battery-operated closed-loop system for 128-channel recording and 128-channel stimulation utilized the 2.4-GHz Bluetooth BLE with an on-chip antenna [89]. The system was demonstrated in non-human primates and allowed bidirectional wireless communication up to a 2-Mbps data stream rate at a distance of 2 m. Another battery-operated transceiver was designed consisting of a UWB transmitter at 3.1–5 GHz and a receiver at 5.2 GHz [90]. A single commercial chip antenna for the 3.1–5.2 GHz band was used. The transceiver supported simultaneous recording and stimulation with a 200-Mbps uplink and 10-Mbps downlink. Table 1 in [89] compares closed-loop neuromodulation systems that have been demonstrated *in vivo*.

The neural recording and/or stimulation interfaces have also been implemented for peripheral nerves. For example, a wireless system recording up to 128 channels with sampling at 50 kHz and stimulation up to 15 channels was demonstrated in animal models [91]. The multiple frequencies for recording from the implant were at 2.7, 3.05 and 3.375 GHz with a signal transmission distance of 2 m. A full duplex digital Wi-Fi radio operating at 2.4 GHz was used to communicate with the stimulation module.

Batteryless or passive neural recording can be accomplished with microwave backscattering methods, besides the inductive coupling with coil antennas for both data transduction and power transfer [92]. A neural recorder based on the short-range radio-frequency identification (RFID) principle was demonstrated with a RFID-tag IC at 915 MHz and loop antennas in both the reader and implant [93]. The backscattering technique does not require active electronic components or power supplies. Thus, there is less heating or power dissipation concern in the brain. Excitation carrier-frequency signals from an external transmitter mix with the neural action potentials to produce third-order intermodulation products by nonlinear varactors. The third-order intermodulation signals then transmitted back to the reader. A system with intermodulation product frequencies at 4.5–4.9 GHz and interrogating frequencies at 2.25–2.45 GHz was demonstrated to carry neural action potentials up to 1 kHz bandwidth [94]. The implant antenna was a planar sub-resonant slot that operated at both frequency bands. A tapered slot antenna was used for both transmitting and receiving due to its wide bandwidth. Another dual-band backscattering neural recorder was demonstrated at 2.4 and 4.8 GHz with the third-order mixing products of neural signals that had a bandwidth up to 5 kHz

[95], [96]. Antiparallel diode pairs were used, and the performance showed a high sensitivity in recording neural action potentials. Utilizing a similar back-scattering technique, an 8-channel recorder was demonstrated at 2.4 and 4.8 GHz [97] in which three photodiodes were integrated in the implant to switch the 8 channels and controlled by external infrared emitters.

D. IMPLANT SENSORS WITH LOW DATA-RATE COMMUNICATIONS

Owing to the wireless signal transduction and communication features providing comfort, convenience and ubiquity, in return the sensing implants enable continuous and more accurate assessment of physiological and biochemical parameters. For example, a batteryless wireless endoscopically-implantable sensor implemented in the esophagus that can detect reflux occurrences and their pH values provide continuous and long-term monitoring of acid and nonacid gastroesophageal reflux [98]. The capability gives comfort to patients so they do not change their daily activities or behaviors. Therefore, the diagnosis is more accurate. The electronic recording and outpatient procedures are suitable for a large population of patients. The comfort in long-term sensing can help greatly in the prognosis of drug treatment.

The monitored parameters may be discrete values thus the system does not need a high data transmission rate. Some examples include pressure sensing in the eyes, vascular system, bladders, and brain.

1) INTRAOCULAR PRESSURE SENSOR

Continuous intraocular pressure (IOP) monitoring for glaucoma patients has been demonstrated in animal models. One exemplary implant had a sensing microelectromechanical system (MEMS) device on a flexible substrate [99]. The variable MEMS capacitor was in connection with a coil antenna behaving as an inductor to form a resonant circuit at around 350 MHz. The measured sensitivity for pressure was 160 kHz/mmHg. A similar approach was implemented on soft contact lenses to monitor IOP. The capacitance signals were read by a commercial RFID tag reader at 860–900 MHz with inductive coupling between the coil on the contact lens and the one in the eyeglasses or a RFID antenna [100], [101]. Another example is a contact lens with a silicon nanomembrane as the strain sensor and a coil antenna made of silver nanofibers and fine silver nanowires that operated at 13.56 MHz [102]. The same carrier frequency was used for both energy delivery and data transmission between the implant coil and reader. Similar system architectures measured the reflection coefficients of the coupling between coils on the lens and eyeglasses at resonant frequencies of 238–241 MHz in animal models [103]. Further advances integrated a drug delivery mechanism with the IOP monitoring lenses that had MEMS capacitive sensors and wireless power transfer to trigger drug delivery via iontophoresis [104]. The resonant frequency shifts between

3.78 and 3.86 GHz indicated pressure changes. The power transfer frequency was at 850 kHz to trigger the iontophoresis electrode to release the brimonidine, an anti-glaucoma drug, loaded in a hydrogel coated on the electrode.

2) CARDIAC PRESSURE SENSOR

Monitoring pulmonary artery pressure *in situ* can provide early information for heart failure. The pressure of blood flowing into the lung indicates the forces generated by the right ventricle. Such information cannot be obtained with conventional cuff-based blood pressure measurements. Continuous *in-situ* cardiac pressure sensing can be realized with a MEMS capacitive sensor embedded in a medical self-expandable stent [105]. The stent was used as an antenna to transmit pressure data at 2.4 GHz and to couple 3.7-GHz signals to power the chip and sensor. A voltage-controlled oscillator (VCO) was used to modulate the data using binary frequency-shift keying (BFSK). The stent was designed at a depth of 3.5 cm under the chest skin and the reader was placed within a 1-m distance from the chest. Currently available, the commercial FDA-approved product CardioMEMS™ HF System consists of a capacitive MEMS pressure sensor, an integrated circuit, and a coil to operate at the resonant frequency of around 35.7 MHz to detect blood pressure and to prevent heart failure [106], [107]. The device is implanted in the distal pulmonary artery with a catheter. By powering the passive sensor externally, the resonant frequency shifts indicate the pulmonary artery pressure changes. Clinical trials show improved outcomes among heart failure patients, particularly because the system can be used in home settings [108].

3) BLADDER PRESSURE SENSOR

Similar system architectures have also been implemented to wirelessly monitor acute and chronic bladder pressures for diagnosis of urinary incontinence [109]. The transmitter was placed on the skin and operated at 27.12 MHz in the ISM band. The device contained a commercial MEMS pressure transducer, an inductive coupling coil, and a rechargeable battery. Signals were transmitted by the frequency-shift keyed (FSK) modulation. A similar method was used to power an implant without a battery at the resonant frequency of 140 kHz via a rectangular coil wrapped around the device. The pressure data was transmitted by Bluetooth BLE after analog-to-digital conversion of pressure signals obtained by a commercial liquid pressure sensor [110]. Another example of a batteryless implantable bladder sensor had a flexible diaphragm that transduced pressure variations to capacitance changes [111]. In series with an inductive coil, the resonant frequency shifted between 160 and 168.4 MHz, detected by an external coil, indicating pressure changes. Without batteries, the lifetime can be extended and the size of the implant allows easier implantation via minimally-invasive procedures. Continuous monitoring at home settings is more accurate to confirm symptomatic leakages in daily activities. Treatment

options such as using neurostimulation on sacral nerves or posterior tibial nerves to treat an overactive bladder by reducing involuntary contractions can manage symptoms in the long term [112], [113], [114]. The *in-situ* pressure monitoring provides feedback signals to control the neurostimulator for closed-loop management. The neurostimulator can also be powered and adjusted by similar wireless power transfer and data transmission mechanisms.

4) INTRACRANIAL PRESSURE SENSOR

The intracranial pressure inside the skull builds up from the cerebrospinal fluid in patients who have brain surgeries or suffer from traumatic brain injury. It can also be due to head impacts in athletes, soldiers, or people in car accidents [115], [116]. The intracranial pressure build-up, or hydrocephalus, is particularly critical for children [117], [118]. Tethered-sensor approaches have been used to monitor the pressures, but they are bulky, painful for patients, and limit patients' mobility. Implants with their subdural placement of a MEMS sensor in contact with the cerebrospinal fluid have been demonstrated *in vivo* in animal models to continuously monitor the intracranial pressures [119], [120], [121]. The wireless data communication between the implant inside the brain and a reader on top of the head operated in the frequency band of 2.4–2.483 GHz via a rectangular-shaped annular slot antenna [120]. The antenna was chosen for its radiation efficiency under the 8-mm thick scalp and less sensitivity to the biocompatible coating on the device. The device with dimensions of $22 \times 26 \times 10$ (thickness) mm³ had a battery as the implantation aimed for monitoring within 250 days.

III. WIRELESS POWER TRANSFER

Besides communication, electromagnetic fields and waves can be used to transfer energy across tissues to power implants. Battery-operated implants require replacement at the end of battery life. The procedures may need surgeries that are costly and painful to patients. Typically, the battery lifespan of a cardiac pacer or implantable cardioverter defibrillator is about 7–8 years [122]. Advanced setting switching between normal and low-power modes may help the battery last 10 years. Commercial neurostimulators used in deep brain stimulation for Parkinson's Disease have a battery lifetime of 3.9–6.4 years in clinical settings [123]. The battery life depends on many factors including individuals' physiological conditions making it difficult to predict their expected replacement schedules. For spinal stimulation, the median lifespan of stimulators containing non-rechargeable batteries was found 8.2 years in a large population study [124].

Wireless power transfer for recharging batteries or direct powering provides an option to reduce required battery capacity or eliminate battery which can significantly reduce the implant's physical size. The size reduction enables minimally-invasive, endoscopic or natural orifice transluminal endoscopic (NOTES) [125] implantation procedures for the implants. Particularly, implants with higher power

consumption due to high transmission data rates, lighting needs in video capsule endoscopy, or delivery of electrical currents for therapeutic purposes can benefit from wireless power transfer. Wireless power transfer techniques for inductive coupling and high-frequency signal propagation, as well as the requirements for capsule endoscopy and miniature devices are discussed in [126]. A comprehensive review of different techniques including non-radiative and radiative power transfer methods, and their applications for implants is in [127]. The strategies for wireless power transfer system designs involving implants are reviewed in [128]. Efficiencies, methods and challenges for near-field resonant inductive coupling, near-field capacitive coupling, mid-field and far-field power transfer are discussed systematically. Medical applications such as cochlear, retinal, cortical, and peripheral nerve implants are introduced with a summary of achievements.

A. NEUROSTIMULATOR

A spinal stimulator is implanted under the skin near the upper buttocks or abdomen with thin wires connecting the stimulator to the electrodes that are placed on the spinal cord. Applying inductive coupling to recharge the implanted pulse generator is convenient for patients in such implantation locations and so rechargeable batteries have been implemented for commercial spinal stimulators [129]. Multiple studies show spinal stimulator longevity is higher for rechargeable devices compared to non-rechargeable ones (7.2 vs 3.7 years and 9 vs 8.2 years, respectively, in [130] and [124]). A comparison of commercial spinal cord neurostimulators with non-rechargeable and rechargeable batteries is in [131]. The charging frequencies through inductive coupling are 77–90 kHz [132], 410–485 kHz [133], and 402–405 MHz [134].

With a different configuration from the spinal stimulators, the present deep brain stimulation system consists of an electrode wire lead placed in the deep brain regions, such as the subthalamic nucleus and globus pallidus interna for the management of Parkinson's disease [135], connecting to an external neurostimulator. After the electrodes are located at the desired target region, the lead comes through a small opening in the skull and connects through an extension wire to the neurostimulator implanted under the skin near the collarbone [56]. It is clear that the extension wires for the stimulator are inconvenient, uncomfortable, potentially dangerous, and susceptible to electromagnetic wave interference. Therefore, wireless power transfer from a wearable device, say in a hat, across the skull into the implant becomes an attractive option to transmit power and control signals. In [136], Table 1 compares different wireless power transfer techniques for deep brain stimulation. The typical thickness for power penetration is about 16 mm. The receiving coils in the implants have cubic or planar square lengths of 1–10 mm. Operating frequencies cover a wide spectrum from 160 kHz to 907.5 MHz with output powers in the range of 16 μ W to 100 mW. The efficiencies are mostly less than 1% which is low due to the distance in the inductive coupling. An example to increase transfer efficiency is by using a multi-stage field coupling

approach. It was proposed with four coils to increase power transfer efficiency by reducing load effects [137]. A dual-layer spiral coil in the implant received energy from an external helical coil. Externally, the primary coil that was connected to the source coupled fields to a passive secondary coil tuned at resonance. The load coil (the fourth one) in the implant coupled fields to a passive coil (the third one) tuned also at the same resonance. Both have small dimensions of $5 \times 5 \text{ mm}^2$. The second and third coils coupled the energy across the skull at 13.56 MHz. An efficiency of 19.1% was achieved with a subcutaneous implant depth of 1 cm. The misalignment issue of small antennas inside and outside the body also reduces power transfer efficiency significantly. An intra-dural approach was proposed for spinal cord stimulation to address pain inhibition efficacy issues due to electrode placement on the spine and overcome the power transfer efficiency loss from the misalignment of coils [138]. Inductive coupling at 1.6 MHz was implemented between the planar micro-coils of 9 mm in diameter on a pial conformal surface implant and the coil in an epidural controller [139]. A power level of 5 mW was transmitted through a tissue thickness of 1 cm.

The cross-section difference between the transmitting coil and implant coil is a major factor for low power transfer efficiencies of inductive coupling in deep tissues. The transmitting coil should be sufficiently large to make sure functional coverage in which the misalignment of coils does not stop the stimulator from working because the implant coil dimensions are small. However, the transmitting coil cannot be too large to wear comfortably by patients. The significantly mismatched implant and transmitter coil sizes mean a large portion of electromagnetic fields are lost. The inhomogeneous distributions of permittivities and conductivities by different types of tissues further make it difficult to tune the coils to reach a high-quality factor. The power decays exponentially, which restricts the penetration depth [140]. At higher frequencies up to a few GHz, evanescent fields generated by plane waves outside the body can induce energy transfer through the propagating waves in the tissues. With an array of radiation elements with tuning phases at their ports, fields can be combined and focused to create a high field density spot deeper in the tissues. This technique can be utilized in mid-field wireless power transfer to a miniature implant [141]. Milliwatt of power was delivered at 1.6 GHz to an implant that had a 2-mm diameter in a tissue depth of 5 cm. Similarly, a 4×4 patch antenna array was proposed to focus fields for a $2 \times 2 \text{ mm}^2$ implant inside the brain at 2.1 GHz [142]. For neural studies in animal model experiments, it is preferred that animals can move and behave freely without being tethered to instruments or confined inside small boxes. For example, electrical neurorecording [81] and neurotransmitter (L-glutamate) monitoring [143] were conducted continuously in freely-moving animals with multiple-coil wireless charging in animal cages. The distances of wireless power transfer are typically considered as far-field coupling in the range of 4–10 cm in the air.

For peripheral nerve stimulation, stimulator miniaturization targeting for minimally invasive implantation limits

the antenna dimensions while still demanding sufficient power to be delivered to tissues. For deep implants, ultrasound and RF coupling have been proposed for power transfer [144]. An injectable stimulator with multi-turn micro-coils wrapped inside a capsule was demonstrated with inductive powering at 2 MHz [145], [146]. Another example is an inductive link at 2 MHz used to power a brain stimulator with 8 channels [147], [148]. A transcutaneous implant with a packaged volume of 0.5 cm^3 for epidural spinal stimulation in rats was demonstrated for 160 stimulation electrodes with inductive power transfer at 2 MHz and differential phase-shift keying (DPSK) data transmission at 22 MHz [149]. A subdermal implant consisting of a coil with a 9.8-mm diameter that resonates at 13.56 MHz with a quality factor of 22 was demonstrated in mouse models to power a μLED for optogenetic stimulation [150]. With a miniature three-layer planar inverted-F antenna to harvest RF energy, an implant for deep brain stimulation was demonstrated at 915 MHz in a phantom [151]. A transcutaneous implant coupled RF energy with a coil of a 1.6-mm diameter at 1.5 GHz for optogenetic stimulation on the premotor cortex, dorsal cord, cutaneous nociceptors in mouse models was also demonstrated [152].

B. ENDOLUMINAL IMPLANTS

For implants that are deeper in the body, they face several challenges for wireless power transfer including the uncertainty of dielectric properties influenced by anatomic and tissue structures, which can be dynamically changing. Particularly, the endoscopic capsule or implant in the GI tract can change their locations and orientations significantly with GI motility. Therefore, the antenna designs, field distributions and power budget tolerance need special attention.

A planar spiral inverted-F antenna with circular polarizations at 673 MHz for a leadless pacemaker that could be implanted in the right ventricle of the heart was demonstrated [153]. The antenna had a diameter of 5 mm and a height of 3.2 mm. With a 10-dBm transmitted power, the implant received a power of -17.8 dBm . A system designed for deep implants was demonstrated in a phantom at 915 MHz [154]. Powers from an external patch antenna enhanced with a reflector transferred energy to the 2-circular-slots on a patch antenna in the implant. Transmission distances were investigated with respect to their SAR values. For GI applications to treat gastroparesis, a batteryless implant attached to the wall inside the stomach that can be delivered by endoscopic procedures without major surgery was developed [155], [156]. The resonant frequencies for power transfer could also be used for switching dosage control eliminating additional circuits in order to keep the implant size as small as possible [157]. It can harvest sufficient electromagnetic energy through coil coupling and generate electrical currents to stimulate the stomach to restore its motility, as demonstrated in live pig models. A mid-field power transfer system was designed for capsule applications and demonstrated in phantoms [158]. The antenna had a volume of 8.43 mm^3 and provided multiple functions of data telemetry at 403 and 915

MHz, power transfer at 1.47 GHz, and switching control at 2.4 GHz. The system power transfer efficiency was 0.67% at 1.47 GHz. Table 1 in [158] summarizes different mid-field, compared to near-field, power transfer systems at 1.2, 1.47, 1.5, 1.6, 2.4, and 2.45 GHz with patch and coil antennas in implants. A wireless power transfer system for an imaging capsule was demonstrated at dual frequencies of 915 MHz and 2.45 GHz [159]. The reasons for using dual or multiple frequencies or antennas depend on applications. One reason is to separate the wireless power transfer and data transmission frequencies to avoid interference as their power levels are significantly different. Because the requirements of using ISM-bands, the frequencies in different bands can be well separated. Another reason is to consider the tissue attenuation effects at different frequencies. Particularly the wireless power transfer needs to maximize its efficiency. Thus the antenna design considerations for power transfer and data transmission may become different. The power transfer should also take the RF-to-dc conversion efficiency into account, while the data modulation and rate require a certain bandwidth. Both factors are frequency-dependent. The tissues were typically assumed to be 6 cm thick in the abdomen area. The implant in [159] utilized a meandered resonator antenna with quasi-omnidirectional radiation patterns located at one end of the capsule and the power transmitter was a log-periodic antenna placed 5 mm from the skin of the abdomen. Transmission coefficients were -37.9 and -23.7 dB at 915 MHz and 2.45 GHz. With a transmitting power of 1 W, 8.3 and 13 mW were received by the implant at 915 MHz and 2.45 GHz.

C. ARTIFICIAL RETINA

Retinal prostheses convert images captured by a camera, and wirelessly transmit the data to an implant, in which electrodes stimulate the retina with electrical pulses to produce light perception [160], [161], [162], [163]. Wireless power transfer is needed to provide energy to the stimulator inside the eye. To have a sufficient image resolution, high electrode counts are desired which presents a challenge to data transmission. A dual-band telemetry for 256-channel stimulator was demonstrated with powering at 2 MHz and signal transmission at 22 MHz via two sets of coils [164]. DPSK modulation was implemented for the 16×16 -pixel and 4-bit grayscale images with 2-Mbps data transmission. Another example: a 5-mW power delivery to the load with a 58.8% efficiency at 2 MHz and 500-kHz data uplink with coils was demonstrated in phantoms [165]. For the commercial epiretinal implant system, the implant received about 45 mW of power at 3.156 MHz [166]. Increasing the carrier frequency can benefit higher electrode counts, data rates and power transfer efficiencies. The physical dimension constraint in the eyes also requires antenna sizes to be miniaturized while maintaining sufficient bandwidths. An electrically small circularly-polarized wire patch antenna that could be operated at 2.45, 5.8, or 8 GHz bands and had a wide -10 dB impedance bandwidth at 2–11 GHz was demonstrated in [167].

D. SMART LENS

The power transfer and data transmission methods suitable for artificial retinas are applicable to smart lens applications. Electronic sensors and actuators integrated into a contact lens, generally called Smart Lens [168], [169], have been attracting a lot of attention due to their convenience, ubiquity and noninvasiveness. Smart lenses have been proposed to measure intraocular pressures for glaucoma diagnosis and drug delivery [170], glucose levels in tears for diabetic diagnosis and therapy [171], lactic acid (lactate) for hypoxia and changes of physiological or pathological conditions [172], and cholesterol [173]. MEMS and electrochemical sensors, MEMS actuators, and drug-loaded hydrogels are utilized for sensing [174], [175] and drug delivery [176], [177], [178]. Signal transduction, sensor and electronics operation require wireless powering because contact lenses are too small or soft to contain a battery. Based on the RFID principle, a planar receiving ring antenna on a 200- μm thick, soft contact lens, made of hydroxyethyl methacrylate hydrogel, harvested inductive coupling energy from a transmitting segmented-loop antenna mounted on a pair of eyeglasses [179]. The lens received a 1.74-mW power at 920 MHz with a distance of 1 cm to the eyeglasses that transmitted a power of 0.45 W. A RF-to-dc converted power of 110 μW was used to drive a capacitive pressure sensor and send back the intraocular pressure data detected. In another example, an intraocular pressure monitoring implant with a capacitive sensor utilized a half-circle monopole antenna at 3.65 GHz for power transfer and data transmission at 2.4 GHz [180]. The received power to the rectifier was 20 mW from a transmitting power of 0.6 W. Although it was intended to be an implant, the principle could be applied to contact lenses.

A soft contact lens with a ring antenna of a 10-mm diameter at 27 MHz was demonstrated in an animal model [181]. Another contact lens with a planar coil on a parylene substrate received power from a coil mounted on a pair of eyeglasses in an eye phantom [182]. The receiver coil has outer and inner diameters of 10 and 6 mm to provide transparency to the human pupil area which has a diameter of 2–6 mm. It was found that the quality factor of the coil was reduced when the coil was placed on the eyes due to the parasitic capacitance from tissues. Designed for operation at 13.56 MHz, the coil can be used up to 100 MHz. Varying carrier frequencies, a power transfer efficiency of 17.5% and a received power of 50 mW from a 2-W power source were obtained at a distance of 2 cm between the eyeglasses and the contact lens. A summary review of the powering, sensing and signal transduction methods for smart lenses can be found in [183].

Effects of microwave powers on eyes and retina at 1.25 GHz have been studied. The results and the prior studies at other frequencies from 1.3 to 35 GHz are summarized in [184]. These studies were conducted on various animal models showing possible effects of cataract formation, corneal endothelia abnormality, retinal degeneration and electroretinogram (ERG) signal variations. A conclusion is drawn that

retinal injury is unlikely at 4 W/kg for the 1.25-GHz RF radiation, which is higher than the FCC safety limit of SAR of 1.6 W/kg, and functional changes occurred at higher SAR (8.4 or 20.2 W/kg) on the retina are probably reversible.

E. COCHLEAR IMPLANT

Cochlear implants have been approved by FDA and are commercially available. Wireless power transfer and wireless transmission of processed audio-signal data eliminate the need for wires between the external module that consists of a microphone and microprocessor, and the implant that connects to an array of electrodes in a flexible wire [185], [186]. The electrodes deliver stimulation pulses to the nerves in the cochlear of the inner ear mimicking the functions of the hair cells that convert sound vibrations in the cochlear to neuronal action potentials. A commercial product [187] is available with wireless charging via the Qi standard [188]. Because the skull thickness between the receiver coil in the implant and the external coil in the transmitter is less than 1 cm and does not vary much for individuals, the near-field coupling is sufficient. The received power ranges from 20 to 40 mW [187], [188]. Recently, a cochlear implant power coupling system was demonstrated with a 50.5% efficiency [189].

IV. NONINVASIVE SENSING

A. REMOTE VITAL SIGN MONITORING

Over the past two decades, the study of using microwave or millimeter-wave signals to sense a subject's vital signs and motions to help assess the subject's health condition gained attention and grew rapidly. The theory is based on the Doppler radar principle or Doppler effect. Originally published by J. C. Lin in his 1975 paper [190] and followed by a few other papers by K.-M. Chen and other researchers [191], [192], this research field did not see rapid growth till the beginning of the 21st century, when researchers in Bell Labs demonstrated the feasibility of using a simple radar front-end architecture fabricated on a radio-frequency integrated circuit (RFIC) chip to detect human heartbeat and respiration from a few meters away [193], [194], [195]. Unlike previous experiments of using heavy and bulky instruments, the research team used a direct-conversion receiver architecture and a free-running oscillator that was not phase-locked to any reference source because the radar transmitter was used as the local oscillator for the radar receiver simultaneously. The simple architecture allows the circuits to be fully integrated on a silicon BiCMOS or CMOS chip without the need for any other external component [193]. The demonstrated low-power RFIC vital-sign radar chips drew attention from both academia and industry during the time that we saw a rapid expansion of wireless communication technologies.

1) RESEARCH BY MTT-28 MEMBERS

Over the past decade, the MTT-28 (formerly TC-10) Biological Effects and Medical Applications Committee has been very active in biomedical radar sensors research. A

significant increase in publications manifested tremendous growth. A subcommittee was created in the International Microwave Symposia (IMS) to promote this topic with technical sessions and workshops on this topic.

Following their enabling works in Bell Labs, O. Boric-Lubecke, V. Lubecke, and J. Lin continued the research efforts on vital-sign radars in academia. O. Boric-Lubecke and V. Lubecke's efforts include but are not limited to arctangent demodulation, heart rate variability (HRV) assessment, patient testing, sleep monitoring, and identity authentication [196], [197], [198], [199], [200]. J. Lin's efforts focused on frequency-tuning techniques for optimal detection, nonlinear analysis on detection sensitivity, random body motion cancellation with multiple radar sensors, and several CMOS radar-on-chip systems from 5.8 to 60 GHz [201], [202], [203], [204], [205]. They also collaborated or mentored many researchers on this promising topic. For example, C. Li's group continued to develop frequency modulated continuous wave (FMCW) radars for indoor positioning, passive biomedical radar sensing, and activity classification such as potential active shooter detection and inattentive driver behavior classification [206], [207], [208], [209]. C. Gu's team focused on touchless human-computer interaction [210] in the Google Soli project, which aimed to develop new human interaction with computers by leveraging accurate sensing and perception of gestures with microwave radar technologies. One application was the first smartphone with a microwave radar inside [211]. The effectiveness of a radar system for Doppler Cardiogram (DCG) has been clinically validated to provide diagnostic information for heart diseases that contained abnormal activities with non-invasive, continuous blood pressure sensing, and the detection of heart failure, atrial fibrillation (AF) and premature heartbeat (PHB) [212], [213], [214].

An exciting innovation in biomedical radar was the self-injection-locking technique pioneered by T.-S. Horng and F.-K. Wang's team in collaboration with J. Lin. Based on the concept, a see-through-wall radar leveraging human vital signs was developed [215]. Their works on random body movement cancellation leveraging mutual injection locking have assisted in removing a major source of error for non-contact vital sign detection [216]. Stepped-frequency continuous wave (CW) radar integrated with self-injection-locking merges the advantages of both architectures into a single system to monitor multiple human subjects [217].

To retain individual heartbeats and correct abnormal beats caused by undesired artifacts, C.-C. Chang and S.-F. Chang's groups have proposed a short-time autocorrelation method for heartbeat segmentation and heart rate variability extraction using a CW Doppler radar [218]. The team has demonstrated considerable advancements in analog beam switching/steering using Butler matrices combined with tunable phase shifters to achieve an efficient tradeoff in beam resolution and system complexity [219]. Integrated circuit versions were demonstrated with a deformed Butler matrix [220] and V-band phase shifter [221] in CMOS technologies.

Antennas, passive structures, and metamaterials were further developed for biomedical radar research. For example, C.-T. M. Wu's team has developed substrate-integrated waveguide filters using the complementary split-ring resonators demonstrated in [222], and K-band vital-sign monitoring using metamaterial leaky wave antennas to passively sweep in the azimuth direction by varying frequencies [223]. A super-regenerative oscillator-integrated system elevated sensitivity in a simplified system [224]. C.-H. Tseng's group developed a leaky wave antenna coupled with coplanar waveguide passive components [225], wearables using envelope detection techniques combined with self-oscillating active antennas [226], and K-band self-injection-locked radar sensors using the CMOS technology [227].

N. Tavassolian's group proposed a noncontact heartbeat signal modeling and estimation method to evaluate human cardiovascular activities [228], and with a beamforming system to receive information from multi-subjects' respiration signals [229]. One of the challenges for remote heartbeat sensing is the high amplitude chest movement due to respiration, which generates harmonics that interfere with the heartbeat signals. To overcome the issue, the chest wall acceleration was exploited instead of its displacement [230]. Antenna radiation characteristics on the performance of a Doppler radar showed that specific antenna arrangements outperform others [231].

Data detected by various radar technologies were classified for human activities by H. Hong and X. Zhu's group [232] in clinical collaboration to identify indicators of breathing disorders [233] and sleep pattern recognition from respiration, heartbeats, and body movements [234], [235]. With machine learning training and identification, radar responses were classified for a wide range of human motions [236]. J.-M. Muñoz-Ferreras and R. Gómez-García's team collaborated with C. Li on range tracking and vital signs detection [237], [238], including clutter reduction and target isolation, multiple-patient gesture recognition [239], vital sign monitoring [240], and body movement mitigation [241]. Wearable and biomedical radar health monitoring systems were developed in D. Schreurs and M. Mercuri's group [242], [243]. The applications focused on fall detection, a major concern for the elderly as a fall could go unnoticed or undetected for a dangerously long time. By measuring target positions and speeds, the algorithms could identify potentially dangerous falls [244], [245] with an embedded telehealth radar system for real-time monitoring [246].

2) RESEARCH BY OTHER MTT-S MEMBERS

Multiple-input multiple-output (MIMO) radar-based vital sign monitoring in scenarios with random body motions has been investigated by A. E. Fathy's group [247]. An algorithm based on a heartbeat template associated with wavelet transforms was used to reduce the effects of random body swaying on vital parameter estimation. The MIMO radar was used for real-time heart rate estimation of multiple subjects [248].

Leveraging precise angular location information, the signal-to-noise ratios of the heartbeats of each subject could be maximized. A UWB radar was used for accurate extraction of the respiration and heart rate of multiple subjects [249], through-the-wall vital parameter estimation [250], and gait analysis of a walking subject in combination with machine learning [251].

An FMCW radar as a handheld guidance aid was developed by N. Pohl's group for visually impaired people [252]. A UWB 80-GHz FMCW radar system was employed for the estimation of respiration and heart rates [253]. Owing to the large bandwidth, the skin surface displacement calculated could reach sub-millimeter accuracy. To linearize vital signs detection and enhance dynamic ranges, L. Ran's group proposed an extended differentiate-and-cross-multiply (DACM) algorithm [254], [255], and investigated the possibility of 1-D images of human cardiac motions for clinical diagnosis of heart diseases [254]. A short-range localization, inverse synthetic aperture radar (ISAR) for imaging, and vital signs tracking was also developed in collaboration with C. Li's group [237].

For clinical applications, A. Koelpin's group investigated the use of radar arrays attached to the bottom side of a hospital bed for through-clothing vital parameter estimation [256]. With artificial intelligent techniques, radar-based HRV studies were implemented in clinical and home-care scenarios [257]. The impact of nonlinearities on the reciprocal distance measurement for vital parameter estimation was also analyzed, showing that intermodulation effects may reduce the accuracy [258]. The group also conducted contactless measurements of the pulse wave velocity with a phased array radar system at 24 GHz [259].

Biomedical radar can assist the mobility of visually impaired people [260], [261]. E. Cardillo's group developed a range alignment method to differentiate human targets from non-human moving objects and stationary obstacles by detecting cardiorespiratory activities. Without additional sensors, the radar self-motion effects could be estimated by analyzing the signals reflected by stationary clutters [262]. In addition, the group used radar to identify head motions and eye blinking to aid people with neurodegenerative disorders [263]. Biomedical radar has also shown great promise for transportation safety. For example, J.-G. Yook's group has developed a radar sensor based on voltage-controlled oscillators (VCOs) combined with a switchable phase-locked loop (PLL) for continuous monitoring of vehicle driver [264].

3) CROSS-SOCIETAL RESEARCH AND INDUSTRIAL DEVELOPMENT

Because of the promising vital-sign radar applications in many fields, significant contributions have been made in societies other than MTT-S. For example, R. Narayanan's group used empirical mode decomposition to produce a unique feature vector from the human micro-Doppler signals to classify human motions [265]. They also analyzed

micro-Doppler signatures from various human activities in free-space and through-wall environments using a C-band coherent radar [266]. M. Amin's group with collaborators developed signal-processing algorithms and techniques for elderly fall detection using Doppler radars to reduce false alarms by deep learning [267], [268]. J. Kerneć and F. Fioranelli used radar systems to recognize respiratory disorders and different sleeping stages [269]. A continuous temporal sequence was used to identify different human activities and transitions between activities [270].

S. Pisa's group developed several UWB radar sensors with sub-millimeter resolutions to monitor breathing activities based on a step recovery diode that excites the UWB antenna and zero-bias Schottky diodes at the receiver. The system improved small-body movement detection [271], [272]. An FMCW vital-sign radar that leveraged a high-gain antenna to spatially filter the clutters was also developed [273]. D. Zito's group has developed multiple UWB system-on-chip biomedical radar sensors with CMOS technologies to sense sub-centimeter chest movements [274]. A wearable system-on-a-chip UWB radar and an IEEE 802.15.4 ZigBee radio interface were developed to transmit real-time patient data [275].

The industry has been actively working on this topic. A dedicated team at the imec has developed several versions of biomedical radar chips and systems [276], [277], capable of tracking multiple patients and measuring their vital signs [278], [279]. The applications have been extended into 2-D localization of patients using frequency-scanning antennas in Internet-of-Things (IoT) [279].

B. BIOLOGICAL CELL PROBING

More than a century ago, visionary physical scientists and engineers were critical to the founding of microbiology or cell biology. For example, in 1902, Bernstein hypothesized [280] that a cell is made of a membrane surrounding a cytoplasm of electrolytes. Indeed, Na, K, or Ca ions could be found after cells were broken down. However, it was challenging to experimentally prove the ions inside living cells were free to move and conduct electric currents. This is because, insulated by the cell membrane, a cell could not conduct any dc current, ac signals were generated [281] by Hertz only a decade earlier, and the concept of capacitance was just emerging. Nevertheless, in 1910, Höber was the first to experimentally validate the cell model by measuring the RC resonance at MHz frequencies [282]. He estimated that the ac resistivity of cytoplasm was on the order of $1 \Omega\cdot\text{m}$. In 1921, Philippson confirmed that the membrane resistivity was much greater at $10^8 \Omega\cdot\text{m}$ [283]. In 1925, Fricke measured the membrane capacitance to be on the order of 0.01 F/m^2 [284]. In comparison, the cytoplasm capacitance, on the order of femtofarads, was difficult to measure at MHz frequency ranges [285].

By the early 1940s, the large dispersion in cell suspensions around 1 MHz had been known from the charging of the membrane capacitance [286]. In 1957, in addition to the β dispersion around 1 MHz, Schwan conceptualized

α and γ dispersions [287] across the electromagnetic spectrum from kHz to THz. Schwan called the dispersion effects relaxations. Unlike atoms or molecules, the heterogeneous structures of cells and tissues do not support sharp resonances, not to mention biological heterogeneity in individuals. It means that we can take advantage of the wide electromagnetic spectrum to gain the whole picture of a single cell or a specific type of tissue. However, despite the foresight of these pioneers, although the impedance spectroscopy of cells and tissues was advanced to a single cell as opposed to a suspension of thousands of cells, its frequency range was mostly limited to 100 MHz due to the experimental setup [288].

In the past 20 years, instrumentation advances and the integration of microwave circuits and microfluidic devices enable *in-situ* probing of small volumes of biomolecules and biological cells with dielectric spectroscopy into microwave and millimeter-wave frequency ranges. A review of biomolecule and cell sensing principles for RF and microwaves is in [289]. The sensing mechanisms for microwaves are mainly based on the detection of polarizations and complex permittivities. Summaries of microfluidics-based microwave sensors including their principles, and applications for liquids, cells, biomolecules and bacteria sensing are in [290]. In this section, we will focus on biological cell probing.

Cells in suspension can be characterized, as a group of certain cells, in a microfluidic channel or well above embedded microwave circuits to detect scattering coefficient changes due to the dielectric contrast between culture media and cells in media. Fibroblast cells were loaded into a 3- μL microwell on a microwave substrate-integrated waveguide (SIW) cavity resonator and probed at a resonant frequency of 13.48 GHz [291]. Cell concentration in the media and the measured resonance frequency shift has a linear relationship. A coplanar waveguide loaded with an interdigitated finger capacitor was used up to 40 GHz to distinguish live and dead lymphoma cell groups by extracting their dielectric properties [292]. A two-port coplanar waveguide transmission line (CPW-TL) and a one-port CPW-fed interdigitated capacitor (CPW-IDC) were proposed to measure the permittivities of yeast cells and mammalian cells from 300 kHz to 50 GHz in a microfluidic channel with different culture media [293].

Benefiting from the microwave/microfluidics integration, a single cell can be captured with mechanical structures in the microfluidic channel or by alternative current (AC) dielectrophoresis [294], which allows the investigation of its intracellular properties. Biological cell microscopy utilizing chemical stains or fluorescent dyes and flow cytometry to study and sort cells has the advantages of high specificity, sensitivity, and efficiency. However, instruments are costly and they involve labeling techniques with stains, fluorochromes and fluorophores that may interact with or even alter biomolecules on the cell membranes or inside the cells affecting the results. Probing cells with electromagnetic fields to model the cells or interrogate the molecular properties however does not involve chemical labels. The principle of

label-free cell probing with microwaves in a microfluidic channel is described in [295]. A comparison of cellular analysis by microwaves to conventional techniques is given in [296]. The dead and living cancer cells could be identified within the microfluidic environment at frequencies up to 40 GHz [295]. Since dead and living cells have similar cell morphology under visual observation, this capability of recognizing and sorting cells by microwaves can be very beneficial in identifying drug efficacy in the development of chemotherapy drugs or treatment methods.

A mechanical trap in a microfluidic channel allowed a single cell to be probed from 40 MHz to 40 GHz with a coplanar line and a capacitive gap underneath the cell [297]. Another example showed a microchamber in a microfluidic channel trapped a single cell above a coplanar waveguide for probing up to 3 GHz [298]. The sensor could distinguish live from dead Jurkat cells in both time and frequency domains. Similarly, live and dead *Escherichia coli* bacterial cells were distinguished with probing in the 0.5–20 GHz frequency range [299]. The frequency range was further extended to 900 Hz–40 GHz [300], bridging the gap between GHz impedance spectroscopy and traditional impedance spectroscopy in kHz and MHz. The extended frequency range allowed better characterization of not only cytoplasm, but also the cell nucleus [301].

The single-cell microfluidic device with a coplanar waveguide and a capacitive gap has also been utilized for cell electroporation with intensities of electric fields from 0.4 to 2 kV/cm [302]. Results indicated that dielectric properties could be monitored and the cell changes or damages from electroporation could be observed with time, confirmed with conventional cell study methods. A review of electroporation techniques and their applications is in [303]. A microstrip line with a capacitive gap sensitive to the dielectric properties of liquid or particles was proposed for dielectric spectroscopy in a microfluidic device [304]. The broadband sensor with a discontinuity in the microstrip line was used to measure s_{21} to extract cell capacitances at 0.5–8 GHz, and a capacitive resonator as a narrowband sensor at 5.49–5.95 GHz detected cancerous colorectal cells with a 30-MHz frequency shift. Another device architecture was demonstrated with a folded circular waveguide cavity integrated in a microfluidic chip [305]. Two resonators at 3 and 6 GHz were used for single Chinese hamster ovary cell measurements. Permittivities were extracted from the scattering coefficients with an ability to detect dielectric constant contrasts less than 0.3.

Utilizing ac dielectrophoresis, a single cell can be precisely placed between the electrodes of a coplanar stripline in the microfluidic channel [294]. The dielectrophoresis signal, in the orders of 1 MHz and 1 V, does not affect the vitality or morphology of cells [306], [307], [308], and can be added onto the probing microwave signals (at GHz) to trap the cell between electrodes within seconds. The method allows high throughput of cells for continuous screening. The device could repeatedly distinguish live from dead cells for two different types of cells. The single-cell intracellular probing and the

wide bandwidths of microwaves allow applying of impedance spectroscopy on a single cell to establish and validate the single-cell model articulated by H.P. Schwan [287], [309] and its equivalent circuit. An equivalent circuit for a single Jurkat cell was established at 9 kHz–9 GHz with ac dielectrophoresis to trap single cells for analysis [310], [311]. The model and equivalent circuit were further expanded to a double-shell model to identify the nucleus in the cytoplasm. The model includes shunt resistance-capacitance pairs in the cell membrane, cytoplasm, nuclear membrane, and nucleoplasm [301]. Although the bifurcation of β and γ relaxations had been previously observed [312], [301] established their correlation with the nucleus size. The ability to characterize the nucleus may lead to a better differentiation of normal and cancerous cells because that is where the major difference resides. To resolve the nucleus of a live cell spatially and noninvasively, a scanning microwave microscope based on the same device architecture was demonstrated [313]. It is quite a lot of progress as the concept was originated more than a century ago, when Höber believed that an ac signal could noninvasively penetrate through a cell membrane to detect what was inside a live cell.

C. MICROWAVE ENHANCED MAGNETIC RESONANCE IMAGING

This section will look at recent advances in the area of magnetic resonance imaging (MRI). While not intended to be an exhaustive update on research in this exciting area, references have been selected in this overview to provide examples of the breadth of research work being done globally in this important technical and medical area. The reader is encouraged to look at various review articles on RF aspects of MRI for a more thorough background on the subject, for example, from literature in [314], [315].

MRI scanners have been used for several decades for imaging of biological specimens including humans. MRI scanners utilize the Zeeman effect [316], as does nuclear magnetic resonance spectroscopy (NMR) and electron spin resonance (ESR) imaging [317], [318], [319], [320], by placing the specimens in a strong magnetic field (B_0) and then manipulating the spin magnetization vectors of the nucleons (MRI, NMR) or electrons (ESR) with a strong transmitted radio frequency (RF) field (B_1) so that, as the spin vectors relax, the net magnetization can be picked by sensitive coils, antennas and receivers. This received signal is related to the image through a Fourier transform (the so-called phase-frequency diagram), with an inverse Fourier transform operation used to generate the actual image. As such, there is a significant interplay between RF electronics and signal processing that creates the sharp images medical diagnosticians require. The traditional method of both exciting the spins and receiving the resulting MR signal is through the use of coils in various sizes, shapes and arrays [321], [322]. This method is used almost exclusively for the static B_0 fields of less than approximately 3 Tesla. Higher B_0 fields yield better signal to noise ratios (SNRs) and so much research work has been done in various

transmit/receive structures that resemble coils, traditional antennas such as dipoles or Yagi-Uda antennas, or combinations [323], [324], [325], [326], [327], [328]. For human imaging, the conductivity of the body increases with frequency and so this affects contrast, location of image light and dark regions and finally, heating increases with increased need for a high B1 field and so much research focus is in this higher B0 range to help better understand the phenomenon for both patient safety and image quality.

To keep SNRs as high as possible requires electronics that are low-noise and have low magnetic moments if they are to be located inside the magnet bore [315]. Having the electronics close to the patient helps to provide better SNRs (reduces the need for lengths of lossy cables to the pre-amplifiers, for example) but at the expense of equipment and cabling being required inside an already crowded magnet bore. To help mitigate some of this bore overcrowding, work has been done on wireless power transfer to power in-bore electronics [329], [330], [331], which also requires low-power in-bore electronics. With low-power in-bore electronics, dynamic ranges can be limited and so methods for resolving this low dynamic range are being studied [332]. For the SNR reasons, it is desirable to have the antennas placed as close as possible to the field of view of interest. Besides traditional external coils and antennas, implantable antennas and associated low-power electronics for imaging are being studied for use at 7 T [329]. Since these implantable electronics are metallic in nature, unwanted heating and hot spots must be studied to prevent injury to the patient. Significant studies have been conducted showing various techniques such as specific placement or decoy elements and show varying degrees of heating and minimization and image impact [333], [334], [335], [336], [337], [338], [339], [340], [341], [342], [343], [344]. These studies include looking at the impact of electromagnetic interactions with implanted lead wires [337], helical stents [338], catheters [339], as well as a wide range of other implantable devices [342], [343], [344].

As computing power increases, machine learning, artificial intelligence, and numerical algorithms and techniques are being increasingly applied to electromagnetics problems, and the MRI arena is no exception. As examples of applications for these computing tools to MRI, significant works have recently used these tools as ways to increase the speeds of image processing [344], [345], [346] so that images can be obtained more quickly, with the goal of imaging movement such as blood flow [347], [348] or for correcting body motion occurring during scanning [349]. An example of improved image quality is by using a deep-learning training approach [346]. For the RF coils used in MRI scanners, researchers attempt to extract the most SNR that can be physically obtained. Recent papers looked at the intrinsic performance of RF coils through a numerical study that should provide a metric for MRI designers to compare coil quality across manufacturers and customers [321], [323], [342]. Increased computing power also allows researchers to electromagnetically model the human body to predict unwanted effects such as heating,

hot spots, or wavelength-dependent light and dark regions in the images [333], [334], [335], [336], [337], [338], [339], [340], [341], [342], [343], [344], [350].

In summary, while MRI may seem to be mature since it has been used for decades and is widely used in the medical industry, there are still many interesting technical problems to tackle.

D. MICROWAVE IMAGING

The principles, algorithms, image reconstruction of microwave imaging are well summarized in [351]. Their applications for medical and non-medical applications are discussed. Microwave imaging techniques for breast are particularly of interest because of breast cancer screening applications. Reviews in [352], [353], [354] provide historic details of microwave breast imaging techniques and achievements.

Early screening and detection for asymptomatic women aged 40 years or older can prevent breast cancer death [355], [356]. Currently X-ray mammography is widely used for breast imaging. For further examination, ultrasound, MRI and positron emission tomography (PET) are used. The mammography utilizes low-energy X-ray which presents some risk factors for radiation exposure and requires painful compression of the breast [357]. The inaccuracy in distinguishing dense tissues and tumors could lead to overtreatment and unnecessary invasive biopsies [356], [358].

Because the temperature of tumors is higher due to increased vascularization and hypermetabolism [359], [360], [361]. Several studies show that the cancer tumor temperatures increase compared to surrounding tissues is in the range of 1.3–3.5 °C [362]. Passive radiometry has been used for breast imaging [363]. A multiprobe radiometer was demonstrated at 3 GHz with a bandwidth of 1 GHz and it was able to detect ± 0.1 °C changes [364]. A commercial system showed better accuracy as an adjunct to mammography that can significantly reduce false positives for tumor screening [365]. Another experiment utilized two single-frequency radio-thermometers at 1.75 GHz (with a bandwidth of 1.5–2 GHz) and 3 GHz (2.75–3.23 GHz), and achieved ± 0.1 °C measurements at a depth of about 5 cm [366]. Clinical results showed tumor detection typically at depths of 5–30 mm. A system with an active L-shape monopole antenna operating at 1.57 GHz spatially scanning for imaging was used to demonstrate the tumor detection [367].

Microwave detection can provide a spatial distribution of permittivities and conductivities of tissues making it possible to distinguish tissue types. The energy absorption due to the whole-body resonance reaches maximum approximately between 30 and 100 MHz because the resonant wavelengths are comparable to body dimensions. Increasing operation frequencies to microwaves, the effects decrease and the contrasts of reflection from different types of tissues increase. A chronicle of investigation of tissues, including healthy and cancerous ones, and at various frequency bands are summarized in [353]. Different normal tissue types including skin, muscle and fat

from 0.1 to 100 GHz were characterized [368]. Excised normal and malignant tissues at 50–900 MHz and 3 MHz–3 GHz were characterized respectively in [369] and [370]. A large-scale study characterizing excised normal, benign and malignant breast tissues from 0.1 to 20 GHz was summarized in [371], [372]. Using a coaxial probe on tissue specimens from patients to measure the reflection coefficient, dielectric properties were extracted at 0.5–8 GHz [373]. Based on dielectric properties, microwave imaging of the breast can be conducted with tomography, radar principles, and microwave-acoustics techniques.

Microwave tomography, as a passive method, maps the dielectric properties of the breast utilizing inverse scattering parameters with reconstruction algorithms [374], [375]. A 32-channel system with 16 monopole transceiving antennas around the breast when the subject lying on her stomach acquired signals at 300 MHz–1 GHz [376]. 900-MHz images were obtained to compare among subjects and later 3-D images were reconstructed [377]. The system has been used for prognosis during patients receiving chemotherapy [378]. A similar technique was used at 500 MHz to 3 GHz for breast imaging, also with 16 antennas [379]. New antenna structures have been proposed for microwave breast tomography including a system with 12 balanced antipodal Vivaldi antennas operating at 0.5 to 5 GHz in which broadband, directive and focused beams were achieved [380]. Image reconstruction methods for 2-D and 3-D illustrations have been demonstrated, for example, in [381], [382], [383].

The radar-based microwave imaging systems, as active methods, reconstruct images by the reflected signals from the breast depending on the permittivity and conductivity differences among tissues, normal or malignant. The methods can be conducted in the time or frequency domains. Frequencies above 1 GHz are needed for a better spatial resolution. UWB pulses are used to illuminate the breast and return signals can be collected by the same antennas. 3-D images can be obtained by focusing algorithms and array rotation mechanisms for calibration [384], [385], [386], [387], [388]. The pulse travel time from one antenna to any selected focal point can be calculated. The focal points are then scanned to create an image for the area of interest. The reflections from the tumor add coherently and the image shows a contrast between tissue types. Microwave imaging via the space-time beamforming (MIST) method is applied with the person lying on her back and antennas are placed on the flattened breast surfaces [389], [390], [391]. Multiple demonstrations with different algorithms and hardware have been conducted. For example, pyramidal single-ridge horn antennas at 6 GHz transmitted UWB pulses with a 110-ps width for such imaging purposes [385]. The signals were collected at 17 antenna locations. 3-D images of $6 \times 6 \times 5 \text{ cm}^3$ with a 1-mm pixel resolution could be achieved. A tumor with 4 mm in diameter under the skin at a depth of 2 cm in phantom experiments could be identified.

The tissue sensing adaptive radar (TSAR) method is applied with the person lying on her stomach and the breast

is extended through a hole and into a tank containing body-temperature liquid and antennas [392], [393], [394]. Antennas physically scan with UWB pulses to synthesize an array that encircles the breast. Resistively loaded monopole and bowtie slot-line antennas were used. Scanning on tissues first determined the location of the breast and then the reflections from the skin were adaptively subtracted. A TSAR system has been used in a clinical experiment [395]. A scanning balanced antipodal Vivaldi antenna [396] with a UWB bandwidth of 2.4–15 GHz moved around the breast and in the vertical direction to acquire signals at 200 locations over the frequency range from 50 MHz to 15 GHz. The TSAR images showed responses consistent with clinical histories.

The microwave-acoustic imaging technique, also termed microwave thermoacoustic tomography, utilizes microwave pulses to induce thermoelastic pressure waves on the subject. Microwave propagation and absorption depend on tissue permittivity and conductivity, while thermoelastic pressure waves depend on heat dissipation, thermal expansion, pressure level, and media. The pressure propagation in the media can be detected by an acoustic (ultrasound) sensor. The imaging principle is similar to a conventional ultrasound imager except the pressure waves are induced by microwave energy instead of acoustic energy. With specific absorptions in different tissues, the image contrasts can be greatly enhanced. The history, principles, techniques, system implementation, performance, and trial results for breast imaging and other tissue or organs are discussed in detail by J. Lin [397], [398]. Short (0.4–25 μs), high-power (up to 40 kW) pulses at 2.45 GHz are typically used and the energy causes a rapid temperature rise ($10^{-6} \text{ }^\circ\text{C}$ in μs). The pressure wave distribution, with fundamental acoustic frequencies at 22 kHz–1.11 MHz in human tissues, is detected by an ultrasound receiver array and forms the image. To cover higher harmonics of the acoustic waves, it is recommended to have a bandwidth of up to 7.75 MHz [398]. Investigations on different microwave pulses, powers and frequencies, as well as the types, array configurations, frequencies and resolutions of the ultrasound detector have been studied. Comparisons of different systems with their operating parameters are in Tables 1 and 2 of [399]. An ultrashort pulse system was demonstrated for whole-breast imaging with a $40 \times 27 \text{ cm}^2$ radiation area [400]. The illumination microwave pulses with a 20-ns pulse duration, a peak power of 200 GW and a repetition rate up to 100 Hz were transmitted from a linearly polarized conical antenna connected to an aperture antenna. A ring ultrasound transducer at a center frequency of 5 MHz and having 256 detectors was used for detection. The system showed a 7-cm imaging depth and a 0.29-mm spatial resolution in a phantom.

Recently, with the intention to reduce microwave powers in the instrument, a handheld coherent microwave-induced thermoacoustic imaging system was demonstrated. It used 120-W pulses at 2.1 GHz and with pulse widths of 200 ns–10 μs . It could generate images that were detected by an ultrasound transducer at center frequencies of 0.5 and 1 MHz for time-domain imaging [401]. The same technique was

also demonstrated in the frequency domain utilizing FMCW and stepped frequency continuous wave (SFCW) modulations with a peak power of 120 W. The results showed significantly improved signal-to-noise ratios in the ultrasound images with microwave SARs limited to 8.74 and 2.47 W/kg. Comparisons of different imaging techniques and their performance characteristics are compared in Table 1 in [402] and Tables 3/A1 in [403]. The microwave-acoustic imaging techniques have also been in research for other tissues and organs [398] including the kidney, prostate, blood vessels, joints, and brain [404], [405], [406], [407], [408], [409], [410].

E. BIOCHEMICAL SENSING

Sensing blood glucose levels is essential for diabetics. Currently, the most used method is by finger prick to extract a drop of blood sample onto a test strip which is coated with glucose oxidase enzyme. The chemical reaction varies the strip impedance providing reading to an electronic reader [411]. The disposable electrochemical test strips as consumables are still costly and have a limited expiration time. Considering each diabetic person may need more than 4 strips a day, a method to eliminate the enzyme-based strips can reduce costs significantly and make the sensor device ubiquitous and universal.

The changes in the dielectric properties of blood plasma with different glucose concentrations at microwave frequencies provide a possible sensing modality. General microwave sensors to detect permittivities and conductivities of materials, such as transmission-line, resonator, open-end coaxial probe, and reflectometry can be applied for blood glucose measurements [412], [413], [414]. The permittivities and conductivities of whole blood and blood plasma as glucose concentrations change are reported in [415], [416], [417]. Blood plasma samples with discrete glucose concentrations up to 16000 mg/dL were measured at 500 MHz–20 GHz [417]. As a reference, blood glucose levels for healthy diabetics should be less than 100 mg/dL after fasting. Above 126 mg/dL after fasting for a healthy person is considered having diabetes. The typical limit of detection for an electrochemical blood glucose test is defined in the range of 20–600 mg/dL. With blood plasma, the relative permittivity decreases with the increase of frequency while conductivity increases [418]. The permittivity and conductivity of glucose in deionized water, termed an aqueous glucose solution, with variations of concentrations were characterized from 500 MHz to 67 GHz [419]. The comparison of glucose in blood plasma and water was discussed for key glucose concentrations and at frequencies of 0.5, 2.5, 5, and 10 GHz in [418]. A Debye relaxation model was used to obtain permittivities of aqueous glucose solutions and blood samples up to 40 GHz [420]. There is also interest to characterize the dielectric properties of human blood beyond the microwave frequencies. Time-domain spectroscopy up to 1 THz found that the absorption coefficients specific in human blood showed a linear relationship with the glucose concentrations [421].

1) BLOOD GLUCOSE SENSOR

For easy access to blood samples and repeated uses without cleaning complications, planar sensing device architectures are preferred. A review on planar microwave devices to detect glucose concentrations is in [422]. Tables 1, 2, 3 and 4 summarize the device configurations, parameters, and performance of sensors based on the detection of resonant frequency, insertion loss, quality factor, and phase variations, respectively. The various demonstrations were conducted on aqueous glucose solutions, blood or blood plasma. The aqueous glucose solutions were for controlled experiments that had fewer chemical variables, compared to blood. A “relative sensitivity” factor was defined as the sensing parameter change in percentage divided by the parameter change in percentage [422] in order to compare different techniques on an equal basis. The tables compare the device performance according to the relative sensitivity.

Among the four main techniques, the detection of resonant frequency shifts is more popular due to the sensitive resonance changes caused by small permittivity changes from glucose concentration variations. Resonators based on interdigitated finger capacitors, inductor-capacitor (LC) pairs, split-rings and complementary split-rings, coplanar transmission lines, microstrip lines, substrate-integrated waveguide resonators, and combinations of them have been used. Among the ones with high relative sensitivities, for example, a triple complementary split-ring on the ground plane of a microstrip line was demonstrated at 1–6 GHz with a molded polydimethylsiloxane (PDMS) microfluidic channel containing synthetic blood samples of 70–150 mg/dL concentrations [423]. Three resonant frequencies at 1.44–1.6 GHz, 3.9–4.3 GHz, and 4.9–5.4 GHz indicated glucose concentration variations. A complementary inductor-capacitor ground plane in a microstrip line forms its resonance at 1.64 GHz when the goat blood sample was loaded into the microfluidic cavity [424]. The frequency shifted when glucose concentration changed and sensitivity was achieved with 56 kHz/(mg/dL).

For the insertion-loss approach, a quarter-wavelength stub, shunt to a microstrip line, connected an interdigitated finger capacitor located below a microfluidic channel was used at 7.5 GHz to measure the transmission coefficient changes [425]. A sensitivity for insertion loss changes of 7.6×10^{-3} dB/(g/L) was achieved with aqueous glucose solutions within the range of 30–8000 mg/dL (0.3–80 g/L). Another example was a microstrip line with a T-shape pattern on a small finger-shaped tube which was tested with aqueous glucose solutions [426]. The reflection coefficients showed a sensitivity of 1.2×10^{-2} dB/(mg/dL) at 6 GHz for 20–120 mg/dL concentrations and 5.4×10^{-3} dB/(mg/dL) for 100–600 mg/dL.

Owing to the permittivity and conductivity variations, the quality factors of a resonator change accordingly. Split-ring resonators were commonly utilized for their planar and high-quality factor features. A split-ring resonator was demonstrated with quality factor changes due to the solution dielectric losses in human blood plasma samples at 5.17 and

7.17 GHz [427]. A resonator with two mutually-coupled split-rings was demonstrated at 4.23 GHz with a quality factor of 48 achieving high relative sensitivity in aqueous glucose solutions [428]. The phase-based sensor depends on the phase shifts of a narrow-band signal. For example, a microstrip line coupled to a split-ring resonator was used at 3.98–4.05 GHz with aqueous glucose solutions and demonstrated sensitivity of less than 50 mg/dL by measuring the s_{21} phase shifts [429]. A microstrip line loaded with open split-ring resonators integrated under a microfluidic channel was used in aqueous glucose solutions to detect the s_{21} resonant frequency shifts and s_{11} phase shifts [430]. A rectangular meandered line resonator on a gallium arsenide substrate was used at 9.2 GHz to detect glucose levels in human serum [431]. A sensitivity of 1.08 MHz/(mg/dL) and a detection limit of 8.01 mg/dL were reached.

The microwave probing methods for blood glucose concentrations are still facing challenges in specificity due to the indirect sensing principle of detecting dielectric parameters, compared to the high specificity of electrochemical methods, such as utilizing glucose oxidase to directly react with glucose. The detection inherently is affected by interferents in blood including many chemical or biochemical compounds. However, microwaves offer label-free and noninvasive features. The fields can penetrate into skin and tissues with a lower energy and less scattering by the heterogeneous biological structures, compared to optics. These features can potentially provide a continuous, ubiquitous, comfortable and convenient means to sense blood glucose levels *in vivo*.

2) IN VIVO BLOOD GLUCOSE MONITOR

The discrete sampling of blood glucose levels by the finger-prick method has two main shortcomings. The capillary blood is obtained by piercing the skin on a finger with a lancet. There are many nerve endings in fingers so the method is painful, especially since it has to be repeated multiple times a day [432]. The discrete nature of blood sampling does not allow real-time feedback to avoid hypoglycemia (low blood sugar) or a means for an electronic interface to control insulin delivery. Hypoglycemia is particularly dangerous for insulin-dependent diabetics as the patients may become shaky, lose coordination, feel dizzy and lose consciousness when the condition worsens quickly within minutes. A continuous monitoring method for blood glucose levels can dramatically benefit many patients to avoid danger, keep long-term blood glucose levels in check and provide a means for automatic closed-loop insulin delivery with an insulin pump. Reviews on general blood glucose monitoring techniques, including invasive and noninvasive ones, are summarized in [433], [434], [435], [436], [437], [438], [439]. [440] reviewed specifically categories of optical and microwave blood glucose sensing to compare with electrochemical sensing of saliva, tears, sweat and interstitial fluids. Similarly, [441] reviewed glucose sensing based on electromagnetic waves.

Noninvasive sensor and parameter extraction algorithms have been proposed to obtain complex permittivities of glucose using an open-ended coaxial probe at 0.3–15 GHz [442]. The permittivities and conductivities of blood with various glucose levels were further analyzed in [418] with measured data from [417] and [442]. It was concluded that dielectric spectroscopy for blood glucose level assessment is possible but faces challenges because of the small changes in permittivity within the blood glucose concentration range of interest. Locations on the body for effective sensing, frequency selections, devices, and case studies are discussed in [418].

A double-ring resonator operating at 1.4 GHz was demonstrated to measure blood glucose variations on the abdomen skin [443]. The resonator has a quality factor of 800 in the air and 80 on the abdomen. *In-vivo* tests on humans with oral glucose tolerance tests were compared to commercial glucometer results and showed similar trends. *In vitro* experiments were also conducted to investigate the effects from interferents in blood. In phantom tests, the resonant frequency shifted linearly by about 600 kHz when glucose concentration increased from zero to about 200 mM. A clinical trial was conducted on diabetic patients and healthy persons in oral tolerance tests using the double-ring resonator [444]. Changes in resonant frequency, bandwidth, and insertion loss were used to analyze the results. The results from microwave measurements follow the clinical glucose analyzer temporally in the range of 250–450 mg/dL. The results in a Clarke Error Grid showed that the majority of measured data were within the zones A and B indicating good repeatability in the blood glucose 100–550 mg/dL range.

As the small permittivity changes induce sensitive variations in millimeter-wave signal propagation, there has been research conducted to investigate the feasibility of probing blood glucose noninvasively with signals above 30 GHz. A circular metal patch resonator fed by a waveguide was used at 31.9–32.2 GHz and the *in-vivo* reflection measurements on a human fingertip showed a frequency shift sensitivity of 9 kHz/(mg/dL) in the 85–114 mg/dL range [445], [446]. Millimeter-wave transmission and reflection were measured in the band of 27–40 GHz with waveguides clamped on the ear of a rat and delivered powers of 0.1–0.2 mW [447], [448]. With insulin and glucose injections, power absorption showed temporal correlations with glucose levels at different frequencies. A millimeter-wave system was tested with an *in vivo* pig model in the frequency range of 58–62 GHz [449]. Two $1.5 \times 1.5 \text{ cm}^2$ patch antennas clamped the pig's ear, or between an acrylic tank filled with aqueous glucose solution, and reflection/transmission coefficients were measured. The phantom measurements showed a linear relationship between magnitude changes of s_{21} and glucose concentrations with a slope of 0.005 dB/(mmol/L). The animal experiments were conducted by injections of glucose and the results showed the millimeter-wave sensor could detect glucose level spikes with a 13-min delay. A possible reason for the delay may be due to the ear area where the millimeter-wave signals detect interstitial fluids instead of blood [450]. Experiments were also

conducted on human subjects. The antennas were clamped on the right hand and measured the signal variations passing the thin tissue between the index and thumb fingers. It was found that the system could detect glucose spikes in humans during *in-vivo* intravenous glucose tolerance tests [451]. Similar spike delays were also observed. A commercial sensor worn on the wrist containing a microstrip line to perform dielectric spectroscopy was proposed to detect blood up to 2 GHz and are under clinical experiments [452], [453], [454].

Beyond millimeter waves, THz time-domain spectroscopy has been used for biological studies [455], [456], such as the effects on DNA damages in human blood leukocytes (white blood cells) [457], skin imaging [458], dysplasia nevus diagnosis [459], [460], breast imaging [461], molecular spectroscopy [462], and analysis of steroid hormones [456]. Terahertz time-domain spectroscopy in the range of 0.05–2.5 THz was used to analyze the blood plasma of rats with diabetes and compared them with healthy ones. The results showed significant differences in spectral absorptions and reflections [463]. An experiment was conducted with six human subjects through palm skin and showed large variations of the attenuated total internal reflection at 0.1–0.5 THz in the standard oral glucose tolerance tests [464]. The attenuated total internal reflection amplitude increased when the blood glucose level rose.

3) HYDRATION SENSOR

Regulation of a proper hydration level in the body is critical for human health. Dehydration affects physical, physiological and mental conditions significantly and acutely, particularly for labor workers, the elderly, and children [465], [466], [467], [468]. Assessment of dehydration levels noninvasively has been a great challenge. Skin impedance and optical reflection measurements are influenced by skin thickness, sweat, and the depth of electrical current or optical signal penetration. At microwave frequencies, fields can penetrate into the dermis and hypodermis layers where more blood vessels and sweat glands exist. A coplanar electrode was used for hydration monitoring with wet and dry skins measured at resonant frequencies of 367 and 302 MHz in reflectometry [469]. A disposable and conformable paper-based patch antenna made of copper foil was demonstrated for sweat monitoring [470]. The paper absorbed sweat and changed dielectric properties affecting the first and second resonances at 2 and 3.5 GHz, with a 140-MHz frequency shift per drop of 0.05-mL 0.2% (0.4-mol/L) NaCl solution for first resonance, and 300 MHz for second resonance. Dielectric spectroscopy at 2–6 GHz was proposed with 8 strip/patch antennas on printed circuit boards (PCBs) around a person's wrist for monitoring hydration levels as a wearable [471]. A system with two UWB shielded and dielectric-loaded antennas was used to assess hydration *in vivo* by measuring the transmission coefficients through the midpoint of the forearm from 1 to 8 GHz [472], [473]. The permittivities of skin after dehydration were estimated from the transmission coefficients. The same system was used for dehydration after fasting

by measuring reflection and transmission coefficients up to 10 GHz [474]. The results indicated the challenges in measuring the hydration levels of human bodies including the creation of controllable and repeatable scenarios and conditions. Phantoms made of polymers also present limitations. A broadband antenna at 7.9 GHz, aiming for the 7.35-GHz resonant frequency of water molecules, was used to measure reflection coefficients from 7 to 9.5 GHz on the tissue-engineered skin equivalents made of specific hydration and density of matrix components including various types of cells, collagen, hydrogel, and electrolytes [475]. Results showed that resonant frequencies and return losses corresponded to different skin equivalents. A flexible and deformable tuned-loop resonator, with significantly improved quality factors operated at 0.9–1.1 GHz was tested on human bodies to assess hydration progress [476], [477], [478]. The resonant frequency shifts indicated hydration levels when a person started getting hydrated from a dehydrated state. The feasibility of detecting permittivity and conductivity changes with resonant fields was demonstrated with dehydration processes in tissue phantoms and fruits. A complementary split-ring resonator directly attached to an SMA connector designed at 5.52 GHz was used on phantoms for demonstration [479]. Resonant frequencies for hydrated, normal, and dehydrated skin phantoms were 5.3, 5.52, and 5.89 GHz, respectively.

4) BIOMARKER SENSOR

With electrochemical coating on microwave resonators, the narrow-band frequency responses enable sensitive detection of small amounts of biochemical or protein targets. Selectivity or specificity is typically determined by the enzyme or binding chemicals. Particularly for medical applications, they can be used to detect bodily fluids or exhaled breath to identify certain markers for diseases. For example, diabetic patients without good blood glucose control may have higher acetone levels in their breath [480]. To measure the low concentration of gases, a sensitive detection principle is needed such as the use of microwave resonance. Metal-oxide gas sensors and optics-based sensors have their respective shortcomings. Microwave resonance circuits do not require high temperatures to operate or bulky electronics to operate optics. It provides an attractive option for a portable instrument. A microstrip ring resonator covered with a layer of swelling PDMS and operated at 5.45 GHz with a quality factor of 150 was used to detect acetone vapor with concentrations of 0–265 ppt by frequency shifts [481]. A circular disk resonator coated with single- or multi-walled carbon nanotubes that adsorbed gas molecules was used at 3.876 GHz to detect ammonia by frequency shifts [482]. Using microbeads (beaded activated carbon and polymer-based beads) for gas adsorbents, a microstrip split-ring was used to sense 2-Butoxyethanol gas by measuring s_{21} frequency shifts of 10 and 160 kHz responded to a 35-ppm concentration with the beaded activated carbon and polymer-based beads, respectively [483]. Using cobalt phthalocyanine as the selective layer, a grounded

coplanar waveguide resonator was demonstrated for ammonia detection of 100–500 ppm and toluene of 500–2000 ppm at 3.65–3.75 GHz [484]. A polycrystalline anatase-phase TiO₂ nanotube membrane was placed in the coupling gap of a microstrip ring resonator for the detection of methanol, ethanol and 2-propanol at 5.12 GHz [485]. Both frequency shifts and quality factor variations provide gas information. Another example used a comb copolymer phthalocyanine thin film on microstrip-line interdigitated fingers as the selective material to detect acetone, ethanol and methanol in the range of 0–200 ppm at 8.64 GHz by measuring resonant frequency shifts and S_{11} magnitude changes [486].

For liquid samples, a coplanar waveguide and slotline ring resonator at the resonant frequency of 3.375 GHz was proposed for biomolecule detection, such as biotin and streptavidin, by resonance shifts [487]. With the intention to detect albumin in the concentration range of 0–100 g/L, an interdigitated finger without enzyme coating was used to measure its concentration of albumin dissolved in water between 4 and 5 GHz [488]. The albumin is a precursor for thoraco-abdominal aneurysms, a lethal vascular disease. A bacterial detector utilizing interdigitated fingers coated with T4 bacteriophage gp37 adhesin, which was to bind *Escherichia coli* B in order to recognize its bacterial host lipopolysaccharide, was demonstrated at the measurement range of 0–3 GHz [489]. A split-ring resonator in parallel to a microstrip line detected at 10.48 GHz the prostate-specific antigen (PSA) and cortisol stress hormone with coatings of PSA and cortisol antibodies on the gold resonance surface [490]. The sensor was designed to quickly assess the risk of prostate cancers in men.

Millimeter waves and THz have been researched in uses of detecting biological macromolecules such as amino acids, peptides, proteins, nucleic acids, and carbohydrates. The vibrations due to molecular structures, and inter-/intra-molecular interactions respond to the short wavelengths. THz spectroscopy provides unique advantages over its wide bandwidths. Spectral characteristics of absorption and resonance with low noise interference and short pulse widths reveal biomolecule features effectively. A review summarizes the advances in frequency uses, instrumentation and the detection of biomolecules in [491]. Some examples include virus detection [492], amino acids examination [493], hydration processes in biological cell membranes [494], detection of carbohydrate isomers [495], and detection of the SARS-CoV-2 virus spike proteins [496].

V. THERAPEUTIC APPLICATIONS

Hyperthermia treatments are performed at around 45 °C and ablation treatments are typically performed at temperatures above 55°C. There has been a several-fold increase in the utilization of microwaves in medicine, since our publication appeared twenty years ago [1]. This increase represents new techniques for therapy, detection, and healthcare communications. Today, the microwave equipment can be found in most hospitals in the US. A summary of

commercially available systems and their applications as well as research development are presented in [497]. In this section, several therapeutic uses of microwaves and ongoing research activities are discussed.

A. ABLATION AND CATHETER ABLATION

Leonard Taylor, the inventor of the microwave scalpel, described the potential utilization of microwaves in the treatment of various types of solid tumors as a tool for microwave surgery [498]. The technology has since evolved, to include microwave treatments of several types of cancer, including cancers of the liver, kidney, breast, and lungs, just to mention a few [499].

Microwave catheter ablation is used to thermally treat and deactivate the heart tissues that produce abnormal electrical activities. Small microwave antennas or waveguides which are sufficiently small to fit within a catheter deliver energy to the tissues directly [500], [501], [502], [503]. Several conditions can lead to the development of abnormal cardiac rhythms (arrhythmias) [504], [505]. When the heart develops an abnormal focus or pathway of electrical activities, a rhythm disturbance becomes the result. In the 1980s, microwave catheter ablation was researched and developed, but this new modality could not compete with RF ablation [506], which had been in use for many years. Recently, however, microwave ablation has been revisited and has become the subject of new research efforts owing to the great advances in high-frequency electronics and the miniaturization of delivery tools [507]. Microwave ablation is not contact-dependent, unlike RF ablation [508]. Different techniques for energy delivery are discussed in [509]. The use of microwave energy allows for greater tissue penetration without a higher risk of endocardial disruption, and a higher transmural efficacy to heat tissues without damaging vessel walls. Thus, it creates a greater volume of tissue necrosis for potentially a greater therapeutic effect. Typically, the frequencies used are in the range of 915 MHz to 2.45 GHz. Lower frequencies can penetrate deeper and have less heating in the connecting cable. Microwave lesion depth increases exponentially over time, unlike the RF ablation [510]. Microwave ablation has been used intra-operatively for open heart surgeries and minimally invasive surgeries [509].

Minimally invasive microwave catheters for percutaneous cardiac ablation require miniature antennas [511], a low reflection back to the cable to avoid heating, and immunity of antenna performance to tissue permittivities. A spiral antenna was used to deliver up to 150-W output powers at 915 MHz for catheter ablation [500], [512]. Monopole and helical coils were also used [510]. A conformal antenna applicator designed for circumferential ablation was demonstrated at 915 MHz [513]. Comparisons of tissue responses and ablation zones with a power of 50 W for 15 minutes at 1.9 and 10 GHz were discussed in [514].

At 2.45 GHz, absorption rates of blood, muscle and fat are different, and signal penetration depths vary so the energy can be purposely delivered into a specific area at a

distance from the applicator. Their different dielectric constants also affect the field distributions in different layers of tissues. The wavelengths are reduced in blood and electrically small antennas thus are preferred. Split-Tip, Cap-Slot, and Cap-Choke antennas that can fit into a 7–9 French (3 Fr = 1 mm) outer diameter catheter introducer were demonstrated for atrioventricular (AV) nodal and ventricular ablation [515]. An expanded tip wire antenna in a 6-Fr catheter [516], a slot array antenna [517], a 13-mm monopole antenna [518], [519], a helical antenna [520], a parallel loop antenna [521], a double slot choked antenna [522] and a double-dipole antenna fed by a substrate-integrated coaxial line [523] were demonstrated at 2.45 GHz in phantoms and/or animals for microwave ablation purposes.

Besides treating cardiac tissues, a coaxial-based antenna was designed for tumor ablation at 2.45 GHz with power radiation to heat up a tumor above 60 °C in order to induce cell death [524]. Coaxial-slot and coaxial-dipole antennas at 2.45 GHz were also used to generate heating in a region 30 mm away in the probe direction for brain tumor ablation [525]. Pancreatic cancer [526], lung cancer [527], colorectal cancer [528], liver cancer [529], and other cancer [530], [531] treatments were demonstrated. 2.45-GHz microwave ablation has been used in minimally invasive endoscopic procedures to treat gastric motility disorders such as gastroparesis. Ablation of GI tissues disrupts irregular electrical activities on the stomach wall that produce abnormal motility and cause gastroparesis symptoms [532].

The effectiveness of using microwave energy at 14.5 GHz for coagulating blood has been shown in [533]. Tumor vascularity in which cancerous cells make blood vessels is an important factor for tumors to become malignant. RF ablation effects on coagulation necrosis have shown effectiveness [534] so microwave ablation that can deliver heating more effectively becomes attractive for treatment. A circular waveguide applicator was designed for skin cancer treatment at 14.5 GHz and 10–50 W powers were demonstrated on ovine skin samples [535]. In another example, microwave energy of 31.8 W was delivered by a waveguide cavity at 14.5 GHz for the treatment of benign skin tumors, skin tag, cutaneous horn, and general warts [536].

A microwave applicator was designed to treat snoring [537]. Chronic snoring is a respiratory disturbance as the soft palate at the back of the roof of the mouth, tonsils, adenoids and tongue vibrate as air passes through the mouth when the airway through the nose is restricted. Long-term snoring can be the result of obstructive sleep apnea [538], [539]. Surgical techniques are applied with ablation of the uvula and of the mucous membrane near the soft palate. Using a surgical laser can create fibrous scars by ablation of the uvula to reduce vibration of the soft palate. A technique that applied ac currents via needle electrodes at 465 MHz showed less postoperative pain in a 22-subject study [540]. The excessive heat by RF contact can result in unwanted tissue damage and scarring. This side effect can potentially be minimized by microwaves. A microwave ablation applicator with a diameter of 1.2 mm

was designed according to the anatomical constraints [537]. Temperatures of above 60 °C at the hot spot and below 40 °C on the surface of the palate were achieved with a maximum 20-W power that was delivered by a two-lead antenna from a coaxial cable at 868 MHz. A similar principle was applied on a tissue resection device with moveable jaws behaving as an antenna that could deliver energy at 5.8 GHz for coagulation of tissues by heating, and voltages at 400 kHz and 350 V for tissue cutting [541].

B. MICROWAVE BALLOON ANGIOPLASTY (MBA)

Percutaneous transluminal balloon angioplasty (PTBA) [542] has been used as an alternative to coronary bypass surgery which redirects blood flow around a blocked artery in the heart [543]. The PTBA technique employs a balloon catheter that is advanced to the site of the atrial stenosis (the narrowing of an artery). Pressure, generated by the balloon inflation, dilates the affected artery. Microwave balloon angioplasty (MBA) provides a major modification for the PTBA [544], [545], [546]. The MBA catheter contains a microwave cable and an end-fire antenna assembly encased within the catheter, similar to the ones mentioned for catheter ablation tools. It is positioned so that the antenna is centered within the balloon [511]. As the balloon is inflated, the surrounding tissue is concurrently heated when microwave energy is applied. The hypothesis, later validated, is that combining pressure and heat creates patent vessels, enhancing the dilatory effect of the balloon, and reduces or eliminates subsequent resistance to blood flow. MBA takes advantage of the volume heating properties of microwave radiation. Similar antennas mentioned for ablation catheters are also applied for angioplasty at 915 MHz and 2.45 GHz. For example, a spiral antenna with a diameter of 10 mm in a balloon of 20 mm in diameter at 915 MHz delivering up to 150 W via a coaxial cable in phantoms [547]. Another example is a balloon catheter with a coaxial antenna at the tip filled with saline that has high dielectric losses at 2.45 GHz was used to produce localized heat in a plaque area to remove blockages inside vessels. The capability was demonstrated in animal models [548].

Gastroesophageal reflux disease (GERD) is due to the reflux of acid or nonacid fluids flow back from the stomach into the esophagus [549], [550]. Acid reflux can irritate and damage the esophagus lining with heartburn feeling. The content can reach the throat or into the lungs causing chronic cough, inflammation of the vocal cords, chest pain and asthma. Non-acid reflux symptoms, which often do not cause painful heartburn and so patients fail to seek treatment, can also be significant [551]. Correction of the lower esophagus sphincter can effectively treat GERD symptoms [552], [553]. Controlled heating on the lower esophageal sphincter muscles can restore and tighten the valve function of the sphincter to stop reflux from the stomach to the esophagus. The tissue thickness is less than 2 mm and the treatment instrument needs to provide the heat quickly in the precise location to avoid motion effects and damage to other tissues. Clinical trials have shown significant efficacy in reducing reflux symptoms using

commercial contact electrodes outside a balloon to deliver 465-kHz, 5-W RF powers onto esophagus tissues [554], [555]. For using microwaves, a center-fed traveling-wave waveguide consisting of a slot antenna array with a width of 5 mm and a length of 40–60 mm was demonstrated [556]. There were 20 slot antennas each with a width of 0.44 mm and a spacing of 1 mm. The antennas were used to deliver energy into the sphincter to produce controlled heating around the sphincter. The radiation structure was mounted outside of the balloon. The energy of 8–600 J was delivered with 4–20 W pulses at 14.5 GHz for a duration of 2–30 s. The operating frequency was chosen at 14.5 GHz because of its limited depth of field penetration which was validated previously in liver and kidney models [533]. Details about the frequency choice and antenna structures are in [557].

C. HYPERTHERMIA IN MEDICINE

Hyperthermia cancer therapy is an established process. An elevated temperature in tissue can help inducing cancer cell death with chemical or radiation treatments [558], [559], [560]. It was heavily researched in the 1980s and 1990s. The popularity of microwave hyperthermia remained relatively high in several countries in Europe, but not in the USA. Today, only a small number of medical centers treat recurrence of breast cancer with microwaves, mostly as adjuvant therapy to enhance the treatment of radiation and chemotherapy. Hyperthermia therapy has been used in a variety of cancers, such as breast, brain, prostate, melanomas, and soft tissues sarcomas, to mention a few. Non-cancer therapies using microwaves are discussed below.

Microwave treatment of benign prostatic hyperplasia (BPH) is based on the basic principles behind microwave balloon angioplasty discussed above. It has been a welcomed procedure in urology [561], [562], [563]. Benign prostatic hyperplasia (BPH) is also called prostate gland enlargement which is common for senior men. The prostate is a gland in males that produces seminal fluid. It is located at the base of the bladder and surround the urethra. As a male grows older, the prostate enlarges and may compress the urethra, obstruct the urinary tract, and block the urine flow out of the bladder. It can also cause discomfort and frequent need to urinate, difficulty in starting urination, and bladder, urinary tract or kidney problems in long term [564], [565], [566].

As a known vascular modality, microwave balloon catheters are now used to treat BPH. The Transurethral Microwave Thermotherapy (TUMT) system is a microwave delivery system built into the transurethral catheter inserted through the tip of the penis into the urethra until it reaches the area of the urethra surrounded by the prostate. TUMT then destroys prostatic tissues by raising the temperature in the prostate to as high as 50 °C [567]. However, the integrity of the urethral mucosa and other nearby structures is preserved by an integrated cooling system. The principle of cell death by heat, the comparison to other thermal treatment techniques, and efficacies are discussed in [568]. Clinical studies suggest that TUMT is a safe and effective treatment option for BPH

[561], [569]. A helical coil antenna used in a TUMT at 915 MHz delivered 45-W power and produced heat to maintain a temperature of 60 °C at the prostate [570], [571]. A coaxial open-slot antenna encapsulated within an elliptical silicone balloon filled with saline connected to a silicone catheter was demonstrated at 2.45 GHz [572]. The temperature can be maintained at 75 °C for 30 minutes with a power of 70 W. Instead of the transurethral approach, transperineal microwave thermoablation used for BPH treatment was also tested in a clinical trial and showed safe and repeatable results [573]. A 2.45-GHz semi-rigid coaxial antenna with an extended center-conductor tip coated with dielectric materials was utilized in the probe with a quarter-wavelength choke section. It delivered a continuous-wave power of 20 W for 5 minutes. The temperature was maintained at 39 °C.

Photodynamic therapy [574], [575] is a treatment modality for Barret's esophagus [576], a pre-cancer growth in the esophagus, often due to reflux [577], [578]. The success of treatment depends on the combination of a photo-sensitizing agent such as Photofrin [579], the oxygen level at the treatment site, and the specific optical wavelength of 635 nm to activate the Photofrin. Microwave hyperthermia increases local blood flow and thus increases the local oxygenation in the tumor [580]. This process results in the generation of an effective level of singlet oxygen, which is needed to destroy the tumor cells. An integrated system was proposed with microwave antennas and laser diodes in a balloon catheter for the treatment of Barret's esophagus [581].

Microwave hyperthermia can also be used in the treatment of hyperhidrosis [582]. Hyperhidrosis is a condition when a person produces sweat excessively and above normal physiological needs, regardless of the ambient temperature [583]. A minimally invasive technique was developed by miraDry[®] (Sientra, Santa Clara, California, USA), that utilizes microwave hyperthermia to reduce sweat and treat primary axillary hyperhidrosis by targeting underarm sweat glands. A cooling system is used to protect the underarm skin while microwave energy is applied [584]. An applicator consisting of an array of four waveguide antennas and a cooling system was designed to maximize energy absorption near the dermal/hypodermal interface [585]. Pre-clinical tests on porcine models were conducted to optimize its thermal performance. At 5.8 GHz, low absorption at the epidermis and maximal absorption at the dermal/hypodermal interface were found, mostly independent of skin thickness. Each antenna delivered 30-W power and microwave energy levels of 599, 630 and 756 J were tested with coolant at 10 °C. The results were examined for safety limits. The published results of clinical trials report that the microwave treatment system is effective in treating both axillary hyperhidrosis [586], [587] and axillary osmidrosis (sweat related odors) [588]. This method is currently available in various plastic surgery centers around the United States.

Microwave techniques in the frequency range of hundreds of MHz to a few GHz will continue to be developed in therapeutic medicine due to their noninvasive, localized

control and remote heating features [589], for biomedical instruments such as blood perfusion measurements [590], [591], [592], and for cosmetic surgery such as the 2.45-GHz microwave-aided tumescent liposuction [593], [594]. Integration in treatment instruments, including for the creation of cavities in solid tumors which will allow for the introduction of high-dose chemotherapy, at dosages that cannot safely be applied systemically today, will create more clinical applications.

VI. CONCLUSION

Microwave technologies in diagnostic and therapeutic medicine will continue to advance and evoke innovative healthcare for a variety of tough diseases, bring comfort and convenience to patients, empower patients and doctors for effective disease management, and enhance the overall welfare of our society. As in many areas of scientific exploration, microwaves in medicine will continue to push the boundaries of the frontier.

VII. THE BIOLOGICAL EFFECTS AND MEDICAL APPLICATIONS COMMITTEE MTT-28 HISTORY

The Biological Effects and Medical Applications Committee in the Microwave Theory and Techniques Society (MTT-S) has been a propelling force to promote RF and microwave technologies in biomedical applications. The committee has a long history in MTT-S. To the best of our knowledge from searching information in IEEE Xplore, the earliest biomedical session in the International Microwave Symposium (IMS) was in 1973 held in Boulder, Colorado, USA. The session titled “XI session: Microwave Techniques in Biological Research” was chaired by H. M. Altschuler with 7 papers presented. Paper titles included “An RF Decoupled Electrode for measurement of Brain Temperature During Microwave Exposure”, “Theoretical and Experimental Studies of Microwave Induced Cataracts in Rabbits” and “Bid Feathers as Dielectric Receptors of RF Field”. In 1974, a session “Analysis and Application of Microwave in Biology and Medicine” was chaired by A. Ecker with 7 papers published. In 1975, the session “Microwave in Medicine” was chaired by P. Polson with 8 papers presented including “Microwave Measurement of Respiration” by J. Lin and J. Salinger [595]. The sessions in IMS for biomedical applications continued. Just a few examples: in 1979, 1980, 1981 and 1983, there were “Microwaves in the Bioenvironment” session chaired by R. Olsen with 5 papers; “Biological Applications and Effects” chaired by E. Bostow; “Biological Effects and Medical Application” chaired by W.R. Adey with 9 papers; and “Microwave Biological Effects” chaired by K. Carr with 8 papers, including papers titled “Microwave Thermo-therapy for the Treatment of Human Cancer” and “A 5.8-GHz Ophthalmic Microwave Applicator for Treatment of Choroidal Melanoma”.

To facilitate and promote the fields, a committee was established in late 1980 by A. Rosen, A. Vander Vorst, and R. Bansal as MTT-S Technical Committee (TC) 10. Papers about medical applications using microwaves were

systematically recruited and presented in the symposia. For example, in 1985 IMS, the session “Biomedical Aspects of Microwaves” was chaired by J. C. Lin with 6 papers. In 1986 and 1987, the sessions chaired by A. Rosen had 6 and 5 papers, respectively. These presentation counts do not include the open-forum papers.

Since 1990, the committee has been steadily growing in memberships and scopes. Consequentially, the committee has sponsored multiple technical sessions, workshops, and short courses each year in the International Microwave Symposia and special issues in the Transactions on Microwave Theory and Techniques, and Microwave Magazine. For example, the “Special Issue on Biomedical Applications of RF/Microwave Technologies” was published in May 2013 of the Transactions on Microwave Theory and Techniques, guest edited by M.-R. Tofighi and J.-C. Chiao. Three special issues on medical applications of RF and microwaves were published in the March, May and July issues of Microwave Magazine, guest edited by D. Kissinger and J.-C. Chiao.

Since 2011, the IEEE BioWireless Conference in the IEEE Radio & Wireless Week (RWW) has been sponsored by TC-10. The IEEE International Microwave Workshop Series - Biomedical (IMWS-Bio) since 2013 was also sponsored by TC-10. In 2017, the BioWireless Conference and IMWS-Bio were integrated into a new conference in 2017. The International Microwave Biomedical Conference (IM-BioC) has been held by rotation on different continents each year since 2017. Several members have served the IEEE MTT-S Distinguished Microwave Lecturers and delivered biomedical-related research lectures all over the world. In 2014, a new electronic journal was proposed by TC-10 members and approved by IEEE in 2017. The IEEE Journal of Electromagnetics, RF, and Microwaves in Medicine and Biology provides a place to share the sciences and applications of medicine and biology related to the utilization of electromagnetics, radio frequency signals, microwaves and millimeter waves [596]. In 2020, the Biological Effects and Medical Applications Committee was renumbered to TC-28 to be included in the technical category of Systems and Applications.

REFERENCES

- [1] A. Rosen, M. A. Stuchly, and A. Vander Vorst, “Applications of RF/microwaves in medicine,” *IEEE Trans. Microw. Theory Techn.*, vol. 50, no. 3, pp. 963–974, Mar. 2002.
- [2] *IEEE Standard for Safety Levels With Respect to Human Exposure to Electric, Magnetic, and Electromagnetic Fields, 0 Hz to 300 GHz*, IEEE C95. 1, 2019.
- [3] International Commission on Non-Ionizing Radiation Protection, “ICNIRP guidelines on limiting exposure to time-varying electric, magnetic and electromagnetic fields (100 kHz to 300 GHz),” 2020. [Online]. Available: <https://www.icnirp.org/>
- [4] P. Bose, A. Khaleghi, S. Mahmood, M. Albatat, J. Bergsland, and I. Balasingham, “Evaluation of data telemetry for future leadless cardiac pacemaker,” *IEEE Access*, vol. 7, pp. 157933–157945, 2019.
- [5] D. Fitzpatrick, *Implantable Electronic Medical Devices*, 1st ed. New York, NY, USA: Elsevier, 2014.
- [6] “Article 5: Frequency allocations,” International Telecommunication Union, 2017. [Online]. Available: <https://life.itu.int/radioclub/rr/art05.htm>

- [7] P. D. Costa, P. P. Rodrigues, A. H. Reis, and A. Costa-Pereira, "A review on remote monitoring technology applied to implantable electronic cardiovascular devices," *Telemed. e-Health*, vol. 16, no. 10, pp. 1042–1050, 2010.
- [8] D. S. Chew and V. Kuriachan, "Leadless cardiac pacemakers: Present and the future," *Curr. Opin. Cardiol.*, vol. 33, no. 1, pp. 7–13, 2018.
- [9] M. A. Miller, P. Neuzil, S. R. Dukkipati, and V. Y. Reddy, "Leadless cardiac pacemakers: Back to the future," *J. Amer. College Cardiol.*, vol. 66, no. 10, pp. 1179–1189, 2015.
- [10] J. Sperzel, C. Hamm, and A. Hain, "Nanostim-leadless pacemaker," *Herzschrittmachtherapie Elektrophysiologie*, vol. 29, no. 4, pp. 327–333, 2018.
- [11] D. Reynolds et al., "A leadless intracardiac transcatheter pacing system," *New England J. Med.*, vol. 374, no. 6, pp. 533–541, 2016.
- [12] D. Sharma, V. Kaim, B. K. Kanaujia, N. Singh, S. Kumar, and K. Rambabu, "A triple band circularly polarized antenna for leadless cardiac transcatheter pacing system," *IEEE Trans. Antennas Propag.*, vol. 70, no. 6, pp. 4287–4298, Jun. 2022.
- [13] M. Zada, I. A. Shah, A. Basir, and H. Yoo, "Ultra-compact implantable antenna with enhanced performance for leadless cardiac pacemaker system," *IEEE Trans. Antennas Propag.*, vol. 69, no. 2, pp. 1152–1157, Feb. 2020.
- [14] F. Faisal, M. Zada, H. Yoo, I. B. Mabrouk, M. Chaker, and T. Djerafi, "An ultra-miniaturized antenna with ultra-wide bandwidth for future cardiac leadless pacemaker," *IEEE Trans. Antennas Propag.*, vol. 70, no. 7, pp. 5923–5928, Jul. 2022.
- [15] M. Oikawa-Kawamoto et al., "Safety and utility of capsule endoscopy for infants and young children," *World J. Gastroenterol.*, vol. 19, no. 45, pp. 8342, 2013.
- [16] I. Iwama et al., "Efficacy and safety of a capsule endoscope delivery device in children," *Eur. J. Gastroenterol. Hepatol.*, vol. 31, no. 12, pp. 1502–1507, 2019.
- [17] F. Fabiola et al., "Applications of wireless capsule endoscopy in pediatric age: An update," *Acta Bio Medica: Atenei Parmensis*, vol. 89, pp. 40–46, 2018.
- [18] G. Iddan, G. Meron, A. Glukhovsky, and P. Swain, "Wireless capsule endoscopy," *Nature*, vol. 405, no. 6785, 2000, Art. no. 417.
- [19] T. Nakamura and A. Terano, "Capsule endoscopy: Past, present, and future," *J. Gastroenterol.*, vol. 43, no. 2, pp. 93–99, 2008.
- [20] A. Wang et al., "Wireless capsule endoscopy," *Gastrointestinal Endoscopy*, vol. 78, no. 6, pp. 805–815, 2013.
- [21] S. Chetcuti Zammit and R. Sidhu, "Capsule endoscopy - Recent developments and future directions," *Expert Rev. Gastroenterol. Hepatol.*, vol. 15, no. 2, pp. 127–137, 2021.
- [22] D. Miley, L. B. Machado, C. Condo, A. E. Jergens, K. Yoon, and S. Pandey, "Video capsule endoscopy and ingestible electronics: Emerging trends in sensors, circuits, materials, telemetry, optics, and rapid reading software," *Adv. Devices Instrum.*, vol. 2021, no. 9854040, pp. 1–50, 2021.
- [23] D. Nikolayev, M. Zhadobov, R. Sauleau, and P. Karban, "Antennas for ingestible capsule telemetry," in *Advances in Body-Centric Wireless Communication: Applications and State-of-the-Art*. London, U.K.: IET, 2016, ch. 6, pp. 143–186.
- [24] S. Gayen, B. Biswas, and A. Karmakar, "The quest for a miniaturized antenna in the wireless capsule endoscopy application: A review," *Int. J. Microw. Wireless Technol.*, vol. 14, no. 9, pp. 1195–1205, 2021.
- [25] F. Merli, L. Bolomey, J. Zurcher, G. Corradini, E. Meurville, and A. K. Skrivervik, "Design, realization and measurements of a miniature antenna for implantable wireless communication systems," *IEEE Trans. Antennas Propag.*, vol. 59, no. 10, pp. 3544–3555, Oct. 2011.
- [26] R. Li and Y. Guo, "A conformal UWB dual-polarized antenna for wireless capsule endoscope systems," *IEEE Antennas Wireless Propag. Lett.*, vol. 20, no. 4, pp. 483–487, Apr. 2021.
- [27] S. A. Osman, M. S. El-Gendy, H. M. Elhennawy, and E. A. Abdallah, "Reconfigurable flexible inverted-F antenna for wireless capsule endoscopy," *AEU-Int. J. Electron. Commun.*, vol. 155, 2022, Art. no. 154377.
- [28] E. Güreş, M. B. Yelten, Ö. Özdemir, and O. Ferhanoglu, "A meandered dual loop antenna for wireless capsule endoscopy," *AEU-Int. J. Electron. Commun.*, vol. 137, Jul. 2021, Art. no. 153792.
- [29] J. Lai et al., "Design of a dual-polarized omnidirectional dielectric resonator antenna for capsule endoscopy system," *IEEE Access*, vol. 9, pp. 14779–14786, 2021.
- [30] G. Wang, X. Xuan, D. Jiang, K. Li, and W. Wang, "A miniaturized implantable antenna sensor for wireless capsule endoscopy system," *AEU-Int. J. Electron. Commun.*, vol. 143, 2022, Art. no. 154022.
- [31] D. H. Werner and S. Ganguly, "An overview of fractal antenna engineering research," *IEEE Antennas Propag. Mag.*, vol. 45, no. 1, pp. 38–57, Feb. 2003.
- [32] J. Anguera et al., "Fractal antennas: An historical perspective," *Fractal Fractional*, vol. 4, no. 1, 2020, Art. no. 3.
- [33] M. A. N. Hamed, R. A. Fayadh, and H. M. Farhan, "UWB pentagonal shaped fractal patch antenna for wireless capsule endoscopy," in *Proc. IOP Conf. Ser., Mater. Sci. Eng.*, 2020, Art. no. 012092.
- [34] B. Biswas, A. Karmakar, and V. Chandra, "Fractal inspired miniaturized wideband ingestible antenna for wireless capsule endoscopy," *AEU-Int. J. Electron. Commun.*, vol. 120, 2020, Art. no. 153192.
- [35] M. A. N. Hamed and R. A. Fayadh, "UWB elliptical antenna using fractal geometry for wireless capsule endoscopy," *IOP Conf. Ser., Mater. Sci. Eng.*, vol. 180, 2020, Art. no. 012103.
- [36] E. A. Johannessen, L. Wang, C. Wyse, D. R. Cumming, and J. M. Cooper, "Biocompatibility of a lab-on-a-pill sensor in artificial gastrointestinal environments," *IEEE Trans. Biomed. Eng.*, vol. 53, no. 11, pp. 2333–2340, Nov. 2006.
- [37] J. L. Gonzalez-Guillaumin, D. C. Sadowski, K. V. I. S. Kaler, and M. P. Mintchev, "Ingestible capsule for impedance and pH monitoring in the esophagus," *IEEE Trans. Biomed. Eng.*, vol. 54, no. 12, pp. 2231–2236, Dec. 2007.
- [38] F. Xu, G. Yan, Z. Wang, and P. Jiang, "Continuous accurate pH measurements of human GI tract using a digital pH-ISFET sensor inside a wireless capsule," *Measurement*, vol. 64, pp. 49–56, 2015.
- [39] H. Weinstein et al., "A new method for determining gastric acid output using a wireless pH-sensing capsule," *Alimentary Pharmacol. Therapeutics*, vol. 37, no. 12, pp. 1198–1209, 2013.
- [40] R. Monnard et al., "Issues in continuous 24-h core body temperature monitoring in humans using an ingestible capsule telemetric sensor," *Front. Endocrinol.*, vol. 8, 2017, Art. no. 130.
- [41] C. C. Bongers, H. A. Daanen, C. P. Bogerd, M. T. Hopman, and T. M. Eijsvogels, "Validity, reliability, and inertia of four different temperature capsule systems," *Med. Sci. Sports Exercise*, vol. 50, pp. 169–175, 2018.
- [42] F. N. Alsunaydih, M. S. Arefin, J. Redoute, and M. R. Yuce, "A navigation and pressure monitoring system toward autonomous wireless capsule endoscopy," *IEEE Sensors J.*, vol. 20, no. 14, pp. 8098–8107, Jul. 2020.
- [43] A. Aburub, M. Fischer, M. Camilleri, J. R. Semler, and H. M. Fadda, "Comparison of pH and motility of the small intestine of healthy subjects and patients with symptomatic constipation using the wireless motility capsule," *Int. J. Pharmaceutics*, vol. 544, no. 1, pp. 158–164, 2018.
- [44] R. J. Saad and W. L. Hasler, "A technical review and clinical assessment of the wireless motility capsule," *Gastroenterol. Hepatol.*, vol. 7, no. 12, pp. 795–804, 2011.
- [45] J. Z. Ou, C. K. Yao, A. Rotbart, J. G. Muir, P. R. Gibson, and K. Kalantar-Zadeh, "Human intestinal gas measurement systems: In vitro fermentation and gas capsules," *Trends Biotechnol.*, vol. 33, no. 4, pp. 208–213, 2015.
- [46] K. Kalantar-Zadeh et al., "A human pilot trial of ingestible electronic capsules capable of sensing different gases in the gut," *Nature Electron.*, vol. 1, no. 1, pp. 79–87, 2018.
- [47] K. Kalantar-Zadeh, K. J. Berean, R. E. Burgell, J. G. Muir, and P. R. Gibson, "Intestinal gases: Influence on gut disorders and the role of dietary manipulations," *Nature Rev. Gastroenterol. Hepatol.*, vol. 16, no. 12, pp. 733–747, 2019.
- [48] S. S. Rao, A. Lembo, W. D. Chey, K. Friedenberg, and E. M. Quigley, "Effects of the vibrating capsule on colonic circadian rhythm and bowel symptoms in chronic idiopathic constipation," *Neurogastroenterol. Motility*, vol. 32, no. 11, 2020, Art. no. e13890.
- [49] J. Yu et al., "Safety and efficacy of a new smartphone-controlled vibrating capsule on defecation in beagles," *Sci. Rep.*, vol. 7, no. 1, pp. 1–7, 2017.

- [50] J. Zhu et al., "Efficacy and safety of vibrating capsule for functional constipation (VICONS): A randomised, double-blind, placebo-controlled, multicenter trial," *eClinicalMedicine Lancet Discov. Sci.*, vol. 47, 2022, Art. no. 101407.
- [51] A. Schulze-Bonhage, "Long-term outcome in neurostimulation of epilepsy," *Epilepsy Behav.*, vol. 91, no. 2, pp. 25–29, 2019.
- [52] D. M. Kusyk, J. Meinert, K. C. Stabingas, Y. Yin, and A. C. Whiting, "Systematic review and meta-analysis of responsive neurostimulation in epilepsy," *World Neurosurg.*, vol. 167, pp. e70–e78, 2022.
- [53] B. Gosselin, "Recent advances in neural recording microsystems," *Sensors*, vol. 11, pp. 4572–4597, 2011.
- [54] H. Noshahr, M. Nabavi, and M. Sawan, "Multi-channel neural recording implants: A review," *Sensors*, vol. 20, no. 3, 2020, Art. no. 904.
- [55] R. E. Gross and A. M. Lozano, "Advances in neurostimulation for movement disorders," *Neurological Res.*, vol. 22, no. 3, pp. 247–258, 2000.
- [56] A. L. Benabid, "Deep brain stimulation for Parkinson's disease," *Curr. Opin. Neurobiol.*, vol. 13, no. 6, pp. 696–706, 2003.
- [57] P. Limousin and I. Martínez-Torres, "Deep brain stimulation for Parkinson's disease," *Neurotherapeutics*, vol. 5, no. 2, pp. 309–319, 2008.
- [58] C. Wu and A. D. Sharan, "Neurostimulation for the treatment of epilepsy: A review of current surgical interventions," *Neuromodulation: Technol. Neural Interface*, vol. 16, no. 1, pp. 10–24, 2013.
- [59] W. J. Marks, "Deep brain stimulation for dystonia," *Curr. Treat. Options Neurol.*, vol. 7, no. 3, pp. 237–243, 2005.
- [60] J. L. Ostrem and P. A. Starr, "Treatment of dystonia with deep brain stimulation," *Neurotherapeutics*, vol. 5, no. 2, pp. 320–330, 2008.
- [61] M. L. Kringsbach, N. Jenkinson, S. L. Owen, and T. Z. Aziz, "Translational principles of deep brain stimulation," *Nature Rev. Neurosci.*, vol. 8, no. 8, pp. 623–635, 2007.
- [62] S. Vanneste and D. De Ridder, "Noninvasive and invasive neuromodulation for the treatment of tinnitus: An overview," *Neuromodulation, Technol. Neural Interface*, vol. 15, no. 4, pp. 350–360, 2012.
- [63] D. J. Hoare, P. Adjajian, and M. Sereda, "Electrical stimulation of the ear, head, cranial nerve, or cortex for the treatment of tinnitus: A scoping review," *Neural Plast.*, vol. 2016, Jun. 2016, Art. no. 5130503.
- [64] W. Xu et al., "Deep brain stimulation for Tourette's syndrome," *Transl. Neurodegener.*, vol. 9, no. 1, pp. 1–19, 2020.
- [65] N. Pedroarena-Leal and D. Ruge, "Toward a symptom-guided neurostimulation for Gilles de la Tourette syndrome," *Front. Psychiatry*, vol. 8, Feb. 2017, Art. no. 29.
- [66] X. Moisset, M. Lanteri-Minet, and D. Fontaine, "Neurostimulation methods in the treatment of chronic pain," *J. Neural Transmiss.*, vol. 127, no. 4, pp. 673–686, 2020.
- [67] M. Hofmeister et al., "Effectiveness of neurostimulation technologies for the management of chronic pain: A systematic review," *Neuromodulation, Technol. Neural Interface*, vol. 23, no. 2, pp. 150–157, 2020.
- [68] S. Hayek, R. Levy, and T. Deer, *Neurostimulation for the Treatment of Chronic Pain (Interventional and Neuromodulatory Techniques For Pain Management Series, vol. 1)*. Amsterdam, The Netherlands: Elsevier, 2012.
- [69] T. da Silva Freitas, B. A. de Monaco, and S. Golovac, *Neuromodulation Techniques for Pain Treatment: A Step-By-Step Guide to Interventional Procedures and Managing Complications*. New York, NY, USA: Springer, 2021.
- [70] Lambru and M. Lanteri-Minet, *Neuromodulation in Headache and Facial Pain Management: Principles, Rationale and Clinical Data*. New York, NY, USA: Springer, 2020.
- [71] L. B. Marangell, M. Martínez, R. A. Jurdi, and H. Zboyan, "Neurostimulation therapies in depression: A review of new modalities," *Acta Psychiatrica Scandinavica*, vol. 116, no. 3, pp. 174–181, 2007.
- [72] H. Akhtar, F. Bukhari, M. Nazir, M. N. Anwar, and A. Shahzad, "Therapeutic efficacy of neurostimulation for depression: Techniques, current modalities, and future challenges," *Neuro-Sci. Bull.*, vol. 32, no. 1, pp. 115–126, 2016.
- [73] D. Perrotta and R. L. Perri, "Mini-review: When neurostimulation joins cognitive-behavioral therapy. on the need of combining evidence-based treatments for addiction disorders," *Neurosci. Lett.*, vol. 777, 2022, Art. no. 136588.
- [74] A. Aleman, S. Enriquez-Geppert, H. Knegtering, and J. J. Dlabac-de Lange, "Moderate effects of noninvasive brain stimulation of the frontal cortex for improving negative symptoms in schizophrenia: Meta-analysis of controlled trials," *Neurosci. Biobehavioral Rev.*, vol. 89, pp. 111–118, 2018.
- [75] F. Rachid, "Neurostimulation techniques in the treatment of nicotine dependence: A review," *Amer. J. Addictions*, vol. 25, no. 6, pp. 436–451, 2016.
- [76] M. Jansen, J. G. Daams, M. W. Koeter, D. J. Veltman, W. Van Den Brink, and A. E. Goudriaan, "Effects of non-invasive neurostimulation on craving: A meta-analysis," *Neurosci. Biobehavioral Rev.*, vol. 37, no. 10, pp. 2472–2480, 2013.
- [77] R. C. Freire, C. Cabrera-Abreu, and R. Milev, "Neurostimulation in anxiety disorders, post-traumatic stress disorder, and obsessive-compulsive disorder," *Anxiety Disord.*, vol. 1191, pp. 331–346, Jan. 2020.
- [78] I. O. Bergfeld et al., "Invasive and non-invasive neurostimulation for OCD," *Neurobiol. Treat. OCD, Accelerating Prog.*, vol. 49, pp. 399–436, Feb. 7, 2021.
- [79] M. D. Johnson et al., "Neuromodulation for brain disorders: Challenges and opportunities," *IEEE Trans. Biomed. Eng.*, vol. 60, no. 3, pp. 610–624, Mar. 2013.
- [80] A. M. Sodagar, G. E. Perlin, Y. Yao, K. Najafi, and K. D. Wise, "An implantable 64-channel wireless microsystem for single-unit neural recording," *IEEE J. Solid-State Circuits*, vol. 44, no. 9, pp. 2591–2604, Sep. 2009.
- [81] Y. Jia et al., "A trimodal wireless implantable neural interface system-on-chip," *IEEE Trans. Biomed. Circuits Syst.*, vol. 14, no. 6, pp. 1207–1217, Dec. 2020.
- [82] T. Kaiju et al., "High spatiotemporal resolution ECoG recording of somatosensory evoked potentials with flexible micro-electrode arrays," *Front. Neural Circuits*, vol. 11, 2017, Art. no. 20.
- [83] A. Obaid et al., "Massively parallel microwire arrays integrated with CMOS chips for neural recording," *Sci. Adv.*, vol. 6, no. 12, 2020, Art. no. eaay2789.
- [84] A. Nurmikko, "Challenges for large-scale cortical interfaces," *Neuron*, vol. 108, no. 2, pp. 259–269, 2020.
- [85] T. Ativanichayaphong, J. W. He, C. E. Hagains, Y. B. Peng, and J. C. Chiao, "A combined wireless neural stimulating and recording system for study of pain processing," *J. Neurosci. Methods*, vol. 170, no. 1, pp. 25–34, 2008.
- [86] C. Zuo et al., "A digital wireless system for closed-loop inhibition of nociceptive signals," *J. Neural Eng.*, vol. 9, no. 5, 2012, Art. no. 056010.
- [87] A. Farajidavar, C. E. Hagains, Y. B. Peng, and J. C. Chiao, "A closed loop feedback system for automatic detection and inhibition of mechano-nociceptive neural activity," *IEEE Trans. Neural Syst. Rehabil. Eng.*, vol. 20, no. 4, pp. 478–487, Jul. 2012.
- [88] A. Farajidavar, S. M. Athar, C. E. Hagains, Y. B. Peng, and J. C. Chiao, "Detection of thermal pain in rodents through wireless electrocorticography," in *Proc. IEEE Annu. Int. Conf. Eng. Med. Biol. Soc.*, 2012, pp. 2535–2538.
- [89] A. Zhou et al., "A wireless and artifact-free 128-channel neuromodulation device for closed-loop stimulation and recording in non-human primates," *Nature Biomed. Eng.*, vol. 3, no. 1, pp. 15–26, 2019.
- [90] Y. Lin et al., "A 3.1–5.2 GHz, energy-efficient single antenna, cancellation-free, bitwise time-division duplex transceiver for high channel count optogenetic neural interface," *IEEE Trans. Biomed. Circuits Syst.*, vol. 16, no. 1, pp. 52–63, Feb. 2022.
- [91] A. Deshmukh et al., "Fully implantable neural recording and stimulation interfaces: Peripheral nerve interface applications," *J. Neurosci. Methods*, vol. 333, 2020, Art. no. 108562.
- [92] K. Guido and A. Kiourti, "Passive RF neural electrodes," in *Neural Interface Engineering*. New York, NY, USA: Springer, 2020, pp. 299–319.
- [93] S. Rao et al., "Miniature implantable and wearable on-body antennas: Towards the new era of wireless body-centric systems [antenna applications corner]," *IEEE Antennas Propag. Mag.*, vol. 56, no. 1, pp. 271–291, Feb. 2014.
- [94] H. N. Schwerdt, F. A. Miranda, and J. Chae, "Analysis of electromagnetic fields induced in operation of a wireless fully passive backscattering neurorecording microsystem in emulated human head tissue," *IEEE Trans. Microw. Theory Techn.*, vol. 61, no. 5, pp. 2170–2176, May 2013.
- [95] C. W. L. Lee, A. Kiourti, J. Chae, and J. L. Volakis, "A high-sensitivity fully passive neurosensing system for wireless brain signal monitoring," *IEEE Trans. Microw. Theory Techn.*, vol. 63, no. 6, pp. 2060–2068, Jun. 2015.

- [96] A. Kiourti, C. W. Lee, J. Chae, and J. L. Volakis, "A wireless fully passive neural recording device for unobtrusive neuropotential monitoring," *IEEE Trans. Biomed. Eng.*, vol. 63, no. 1, pp. 131–137, Jan. 2016.
- [97] W. Chen, C. W. Lee, A. Kiourti, and J. L. Volakis, "A multi-channel passive brain implant for wireless neuropotential monitoring," *IEEE J. Electromagn. RF Microw. Med. Biol.*, vol. 2, no. 4, pp. 262–269, Dec. 2018.
- [98] H. Cao et al., "An implantable, batteryless, and wireless capsule with integrated impedance and pH sensors for gastroesophageal reflux monitoring," *IEEE Trans. Biomed. Eng.*, vol. 59, no. 11, pp. 3131–3139, Nov. 2012.
- [99] P. Chen, S. Saati, R. Varma, M. S. Humayun, and Y. Tai, "Wireless intraocular pressure sensing using microfabricated minimally invasive flexible-coiled LC sensor implant," *J. Microelectromech. Syst.*, vol. 19, no. 4, pp. 721–734, 2010.
- [100] J. C. Chiou, Y. Huang, and G. Yeh, "A capacitor-based sensor and a contact lens sensing system for intraocular pressure monitoring," *J. Micromech. Microeng.*, vol. 26, no. 1, 2015, Art. no. 015001.
- [101] G. Yeh, T. Wu, S. Tsai, S. Hsu, and J. Chiou, "Toward a wireless contact lens sensor system with a micro-capacitor for intraocular pressure monitoring on in-vitro porcine eye," in *Proc. IEEE Sensors Conf.*, 2015, pp. 1–4.
- [102] J. Kim et al., "A soft and transparent contact lens for the wireless quantitative monitoring of intraocular pressure," *Nature Biomed. Eng.*, vol. 5, no. 7, pp. 772–782, 2021.
- [103] J. Zhang et al., "Smart soft contact lenses for continuous 24-hour monitoring of intraocular pressure in glaucoma care," *Nature Commun.*, vol. 13, no. 1, pp. 1–15, 2022.
- [104] C. Yang et al., "Intelligent wireless theranostic contact lens for electrical sensing and regulation of intraocular pressure," *Nature Commun.*, vol. 13, no. 1, pp. 1–15, 2022.
- [105] E. Y. Chow, A. L. Chlebowski, S. Chakraborty, W. J. Chappell, and P. P. Irazoqui, "Fully wireless implantable cardiovascular pressure monitor integrated with a medical stent," *IEEE Trans. Biomed. Eng.*, vol. 57, no. 6, pp. 1487–1496, Jun. 2010.
- [106] I. Pour-Ghaz, D. Hana, J. Raja, U. N. Ibebuogu, and R. N. Khouzam, "CardioMEMS: Where we are and where can we go?," *Ann. Transl. Med.*, vol. 7, no. 17, 2019, Art. no. 418.
- [107] M. A. Fonseca, M. G. Allen, J. Kroh, and J. White, "Flexible wireless passive pressure sensors for biomedical applications," in *Proc. Solid-State Sensor Actuator Microsyst. Workshop (Hilton Head)*, 2006, pp. 37–42.
- [108] A. Kotalczyk, J. F. Imberti, G. Y. Lip, and D. J. Wright, "Telemedical monitoring based on implantable devices—the evolution beyond the cardiomeems™ technology," *Curr. Heart Failure Rep.*, vol. 19, pp. 7–14, 2022.
- [109] S. J. Majerus, P. C. Fletter, M. S. Damaser, and S. L. Garverick, "Low-power wireless micromanometer system for acute and chronic bladder-pressure monitoring," *IEEE Trans. Biomed. Eng.*, vol. 58, no. 3, pp. 763–767, Mar. 2011.
- [110] Y. Zhong et al., "Development of an implantable wireless and batteryless bladder pressure monitor system for lower urinary tract dysfunction," *IEEE J. Transl. Eng. Health Med.*, vol. 8, 2019, Art. no. 2500107.
- [111] H. Y. Lee, B. Choi, S. Kim, S. J. Kim, W. J. Bae, and S. W. Kim, "Sensitivity-enhanced LC pressure sensor for wireless bladder pressure monitoring," *IEEE Sensors J.*, vol. 16, no. 12, pp. 4715–4724, Jun. 2016.
- [112] S. W. Siegel et al., "Long-term results of a multicenter study on sacral nerve stimulation for treatment of urinary urge incontinence, urgency-frequency, and retention," *Urology*, vol. 56, no. 6, pp. 87–91, 2000.
- [113] N. Y. Siddiqui, J. M. Wu, and C. L. Amundsen, "Efficacy and adverse events of sacral nerve stimulation for overactive bladder: A systematic review," *Neurourol. Urodyn.*, vol. 29, no. S1, pp. S18–S23, 2010.
- [114] A. A. Bhide, V. Tailor, R. Fernando, V. Khullar, and G. A. Digesu, "Posterior tibial nerve stimulation for overactive bladder—techniques and efficacy," *Int. Urogynecology J.*, vol. 31, no. 5, pp. 865–870, 2020.
- [115] R. C. Cantu, "Head injuries in sport," *Brit. J. Sports Med.*, vol. 30, no. 4, pp. 289–296, 1996.
- [116] N. Haider et al., "Intracranial pressure changes after mild traumatic brain injury: A systematic review," *Brain Inj.*, vol. 32, no. 7, pp. 809–815, 2018.
- [117] D. Shprecher, J. Schwalb, and R. Kurlan, "Normal pressure hydrocephalus: Diagnosis and treatment," *Curr. Neurol. Neurosci. Rep.*, vol. 8, no. 5, pp. 371–376, 2008.
- [118] K. T. Kahle, A. V. Kulkarni, D. D. Limbrick Jr., and B. C. Warf, "Hydrocephalus in children," *Lancet*, vol. 387, no. 10020, pp. 788–799, 2016.
- [119] U. Kawoos, M. Tofighi, R. Warty, F. A. Kralick, and A. Rosen, "In-vitro and in-vivo trans-scalp evaluation of an intracranial pressure implant at 2.4 GHz," *IEEE Trans. Microw. Theory Techn.*, vol. 56, no. 10, pp. 2356–2365, Oct. 2008.
- [120] X. Meng et al., "Dynamic evaluation of a digital wireless intracranial pressure sensor for the assessment of traumatic brain injury in a swine model," *IEEE Trans. Microw. Theory Techn.*, vol. 61, no. 1, pp. 316–325, Jan. 2013.
- [121] U. Kawoos, X. Meng, M. Tofighi, and A. Rosen, "Too much pressure: Wireless intracranial pressure monitoring and its application in traumatic brain injuries," *IEEE Microw. Mag.*, vol. 16, no. 2, pp. 39–53, Mar. 2015.
- [122] F. Morady, *Electrophysiologic Interventional Procedures and Surgery*. Philadelphia, PA, USA: Elsevier, 2012.
- [123] A. L. Sette et al., "Battery longevity of neurostimulators in Parkinson disease: A historic cohort study," *Brain Stimulation*, vol. 12, no. 4, pp. 851–857, 2019.
- [124] T. R. Deer et al., "Clinical longevity of 106,462 rechargeable and primary cell spinal cord stimulators: Real world study in the medicare population," *Neuromodulation, Technol. Neural Interface*, pp. 1–8, Jun. 9, 2022.
- [125] S. Atallah, B. Martin-Perez, D. Keller, J. Burke, and L. Hunter, "Natural-orifice transluminal endoscopic surgery," *J. Brit. Surg.*, vol. 102, no. 2, pp. e73–e92, 2015.
- [126] S. Rao and J. C. Chiao, "Body electric: Wireless power transfer for implant applications," *IEEE Microw. Mag.*, vol. 16, no. 2, pp. 54–64, Mar. 2015.
- [127] S. R. Khan, S. K. Pavuluri, G. Cummins, and M. P. Desmulliez, "Wireless power transfer techniques for implantable medical devices: A review," *Sensors*, vol. 20, no. 12, 2020, Art. no. 3487.
- [128] S. Yoo, J. Lee, H. Joo, S. Sunwoo, S. Kim, and D. Kim, "Wireless power transfer and telemetry for implantable bioelectronics," *Adv. Healthcare Mater.*, vol. 10, no. 17, 2021, Art. no. 2100614.
- [129] J. Parker and P. Single, "Power use in neurostimulators," in *Essential Neuromodulation*. Amsterdam, Netherlands: Elsevier, 2022, ch. 10, pp. 231–253.
- [130] S. Costandi et al., "Longevity and utilization cost of rechargeable and non-rechargeable spinal cord stimulation implants: A comparative study," *Pain Pract.*, vol. 20, no. 8, pp. 937–945, 2020.
- [131] C. Davies, C. Komoroski, and L. Roy, "Evaluation of an innovative spinal cord stimulator platform for the treatment of chronic pain," *Pain Manage.*, vol. 8, no. 3, pp. 167–174, 2018.
- [132] Manuel, *Precision Spectra Spinal Cord Stimulator System Information for Prescribers*. Boston Scientific Corporation, 2017, ISBN: 91008787-03.
- [133] Manual, *Nevro Patient Manual*. Nevro Corp., 2015. [Online]. Available: <https://nevro.com/English/us/patients/overview/default.aspx>
- [134] Manuel, *Algovita Spinal Cord Stimulation System Programmer Charger and Pocket Programmer*. Algostim, LLC, 2014. [Online]. Available: <https://fccid.io/2ABU84200/User-Manual/User-Manual-2334847>
- [135] R. F. Dallapiazza et al., "Considerations for patient and target selection in deep brain stimulation surgery for Parkinson's disease," in *Parkinson's Disease: Pathogenesis and Clinical Aspects*. Brisbane, QLD, Australia: Exon Publications, 2018, ch. 8, pp. 145–160.
- [136] Y. Zhou, C. Liu, and Y. Huang, "Wireless power transfer for implanted medical application: A review," *Energies*, vol. 13, no. 11, 2020, Art. no. 2837.
- [137] C. J. Yang, C. Chang, S. Lee, S. Chang, and L. Chiou, "Efficient four-coil wireless power transfer for deep brain stimulation," *IEEE Trans. Microw. Theory Techn.*, vol. 65, no. 7, pp. 2496–2507, Jul. 2017.
- [138] H. K. P. Feirabend, H. Choufoer, S. Ploeger, J. Holsheimer, and J. D. Van Gool, "Morphometry of human superficial dorsal and dorso-lateral column fibres: Significance to spinal cord stimulation," *Brain*, vol. 125, no. 5, pp. 1137–1149, 2002.
- [139] A. Howard III et al., "Intradural approach to selective stimulation in the spinal cord for treatment of intractable pain: Design principles and wireless protocol," *J. Appl. Phys.*, vol. 110, no. 4, 2011, Art. no. 044702.

- [140] D. K. Freeman and S. J. Byrnes, "Optimal frequency for wireless power transmission into the body: Efficiency versus received power," *IEEE Trans. Antennas Propag.*, vol. 67, no. 6, pp. 4073–4083, Jun. 2019.
- [141] J. S. Ho et al., "Wireless power transfer to deep-tissue microimplants," *Proc. Nat. Acad. Sci.*, vol. 111, no. 22, pp. 7974–7979, 2014.
- [142] M. Abdolrazzagli, R. Genov, and G. V. Eleftheriades, "Antenna array for wireless power transfer to deep-brain implants," in *Proc. IEEE Int. Symp. Antennas Propag. USNC-URSI Radio Sci. Meeting*, 2022, pp. 2018–2019.
- [143] M. Nguyen et al., "Wireless power transfer for autonomous wearable neurotransmitter sensors," *Sensors*, vol. 15, no. 9, pp. 24553–24572, 2015.
- [144] J. Charthad et al., "A mm-sized wireless implantable device for electrical stimulation of peripheral nerves," *IEEE Trans. Biomed. Circuits Syst.*, vol. 12, no. 2, pp. 257–270, Apr. 2018.
- [145] E. Loeb, C. J. Zamin, J. H. Schulman, and P. R. Troyk, "Injectable microstimulator for functional electrical stimulation," *Med. Biol. Eng. Comput.*, vol. 29, no. 6, pp. NS13–NS19, 1991.
- [146] R. Troyk, "Injectable electronic identification, monitoring, and stimulation systems," *Annu. Rev. Biomed. Eng.*, vol. 1, no. 1, pp. 177–209, 1999.
- [147] H.-M. Lee and M. Ghovanloo, "A power-efficient wireless capacitor charging system through an inductive link," *IEEE Trans. Circuits Syst. II, Exp. Briefs*, vol. 60, no. 10, pp. 707–711, Oct. 2013.
- [148] H. Lee, K. Y. Kwon, W. Li, and M. Ghovanloo, "A power-efficient switched-capacitor stimulating system for electrical/optical deep brain stimulation," *IEEE J. Solid-State Circuits*, vol. 50, no. 1, pp. 360–374, Jan. 2015.
- [149] Y. Lo et al., "22.2 A 176-channel 0.5 cm³ 0.7 g wireless implant for motor function recovery after spinal cord injury," in *Proc. IEEE Int. Solid-State Circuits Conf.*, 2016, pp. 382–383.
- [150] G. Shin et al., "Flexible near-field wireless optoelectronics as subdermal implants for broad applications in optogenetics," *Neuron*, vol. 93, no. 3, pp. 509–521, 2017.
- [151] M. K. Hosain, A. Z. Kouzani, M. F. Samad, and S. J. Tye, "A miniature energy harvesting rectenna for operating a head-mountable deep brain stimulation device," *IEEE Access*, vol. 3, pp. 223–234, 2015.
- [152] L. Montgomery et al., "Wirelessly powered, fully internal optogenetics for brain, spinal and peripheral circuits in mice," *Nature Methods*, vol. 12, no. 10, pp. 969–974, 2015.
- [153] A. Abdi and H. Aliakbarian, "A miniaturized UHF-band rectenna for power transmission to deep-body implantable devices," *IEEE J. Transl. Eng. Health Med.*, vol. 7, 2019, Art. no. 1900311.
- [154] S. Ding, S. Koulouridis, and L. Pichon, "Implantable wireless transmission rectenna system for biomedical wireless applications," *IEEE Access*, vol. 8, pp. 195551–195558, 2020.
- [155] S. Deb et al., "An endoscopic wireless gastrostimulator (with video)," *Gastrointestinal Endoscopy*, vol. 75, no. 2, pp. 411–415, 2012.
- [156] S. Deb et al., "Development of innovative techniques for the endoscopic implantation and securing of a novel, wireless, miniature gastrostimulator (with videos)," *Gastrointestinal Endoscopy*, vol. 76, no. 1, pp. 179–184, 2012.
- [157] S. Dubey and J. C. Chiao, "Implantable radio frequency powered gastric electrical stimulator," *IEEE J. Electromagn. RF Microw. Med. Biol.*, vol. 6, no. 3, pp. 340–347, Sep. 2022.
- [158] A. Basir and H. Yoo, "Efficient wireless power transfer system with a miniaturized quad-band implantable antenna for deep-body multi-tasking implants," *IEEE Trans. Microw. Theory Techn.*, vol. 68, no. 5, pp. 1943–1953, May 2020.
- [159] A. Iqbal, P. R. Sura, M. Al-Hasan, I. B. Mabrouk, and T. A. Denidni, "Wireless power transfer system for deep-implanted biomedical devices," *Sci. Rep.*, vol. 12, no. 1, pp. 1–13, 2022.
- [160] D. Weiland, W. Liu, and M. S. Humayun, "Retinal prosthesis," *Annu. Rev. Biomed. Eng.*, vol. 7, pp. 361–401, 2005.
- [161] K. Nowik, E. Langwińska-Wośko, P. Skopiński, K. E. Nowik, and J. P. Szaflik, "Bionic eye review-An update," *J. Clin. Neurosci.*, vol. 78, pp. 8–19, 2020.
- [162] S. Humayun, E. de Juan Jr, and G. Dagnelie, "The bionic eye: A quarter century of retinal prosthesis research and development," *Ophthalmology*, vol. 123, no. 10, pp. S89–S97, 2016.
- [163] Y. H. Luo and L. Da Cruz, "The Argus II retinal prosthesis system," *Prog. Retinal Eye Res.*, vol. 50, pp. 89–107, 2016.
- [164] K. Chen, Y. Lo, Z. Yang, J. D. Weiland, M. S. Humayun, and W. Liu, "A system verification platform for high-density epiretinal prostheses," *IEEE Trans. Biomed. Circuits Syst.*, vol. 7, no. 3, pp. 326–337, Jun. 2013.
- [165] C. Gong, D. Liu, Z. Miao, and M. Li, "A magnetic-balanced inductive link for the simultaneous uplink data and power telemetry," *Sensors*, vol. 17, no. 8, 2017, Art. no. 1768.
- [166] H. C. Stronks and G. Dagnelie, "The functional performance of the Argus II retinal prosthesis," *Expert Rev. Med. Devices*, vol. 11, no. 1, pp. 23–30, 2014.
- [167] V. Kaim, B. Kanaujia, S. Kumar, H. C. Choi, K. W. Kim, and K. Rambabu, "Electrically small circularly polarized UWB intraocular antenna system for retinal prosthesis," *IEEE Trans. Biomed. Eng.*, vol. 69, no. 11, pp. 3504–3515, Nov. 2022.
- [168] J. Kim, E. Cha, and J. Park, "Recent advances in smart contact lenses," *Adv. Mater. Technol.*, vol. 5, no. 1, 2020, Art. no. 1900728.
- [169] X. Ma et al., "Smart contact lenses for biosensing applications," *Adv. Intell. Syst.*, vol. 3, no. 5, 2021, Art. no. 2000263.
- [170] C. Song, G. Ben-Shlomo, and L. Que, "A multifunctional smart soft contact lens device enabled by nanopore thin film for glaucoma diagnostics and in situ drug delivery," *J. Microelectromech. Syst.*, vol. 28, no. 5, pp. 810–816, 2019.
- [171] H. Keum et al., "Wireless smart contact lens for diabetic diagnosis and therapy," *Sci. Adv.*, vol. 6, no. 17, 2020, Art. no. eaba3252.
- [172] N. Thomas, I. Lähdesmäki, and B. A. Parviz, "A contact lens with an integrated lactate sensor," *Sensors Actuators B, Chem.*, vol. 162, no. 1, pp. 128–134, 2012.
- [173] H. Song et al., "Wireless non-invasive monitoring of cholesterol using a smart contact lens," *Adv. Sci.*, vol. 9, no. 28, 2022, Art. no. 2203597.
- [174] Y. Ye et al., "Smart contact lens with dual-sensing platform for monitoring intraocular pressure and matrix metalloproteinase-9," *Adv. Sci.*, vol. 9, no. 12, 2022, Art. no. 2104738.
- [175] M. Donora, A. V. Quintero, H. De Smet, and I. Underwood, "Spatiotemporal electrochemical sensing in a smart contact lens," *Sensors Actuators B, Chem.*, vol. 303, 2020, Art. no. 127203.
- [176] A. Guzman-Arangué, B. Colligris, and J. Pintor, "Contact lenses: Promising devices for ocular drug delivery," *J. Ocular Pharmacol. Therapeutics*, vol. 29, no. 2, pp. 189–199, 2013.
- [177] Z. Duru, N. Duru, and D. M. Ulusoy, "Effects of senofilcon A and lotrafalcon B bandage contact lenses on epithelial healing and pain management after bilateral photorefractive keratectomy," *Contact Lens Anterior Eye*, vol. 43, no. 2, pp. 169–172, 2020.
- [178] P. Chaudhari, V. M. Ghate, and S. A. Lewis, "Next-generation contact lenses: Towards bioresponsive drug delivery and smart technologies in ocular therapeutics," *Eur. J. Pharmacology Biopharmaceutics*, vol. 161, pp. 80–99, 2021.
- [179] J. Chiou, S. Hsu, Y. Huang, G. Yeh, W. Liou, and C. Kuei, "A wirelessly powered smart contact lens with reconfigurable wide range and tunable sensitivity sensor readout circuitry," *Sensors*, vol. 17, no. 1, 2017, Art. no. 108.
- [180] E. Y. Chow, A. L. Chlebowski, and P. P. Irazoqui, "A miniature-implantable RF-wireless active glaucoma intraocular pressure monitor," *IEEE Trans. Biomed. Circuits Syst.*, vol. 4, no. 6, pp. 340–349, Dec. 2010.
- [181] M. Leonardi, E. M. Pitchon, A. Bertsch, P. Renaud, and A. Mermoud, "Wireless contact lens sensor for intraocular pressure monitoring: Assessment on enucleated pig eyes," *Acta Ophthalmologica*, vol. 87, no. 4, pp. 433–437, 2009.
- [182] Y. Kim, J. Maeng, and P. P. Irazoqui, "Eyeglasses-powered, contact lens-like platform with high power transfer efficiency," *Biomed. Microdevices*, vol. 17, no. 4, pp. 1–9, 2015.
- [183] H. Mirzajani, F. Mirlou, E. Istif, R. Singh, and L. Beker, "Powering smart contact lenses for continuous health monitoring: Recent advancements and future challenges," *Biosensors Bioelectron.*, vol. 197, 2022, Art. no. 113761.
- [184] S. Lu et al., "Effects of high peak power microwaves on the retina of the rhesus monkey," *Bioelectromagnetics*, vol. 21, no. 6, pp. 439–454, 2000.
- [185] S. DeSaSouza, *Cochlear Implants in Clinical Use Worldwide Today*. Singapore: Springer, 2022.

- [186] J. K. Niparko, *Cochlear Implants: Principles & Practices*. Philadelphia, PA, USA: Lippincott Williams & Wilkins, 2009.
- [187] I. Hochmair et al., "MED-EL cochlear implants: State of the art and a glimpse into the future," *Trends Amplification*, vol. 10, no. 4, pp. 201–219, 2006.
- [188] W. Sun and H. Yang, "Research of wireless power transmitter sub-system based on Qi specification," *IOP Conf. Ser. Earth Environ. Sci.*, vol. 440, 2020, Art. no. 032029.
- [189] S. Hong et al., "Cochlear implant wireless power transfer system design for high efficiency and link gain stability using a proposed stagger tuning method," in *Proc. IEEE Wireless Power Transfer Conf.*, 2020, pp. 26–29.
- [190] J. C. Lin, "Noninvasive microwave measurement of respiration," *Proc. IEEE*, vol. 63, no. 10, Oct. 1975, Art. no. 1530.
- [191] K. Chen, D. Misra, H. Wang, H. Chuang, and E. Postow, "An X-band microwave life-detection system," *IEEE Trans. Biomed. Eng.*, vol. BME-33, no. 7, pp. 697–701, Jul. 1986.
- [192] H. Chuang, Y. F. Chen, and K. Chen, "Automatic clutter-canceller for microwave life-detection systems," *IEEE Trans. Instrum. Meas.*, vol. 40, no. 4, pp. 747–750, Aug. 1991.
- [193] A. D. Droitcour, O. Boric-Lubecke, V. M. Lubecke, and J. Lin, "0.25 μm CMOS and BiCMOS single-chip direct-conversion Doppler radars for remote sensing of vital signs," in *Proc. IEEE Int. Solid-State Circuits Conf.*, 2002, pp. 348–349.
- [194] A. D. Droitcour, O. Boric-Lubecke, V. M. Lubecke, J. Lin, and G. T. Kovacs, "Range correlation effect on ISM band I/Q CMOS radar for non-contact vital signs sensing," in *Proc. IEEE MTT-S Int. Microw. Symp.*, 2003, pp. 1945–1948.
- [195] A. D. Droitcour, O. Boric-Lubecke, V. M. Lubecke, J. Lin, and G. T. Kovacs, "Range correlation and I/Q performance benefits in single-chip silicon Doppler radars for noncontact cardiopulmonary monitoring," *IEEE Trans. Microw. Theory Techn.*, vol. 52, no. 3, pp. 838–848, Mar. 2004.
- [196] S. M. M. Islam, O. Boric-Lubecke, Y. Zheng, and V. M. Lubecke, "Radar-based non-contact continuous identity authentication," *Remote Sens.*, vol. 12, no. 14, 2020, Art. no. 2279.
- [197] M. Baboli, A. Singh, B. Soll, O. Boric-Lubecke, and V. M. Lubecke, "Good night: Sleep monitoring using a physiological radar monitoring system integrated with a polysomnography system," *IEEE Microw. Mag.*, vol. 16, no. 6, pp. 34–41, Jul. 2015.
- [198] A. D. Droitcour et al., "Non-contact respiratory rate measurement validation for hospitalized patients," in *Proc. Annu. Int. Conf. IEEE Eng. Med. Biol. Soc.*, 2009, pp. 4812–4815.
- [199] W. Massagram, V. M. Lubecke, A. Høst-Madsen, and O. Boric-Lubecke, "Assessment of heart rate variability and respiratory sinus arrhythmia via Doppler radar," *IEEE Trans. Microw. Theory Techn.*, vol. 57, no. 10, pp. 2542–2549, Oct. 2009.
- [200] B. Park, O. Boric-Lubecke, and V. M. Lubecke, "Arctangent demodulation with DC offset compensation in quadrature Doppler radar receiver systems," *IEEE Trans. Microw. Theory Techn.*, vol. 55, no. 5, pp. 1073–1079, May 2007.
- [201] C. Li, X. Yu, C. Lee, D. Li, L. Ran, and J. Lin, "High-sensitivity software-configurable 5.8-GHz radar sensor receiver chip in 0.13- μm CMOS for noncontact vital sign detection," *IEEE Trans. Microw. Theory Techn.*, vol. 58, no. 5, pp. 1410–1419, May 2010.
- [202] T. J. Kao, Y. Yan, T. Shen, A. Y. Chen, and J. Lin, "Design and analysis of a 60-GHz CMOS Doppler micro-radar system-in-package for vital-sign and vibration detection," *IEEE Trans. Microw. Theory Techn.*, vol. 61, no. 4, pp. 1649–1659, Apr. 2013.
- [203] C. Li and J. Lin, "Random body movement cancellation in Doppler radar vital sign detection," *IEEE Trans. Microw. Theory Techn.*, vol. 56, no. 12, pp. 3143–3152, Dec. 2008.
- [204] C. Li, Y. Xiao, and J. Lin, "Experiment and spectral analysis of a low-power Ka-band heartbeat detector measuring from four sides of a human body," *IEEE Trans. Microw. Theory Techn.*, vol. 54, no. 12, pp. 4464–4471, Dec. 2006.
- [205] Y. Xiao, J. Lin, O. Boric-Lubecke, and M. Lubecke, "Frequency-tuning technique for remote detection of heartbeat and respiration using low-power double-sideband transmission in the Ka-band," *IEEE Trans. Microw. Theory Techn.*, vol. 54, no. 5, pp. 2023–2032, May 2006.
- [206] C. Ding et al., "Inattentive driving behavior detection based on portable FMCW radar," *IEEE Trans. Microw. Theory Techn.*, vol. 67, no. 10, pp. 4031–4041, Oct. 2019.
- [207] Y. Li, Z. Peng, R. Pal, and C. Li, "Potential active shooter detection based on radar micro-Doppler and range-Doppler analysis using artificial neural network," *IEEE Sensors J.*, vol. 19, no. 3, pp. 1052–1063, Feb. 2019.
- [208] D. Tang, V. G. R. Varela, D. V. Q. Rodrigues, D. Rodriguez, and C. Li, "A Wi-Fi frequency band passive biomedical Doppler radar sensor," *IEEE Trans. Microw. Theory Techn.*, early access, Aug., 2022, doi: [10.1109/TMTT.2022.3193408](https://doi.org/10.1109/TMTT.2022.3193408).
- [209] G. Wang, C. Gu, T. Inoue, and C. Li, "A hybrid FMCW-interferometry radar for indoor precise positioning and versatile life activity monitoring," *IEEE Trans. Microw. Theory Techn.*, vol. 62, no. 11, pp. 2812–2822, Nov. 2014.
- [210] Y. Li, C. Gu, and J. Mao, "4-D gesture sensing using reconfigurable virtual array based on a 60-GHz FMCW MIMO radar sensor," *IEEE Trans. Microw. Theory Techn.*, vol. 70, no. 7, 3652–3665, Jul. 2022.
- [211] C. Gu, J. Wang, and J. Lien, "Motion sensing using radar: Gesture interaction and beyond," *IEEE Microw. Mag.*, vol. 20, no. 8, pp. 44–57, Aug. 2019.
- [212] S. Dong, Y. Li, J. Lu, Z. Zhang, C. Gu, and J. Mao, "Accurate detection of Doppler cardiograms with a parameterized respiratory filter technique using a K-band radar sensor," *IEEE Trans. Microw. Theory Techn.*, early access, Jun. 24, 2022, doi: [10.1109/TMTT.2022.3184019](https://doi.org/10.1109/TMTT.2022.3184019).
- [213] S. Dong, L. Wen, Z. Zhang, C. Gu, and J. Mao, "Contactless measurement of human systolic time intervals based on Doppler cardiograms in clinical environment," *IEEE Microw. Wireless Compon. Lett.*, vol. 32, no. 6, pp. 796–799, Jun. 2022.
- [214] L. Wen, S. Dong, Z. Zhang, C. Gu, and J. Mao, "Noninvasive continuous blood pressure monitoring based on wearable radar sensor with preliminary clinical validation," in *Proc. IEEE MTT-S Int. Microw. Symp.*, 2022, pp. 707–710.
- [215] F. K. Wang, T. Horng, K. Peng, J. Jau, J. Li, and C. Chen, "Detection of concealed individuals based on their vital signs by using a see-through-wall imaging system with a self-injection-locked radar," *IEEE Trans. Microw. Theory Techn.*, vol. 61, no. 1, pp. 696–704, Jan. 2013.
- [216] F. K. Wang, T. Horng, K. Peng, J. Jau, J. Li, and C. Chen, "Single-antenna Doppler radars using self and mutual injection locking for vital sign detection with random body movement cancellation," *IEEE Trans. Microw. Theory Techn.*, vol. 59, no. 12, pp. 3577–3587, Dec. 2011.
- [217] W. Su, M. Tang, R. El Arif, T. Horng, and F. Wang, "Stepped-frequency continuous-wave radar with self-injection-locking technology for monitoring multiple human vital signs," *IEEE Trans. Microw. Theory Techn.*, vol. 67, no. 12, pp. 5396–5405, Dec. 2019.
- [218] N. T. P. Nguyen, P. Lyu, M. H. Lin, C. Chang, and S. Chang, "A short-time autocorrelation method for noncontact detection of heart rate variability using CW Doppler radar," in *Proc. IEEE MTT-S Int. Microw. Biomed. Conf.*, 2019, pp. 1–4.
- [219] C. Chang, R. Lee, and T. Shih, "Design of a beam switching/steering butler matrix for phased array system," *IEEE Trans. Antennas Propag.*, vol. 58, no. 2, pp. 367–374, Feb. 2010.
- [220] Y. Hsieh, C. Chang, and S. Chang, "Designs of deformed butler matrix in 0.18 μm -CMOS for array beamforming," in *Proc. IEEE Asia-Pacific Conf. Appl. Electromagnetics*, 2019, pp. 1–4.
- [221] Y. Liu, M. Lin, and C. Chang, "A V-band nine-state CMOS-MEMS phase shifter MMIC," in *Proc. IEEE 22nd Topical Meeting Silicon Monolithic Integr. Circuits RF Syst.*, 2022, pp. 88–90.
- [222] Y. Dong, C. Wu, and T. Itoh, "Miniaturised multi-band substrate integrated waveguide filters using complementary split-ring resonators," *IET Microw. Antennas Propag.*, vol. 6, no. 6, pp. 611–620, 2012.
- [223] C. Lu, Y. Yuan, C. Tseng, and C. M. Wu, "Multi-target continuous-wave vital sign radar using 24 GHz metamaterial leaky wave antennas," in *Proc. IEEE MTT-S Int. Microw. Biomed. Conf.*, 2019, pp. 1–4.
- [224] Y. Yuan and C. M. Wu, "Super-regenerative oscillator integrated metamaterial leaky wave antenna for multi-target vital sign and motion detection," *IEEE J. Electromagn. RF Microw. Med. Biol.*, vol. 6, no. 2, pp. 238–245, Jun. 2022.
- [225] C. Tseng and C. Chao, "Noncontact vital-sign radar sensor using metamaterial-based scanning leaky-wave antenna," in *Proc. IEEE MTT-S Int. Microw. Symp.*, 2016, pp. 1–3.

- [226] C. Tseng, J. Huang, L. Yu, and C. Chang, "A cost-effective wearable vital-sign sensor with self-oscillating active antenna based on envelope detection technique," in *Proc. IEEE MTT-S Int. Microw. Symp.*, 2017, pp. 1222–1224.
- [227] C. Tseng and Y. Lin, "24-GHz self-injection-locked vital-sign radar sensor with CMOS injection-locked frequency divider based on push-push oscillator topology," *IEEE Microw. Wireless Compon. Lett.*, vol. 28, no. 11, pp. 1053–1055, Nov. 2018.
- [228] M. Nosrati and N. Tavassolian, "High-accuracy heart rate variability monitoring using Doppler radar based on Gaussian pulse train modeling and FTPR algorithm," *IEEE Trans. Microw. Theory Techn.*, vol. 66, no. 1, pp. 556–567, Jan. 2018.
- [229] M. Nosrati, S. Shahsavari, S. Lee, H. Wang, and N. Tavassolian, "A concurrent dual-beam phased-array Doppler radar using MIMO beamforming techniques for short-range vital-signs monitoring," *IEEE Trans. Antennas Propag.*, vol. 67, no. 4, pp. 2390–2404, Apr. 2019.
- [230] M. Nosrati and N. Tavassolian, "Accurate Doppler radar-based cardiopulmonary sensing using chest-wall acceleration," *IEEE J. Electromagn. RF Microw. Med. Biol.*, vol. 3, no. 1, pp. 41–47, Mar. 2019.
- [231] M. Nosrati and N. Tavassolian, "Effects of antenna characteristics on the performance of heart rate monitoring radar systems," *IEEE Trans. Antennas Propag.*, vol. 65, no. 6, pp. 3296–3301, Jun. 2017.
- [232] C. Ding, L. Zhang, H. Chen, H. Hong, X. Zhu, and C. Li, "Human motion recognition with spatial-temporal-convLSTM network using dynamic range-doppler frames based on portable FMCW radar," *IEEE Trans. Microw. Theory Techn.*, vol. 70, no. 11, pp. 5029–5038, Nov. 2022.
- [233] H. Zhao et al., "A noncontact breathing disorder recognition system using 2.4-GHz digital-IF Doppler radar," *IEEE J. Biomed. Health Inform.*, vol. 23, no. 1, pp. 208–217, Jan. 2019.
- [234] H. Hong et al., "Microwave sensing and sleep: Noncontact sleep-monitoring technology with microwave biomedical radar," *IEEE Microw. Mag.*, vol. 20, no. 8, pp. 18–29, Aug. 2019.
- [235] H. Hong, L. Zhang, C. Gu, Y. Li, G. Zhou, and X. Zhu, "Noncontact sleep stage estimation using a CW Doppler radar," *IEEE J. Emerg. Sel. Topics Circuits Syst.*, vol. 8, no. 2, pp. 260–270, Jun. 2018.
- [236] C. Ding et al., "Continuous human motion recognition with a dynamic range-Doppler trajectory method based on FMCW radar," *IEEE Trans. Geosci. Remote Sens.*, vol. 57, no. 9, pp. 6821–6831, Sep. 2019.
- [237] Z. Peng et al., "A portable FMCW interferometry radar with programmable low-IF architecture for localization, ISAR imaging, and vital sign tracking," *IEEE Trans. Microw. Theory Techn.*, vol. 65, no. 4, pp. 1334–1344, Apr. 2017.
- [238] G. Wang, J. Muñoz-Ferreras, C. Gu, C. Li, and R. Gomez-García, "Application of linear-frequency-modulated continuous-wave (LFMCW) radars for tracking of vital signs," *IEEE Trans. Microw. Theory Techn.*, vol. 62, no. 6, pp. 1387–1399, Jun. 2014.
- [239] Z. Peng, C. Li, J. Muñoz-Ferreras, and R. Gómez-García, "An FMCW radar sensor for human gesture recognition in the presence of multiple targets," in *Proc. IEEE 1st MTT-S Int. Microw. Biomed. Conf.*, 2017, pp. 1–3.
- [240] J.-M. Muñoz-Ferreras, J. Wang, Z. Peng, C. Li, and R. Gómez-García, "FMCW-radar-based vital-sign monitoring of multiple patients," in *Proc. IEEE MTT-S Int. Microw. Biomed. Conf.*, 2019, pp. 1–3.
- [241] J.-M. Muñoz-Ferreras, Z. Peng, R. Gómez-García, and C. Li, "Random body movement mitigation for FMCW-radar-based vital-sign monitoring," in *Proc. IEEE Topical Conf. Biomed. Wireless Technol. Netw. Sens. Syst.*, 2016, pp. 22–24.
- [242] M. Mercuri et al., "Analysis of an indoor biomedical radar-based system for health monitoring," *IEEE Trans. Microw. Theory Techn.*, vol. 61, no. 5, pp. 2061–2068, May 2013.
- [243] P. J. Soh, G. A. Vandenbosch, M. Mercuri, and D. M. Schreurs, "Wearable wireless health monitoring: Current developments, challenges, and future trends," *IEEE Microw. Mag.*, vol. 16, no. 4, pp. 55–70, May 2015.
- [244] M. Mercuri, D. Schreurs, and P. Leroux, "SFCW microwave radar for in-door fall detection," in *Proc. IEEE Topical Conf. Biomed. Wireless Technol. Netw. Sens. Syst.*, 2012, pp. 53–56.
- [245] P. Karsmakers, T. Croonenborghs, M. Mercuri, D. Schreurs, and P. Leroux, "Automatic in-door fall detection based on microwave radar measurements," in *Proc. IEEE 9th Eur. Radar Conf.*, 2012, pp. 202–205.
- [246] C. Garripoli et al., "Embedded DSP-based telehealth radar system for remote in-door fall detection," *IEEE J. Biomed. Health Inform.*, vol. 19, no. 1, pp. 92–101, Jan. 2015.
- [247] T. K. V. Dai, Y. Yu, P. Theilmann, A. E. Fathy, and O. Kilic, "Remote vital sign monitoring with reduced random body swaying motion using heartbeat template and wavelet transform based on constellation diagrams," *IEEE J. Electromagn. RF Microw. Med. Biol.*, vol. 6, no. 3, pp. 429–436, Sep. 2022.
- [248] C. J. Bauder, A. Moadi, M. Joshi, and A. E. Fathy, "Multi-subject heart rate estimation and real-time tracking using a mmWave radar and trace carving algorithm," in *Proc. IEEE MTT-S Int. Microw. Symp.*, 2022, pp. 955–958.
- [249] A. Moadi, M. Joshi, O. Kilic, and A. E. Fathy, "Low cost IR-UWB radar for multisubject non-contact vital sign detection," in *Proc. IEEE Int. Symp. Antennas Propag. USNC-URSI Radio Sci. Meeting*, 2021, pp. 135–136.
- [250] V. M. Lubecke, O. Boric-Lubecke, A. Host-Madsen, and A. E. Fathy, "Through-the-wall radar life detection and monitoring," in *Proc. IEEE MTT-S Int. Microw. Symp.*, 2007, pp. 769–772.
- [251] L. Ren et al., "Short-time state-space method for micro-Doppler identification of walking subject using UWB impulse Doppler radar," *IEEE Trans. Microw. Theory Techn.*, vol. 66, no. 7, pp. 3521–3534, Jul. 2018.
- [252] A. Orth, P. Kwiatkowski, and N. Pohl, "A radar-based hand-held guidance aid for the visually impaired," in *Proc. IEEE German Microw. Conf.*, 2020, pp. 180–183.
- [253] S. Wang et al., "A novel ultra-wideband 80 GHz FMCW radar system for contactless monitoring of vital signs," in *Proc. IEEE 37th Annu. Int. Conf. Eng. Med. Biol. Soc.*, 2015, pp. 4978–4981.
- [254] Q. Lv et al., "High dynamic-range motion imaging based on linearized Doppler radar sensor," *IEEE Trans. Microw. Theory Techn.*, vol. 62, no. 9, pp. 1837–1846, Sep. 2014.
- [255] J. Wang, X. Wang, L. Chen, J. Huangfu, C. Li, and L. Ran, "Non-contact distance and amplitude-independent vibration measurement based on an extended DACM algorithm," *IEEE Trans. Instrum. Meas.*, vol. 63, no. 1, pp. 145–153, Jan. 2014.
- [256] A. Schellenberger, K. Shi, F. Michler, F. Lurz, R. Weigel, and A. Koelpin, "Continuous in-bed monitoring of vital signs using a multi radar setup for freely moving patients," *Sensors*, vol. 20, no. 20, 2020, Art. no. 5827.
- [257] K. Shi et al., "Contactless analysis of heart rate variability during cold pressor test using radar interferometry and bidirectional LSTM networks," *Sci. Rep.*, vol. 11, no. 1, pp. 1–13, 2021.
- [258] F. Michler et al., "On the impact of system nonlinearities in continuous-wave radar systems for vital parameter sensing," in *Proc. IEEE Topical Conf. Wireless Sensors Sensor Netw.*, 2020, pp. 13–15.
- [259] F. Michler et al., "Pulse wave velocity detection using a 24 GHz six-port based Doppler radar," in *Proc. IEEE Radio Wireless Symp.*, 2019, pp. 1–3.
- [260] E. Cardillo, C. Li, and A. Caddemi, "Empowering blind people mobility: A millimeter-wave radar cane," in *Proc. IEEE Int. Workshop Metrology Ind. 4.0 IoT*, 2020, pp. 213–217.
- [261] E. Cardillo, C. Li, and A. Caddemi, "Millimeter-wave radar cane: A blind people aid with moving human recognition capabilities," *IEEE J. Electromagn. RF Microw. Med. Biol.*, vol. 6, no. 2, pp. 204–211, Jun. 2022.
- [262] E. Cardillo, C. Li, and A. Caddemi, "Vital sign detection and radar self-motion cancellation through clutter identification," *IEEE Trans. Microw. Theory Techn.*, vol. 69, no. 3, pp. 1932–1942, Mar. 2021.
- [263] E. Cardillo, G. Sapienza, C. Li, and A. Caddemi, "Head motion and eyes blinking detection: A mm-wave radar for assisting people with neurodegenerative disorders," in *Proc. IEEE 50th Eur. Microw. Conf.*, 2021, pp. 925–928.
- [264] J. Park et al., "Noncontact RF vital sign sensor for continuous monitoring of driver status," *IEEE Trans. Biomed. Circuits Syst.*, vol. 13, no. 3, pp. 493–502, Jun. 2019.
- [265] D. P. Fairchild and R. M. Narayanan, "Classification of human motions using empirical mode decomposition of human micro-Doppler signatures," *IET Radar Sonar Navigation*, vol. 8, no. 5, pp. 425–434, 2014.
- [266] M. Narayanan and M. Zenaldin, "Radar micro-Doppler signatures of various human activities," *IET Radar Sonar Navigation*, vol. 9, no. 9, pp. 1205–1215, 2015.

- [267] B. Jokanović and M. Amin, "Fall detection using deep learning in range-Doppler radars," *IEEE Trans. Aerosp. Electron. Syst.*, vol. 54, no. 1, pp. 180–189, Feb. 2018.
- [268] M. G. Amin, Y. D. Zhang, F. Ahmad, and K. D. Ho, "Radar signal processing for elderly fall detection: The future for in-home monitoring," *IEEE Signal Process. Mag.*, vol. 33, no. 2, pp. 71–80, Mar. 2016.
- [269] J. Le Kernec et al., "Radar signal processing for sensing in assisted living: The challenges associated with real-time implementation of emerging algorithms," *IEEE Signal Process. Mag.*, vol. 36, no. 4, pp. 29–41, Jul. 2019.
- [270] A. Shrestha, H. Li, J. Le Kernec, and F. Fioranelli, "Continuous human activity classification from FMCW radar with bi-LSTM networks," *IEEE Sensors J.*, vol. 20, no. 22, pp. 13607–13619, Nov. 2020.
- [271] S. Pisa, E. Pittella, and E. Piuze, "A survey of radar systems for medical applications," *IEEE Aerosp. Electron. Syst. Mag.*, vol. 31, no. 11, pp. 64–81, Nov. 2016.
- [272] P. Bernardi, R. Cicchetti, S. Pisa, E. Pittella, E. Piuze, and O. Testa, "Design, realization, and test of a UWB radar sensor for breath activity monitoring," *IEEE Sensors J.*, vol. 14, no. 2, pp. 584–596, Feb. 2014.
- [273] G. Sacco, E. Piuze, E. Pittella, and S. Pisa, "An FMCW radar for localization and vital signs measurement for different chest orientations," *Sensors*, vol. 20, no. 12, 2020, Art. no. 3489.
- [274] D. Zito et al., "SoC CMOS UWB pulse radar sensor for contactless respiratory rate monitoring," *IEEE Trans. Biomed. Circuits Syst.*, vol. 5, no. 6, pp. 503–510, Dec. 2011.
- [275] D. Zito et al., "Wearable system-on-a-chip UWB radar for health care and its application to the safety improvement of emergency operators," in *Proc. IEEE 29th Annu. Int. Conf. Eng. Med. Biol. Soc.*, 2007, pp. 2651–2654.
- [276] M. Mercuri, Y. Liu, I. Lorato, T. Torfs, A. Bourdoux, and C. Van Hoof, "Frequency-tracking CW Doppler radar solving small-angle approximation and null point issues in non-contact vital signs monitoring," *IEEE Trans. Biomed. Circuits Syst.*, vol. 11, no. 3, pp. 671–680, Jun. 2017.
- [277] M. Mercuri et al., "A direct phase-tracking Doppler radar using wavelet independent component analysis for non-contact respiratory and heart rate monitoring," *IEEE Trans. Biomed. Circuits Syst.*, vol. 12, no. 3, pp. 632–643, Jun. 2018.
- [278] M. Mercuri, I. Lorato, Y. Liu, F. Wieringa, C. V. Hoof, and T. Torfs, "Vital-sign monitoring and spatial tracking of multiple people using a contactless radar-based sensor," *Nature Electron.*, vol. 2, no. 6, pp. 252–262, 2019.
- [279] M. Mercuri et al., "2-D localization, angular separation and vital signs monitoring using a SISO FMCW radar for smart long-term health monitoring environments," *IEEE Internet Things J.*, vol. 8, no. 14, pp. 11065–11077, Jul. 2021.
- [280] J. Bernstein, "Untersuchungen zur thermodynamik der bioelektrischen ströme," *Archiv Für Die Gesamte Physiologie Des Menschen Und Der Tiere*, vol. 92, no. 10, pp. 521–562, 1902.
- [281] H. Hertz, *Electric Waves: Being Researches On the Propagation of Electric Action With Finite Velocity Through Space*. Mineola, NY, USA: Dover Publications, 1893.
- [282] R. Höber, "Eine methode, die elektrische leitfähigkeit im innern von zellen zu messen," *Pflüger's Archiv Für Die Gesamte Physiologie Des Menschen Und Der Tiere*, vol. 133, no. 4, pp. 237–253, 1910.
- [283] M. Philippson, "Les lois de la résistance électrique des tissus vivants," *Bulletins De L'Académie Royale De Belg.*, vol. 7, pp. 387–403, 1921.
- [284] H. Fricke, "The electric capacity of suspensions of red corpuscles of a dog," *Phys. Rev.*, vol. 26, no. 5, 1925, Art. no. 682.
- [285] J. C. M. Hwang, "Label-free noninvasive cell characterization: A methodology using broadband impedance spectroscopy," *IEEE Microw. Mag.*, vol. 22, no. 5, pp. 78–87, May 2021.
- [286] R. Foster and P. Herman, "Schwan: A scientist and pioneer in biomedical engineering," Departmental Papers (BE) Dept. Bioeng. Univ. Pennsylvania, vol. 4, pp. 1–27, Aug. 2002.
- [287] H. P. Schwan, "Electrical properties of tissue and cell suspensions," in *Advances in Biological and Medical Physics*. Amsterdam, The Netherlands: Elsevier, 1957, pp. 147–209.
- [288] H. Morgan, T. Sun, D. Holmes, S. Gawad, and N. G. Green, "Single cell dielectric spectroscopy," *J. Phys. D, Appl. Phys.*, vol. 40, no. 1, 2006, Art. no. 61.
- [289] P. Mehrotra, B. Chatterjee, and S. Sen, "EM-wave biosensors: A review of RF, microwave, mm-wave and optical sensing," *Sensors*, vol. 19, no. 5, 2019, Art. no. 1013.
- [290] L. Dai et al., "Microfluidics-based microwave sensor," *Sensors Actuators A, Phys.*, vol. 309, 2020, Art. no. 111910.
- [291] S. Ahmed, K. Sung-Hwan, J. Y. Park, and S. Lim, "Microfluidic biosensor based on microwave substrate-integrated waveguide cavity resonator," *J. Sensors*, vol. 2018, 2018, Art. no. 1324145.
- [292] D. Dubuc et al., "Microwave-based biosensor for on-chip biological cell analysis," *Analog Integr. Circuits Signal Process.*, vol. 77, no. 2, pp. 135–142, 2013.
- [293] X. Bao et al., "Broadband dielectric spectroscopy of cell cultures," *IEEE Trans. Microw. Theory Techn.*, vol. 66, no. 12, pp. 5750–5759, Dec. 2018.
- [294] Y. Ning et al., "Broadband electrical detection of individual biological cells," *IEEE Trans. Microw. Theory Techn.*, vol. 62, no. 9, pp. 1905–1911, Sep. 2014.
- [295] K. Grenier et al., "Recent advances in microwave-based dielectric spectroscopy at the cellular level for cancer investigations," *IEEE Trans. Microw. Theory Techn.*, vol. 61, no. 5, pp. 2023–2030, May 2013.
- [296] F. Artis et al., "Microwaving biological cells: Intracellular analysis with microwave dielectric spectroscopy," *IEEE Microw. Mag.*, vol. 16, no. 4, pp. 87–96, May 2015.
- [297] T. Chen, F. Artis, D. Dubuc, J. J. Fournie, M. Poupot, and K. Grenier, "Microwave biosensor dedicated to the dielectric spectroscopy of a single alive biological cell in its culture medium," in *Proc. IEEE MTT-S Int. Microw. Symp.*, 2013, pp. 1–4.
- [298] C. Palego et al., "Broadband microchamber for electrical detection of live and dead biological cells," in *Proc. IEEE MTT-S Int. Microw. Symp.*, 2013, pp. 1–3.
- [299] H. Li et al., "Differentiation of live and heat-killed E. coli by microwave impedance spectroscopy," *Sensors Actuators B, Chem.*, vol. 255, pp. 1614–1622, 2018.
- [300] X. Du, C. Ladegard, X. Ma, X. Cheng, and J. C. Hwang, "Broadband electrical sensing of nucleus size in a live cell from 900 Hz to 40 GHz," in *Proc. IEEE MTT-S Int. Microw. Biomed. Conf.*, 2020, pp. 1–4.
- [301] X. Du, C. Ferguson, X. Ma, X. Cheng, and J. C. Hwang, "Ultra-wideband impedance spectroscopy of the nucleus in a live cell," *IEEE J. Electromagn. RF Microw. Med. Biol.*, vol. 6, no. 2, pp. 267–272, Jun. 2022.
- [302] A. Tamra, D. Dubuc, M. Rols, and K. Grenier, "Microwave monitoring of single cell monocytes subjected to electroporation," *IEEE Trans. Microw. Theory Techn.*, vol. 65, no. 9, pp. 3512–3518, Sep. 2017.
- [303] T. Kotnik, W. Frey, M. Sack, S. H. Meglič, M. Peterka, and D. Miklavčič, "Electroporation-based applications in biotechnology," *Trends Biotechnol.*, vol. 33, no. 8, pp. 480–488, 2015.
- [304] J. Leroy et al., "Microfluidic biosensors for microwave dielectric spectroscopy," *Sensors Actuators A, Phys.*, vol. 229, pp. 172–181, 2015.
- [305] N. Meyne, G. Fuge, A. Zeng, and A. F. Jacob, "Resonant microwave sensors for picoliter liquid characterization and nondestructive detection of single biological cells," *IEEE J. Electromagn. RF Microw. Med. Biol.*, vol. 1, no. 2, pp. 98–104, Dec. 2017.
- [306] Z. R. Gagnon, "Cellular dielectrophoresis: Applications to the characterization, manipulation, separation and patterning of cells," *Electrophoresis*, vol. 32, no. 18, pp. 2466–2487, 2011.
- [307] M. Li and R. K. Anand, "Cellular dielectrophoresis coupled with single-cell analysis," *Anal. Bioanal. Chem.*, vol. 410, no. 10, pp. 2499–2515, 2018.
- [308] J. Yao, G. Zhu, T. Zhao, and M. Takei, "Microfluidic device embedding electrodes for dielectrophoretic manipulation of cells -A review," *Electrophoresis*, vol. 40, no. 8, pp. 1166–1177, 2019.
- [309] H. P. Schwan, "Electrode polarization impedance and measurements in biological materials," *Ann. New York Acad. Sci.*, vol. 148, no. 1, pp. 191–209, 1968.
- [310] X. Ma, X. Du, H. Li, X. Cheng, and J. C. Hwang, "Ultra-wideband impedance spectroscopy of a live biological cell," *IEEE Trans. Microw. Theory Techn.*, vol. 66, no. 8, pp. 3690–3696, Aug. 2018.
- [311] X. Ma, X. Du, L. Li, H. Li, X. Cheng, and J. C. Hwang, "Sensitivity analysis for ultra-wideband 2-port impedance spectroscopy of a live cell," *IEEE J. Electromagn. RF Microw. Med. Biol.*, vol. 4, no. 1, pp. 37–44, Mar. 2020.
- [312] A. Irimajiri, T. Hanai, and A. Inouye, "A dielectric theory of "multi-stratified shell" model with its application to a lymphoma cell," *J. Theor. Biol.*, vol. 78, no. 2, pp. 251–269, 1979.

- [313] X. Jin, M. Farina, X. Wang, G. Fabi, X. Cheng, and J. C. Hwang, "Quantitative scanning microwave microscopy of the evolution of a live biological cell in a physiological buffer," *IEEE Trans. Microw. Theory Techn.*, vol. 67, no. 12, pp. 5438–5445, Dec. 2019.
- [314] M. E. Ladd et al., "Pros and cons of ultra-high-field MRI/MRS for human application," *Prog. Nucl. Magn. Reson. Spectrosc.*, vol. 109, pp. 1–50, 2018.
- [315] R. H. Caverly, "RF aspects of high-field magnetic resonance imaging (HF-MRI): Recent advances," *IEEE J. Electromagn. RF Microw. Med. Biol.*, vol. 3, no. 2, pp. 111–119, Jun. 2019.
- [316] K. P. Rajapran Nair, "The effect of magnetic and electric fields on the spectral transitions," in *Atomic Spectroscopy*. Tamil Nadu, India: MJP Publishers, ch. 9, p. 326.
- [317] A. Bottomley, "NMR imaging techniques and applications: A review," *Rev. Sci. Instruments*, vol. 53, no. 9, pp. 1319–1337, 1982.
- [318] B. Blümich, "Introduction to compact NMR: A review of methods," *TrAC Trends Anal. Chem.*, vol. 83, pp. 2–11, 2016.
- [319] K. Ohno, "ESR imaging and its applications," *Appl. Spectrosc. Rev.*, vol. 22, no. 1, pp. 1–56, 1986.
- [320] K. Takeshita and T. Ozawa, "Recent progress in in vivo ESR spectroscopy," *J. Radiat. Res.*, vol. 45, no. 3, pp. 373–384, 2004.
- [321] Y. Gao and X. Zhang, "Intrinsic temporal performance of the RF receive coil in magnetic resonance imaging," *IEEE Trans. Med. Imag.*, vol. 14, no. 11, pp. 3432–3444, Jun. 2022.
- [322] J. T. Vaughan and J. R. Griffiths, *RF Coils for MRI*. Hoboken, NJ, USA: Wiley, 2012.
- [323] S. Qu, Y. Gao, J. Zhao, Y. Sun, and X. Zhang, "Attachable DC coil array for improved functional MRI at 7 T," *IEEE J. Electromagn. RF Microwave Med. Biol.*, early access, Aug. 10, 2022, doi: [10.1109/JERM.2022.3195752](https://doi.org/10.1109/JERM.2022.3195752).
- [324] M. Zheng, Y. Gao, and X. Zhang, "Loopole antenna for uniform RF transmission in 7T MRI," in *Proc. IEEE Int. Conf. Microw. Millimeter Wave Technol.*, 2021, pp. 1–2.
- [325] I. A. Elabyad, M. Terekhov, M. Bille, and L. M. Schreiber, "Design and implementation of two 16-element antisymmetric transceiver coil arrays for parallel transmission human cardiac MRI at 7 T," *IEEE Trans. Microw. Theory Techn.*, vol. 69, no. 7, pp. 3540–3557, Jul. 2021.
- [326] B. Kahraman-Agir, K. Yegin, and E. Ozturk-Isik, "Wearable and elastic surface coil for 1H magnetic resonance imaging," *IEEE Microw. Wireless Compon. Lett.*, vol. 31, no. 5, pp. 517–520, May 2021.
- [327] Y. Cho, A. Basir, and H. Yoo, "Adjustable RF transmitter head coil: Improving transmit efficiency with SAR management for 7-T magnetic resonance imaging," *IEEE Trans. Microw. Theory Techn.*, vol. 69, no. 5, pp. 2686–2696, May 2021.
- [328] N. Mortensen, L. Hinge, V. Zhurbenko, and V. O. Boer, "7T MRI fractionated dipole antenna for carotid imaging," in *Proc. IEEE 50th Eur. Microw. Conf.*, 2021, pp. 1063–1066.
- [329] S. Ullah, M. Zada, A. Basir, and H. Yoo, "Wireless, battery-free, and fully implantable micro-coil system for 7 T brain MRI," *IEEE Trans. Biomed. Circuits Syst.*, vol. 16, no. 3, pp. 430–441, Jun. 2022.
- [330] M. Rajendran, J. E. H. Yang, J. L. Kaibin, L. C. Ping, and S. Y. Huang, "Birdcage transmitter for wireless power transfer," *IEEE Microw. Wireless Compon. Lett.*, vol. 32, no. 7, pp. 919–922, Jul. 2022.
- [331] T. Sun, X. Xie, and Z. Wang, "Design cases," in *Wireless Power Transfer for Medical Microsystems*. New York, NY, USA: Springer, 2013, pp. 145–168.
- [332] C. Vassos, F. Robb, S. Vasanawala, J. Pauly, and G. Scott, "A semi-blind calibration and compensation method for dynamic range recovery of low-power pre-amplifiers in MRI receive chains," *IEEE Trans. Med. Imag.*, early access, Aug. 01, 2022, doi: [10.1109/TMI.2022.3195656](https://doi.org/10.1109/TMI.2022.3195656).
- [333] R. Das and H. Yoo, "RF heating study of a new medical implant lead for 1.5 T, 3 T, and 7 T MRI systems," *IEEE Trans. Electromagn. Compat.*, vol. 59, no. 2, pp. 360–366, Apr. 2017.
- [334] Y. Cho and H. Yoo, "RF heating of implants in MRI: Electromagnetic analysis and solutions," *Invest. Magn. Reson. Imag.*, vol. 24, no. 2, pp. 67–75, 2020.
- [335] L. Winter, F. Seifert, L. Zilberti, M. Murbach, and B. Ittermann, "MRI-related heating of implants and devices: A review," *J. Magn. Reson. Imag.*, vol. 53, no. 6, pp. 1646–1665, 2021.
- [336] A. Gill and F. G. Shellock, "Assessment of MRI issues at 3-Tesla for metallic surgical implants: Findings applied to 61 additional skin closure staples and vessel ligation clips," *J. Cardiovasc. Magn. Reson.*, vol. 14, no. 1, pp. 1–7, 2012.
- [337] S. M. Park, R. Kamondetdacha, A. Amjad, and J. A. Nyenhuis, "MRI safety: RF-induced heating near straight wires," *IEEE Trans. Magn.*, vol. 41, no. 10, pp. 4197–4199, Oct. 2005.
- [338] X. Ji, J. Zheng, R. Yang, W. Kainz, and J. Chen, "Evaluations of the MRI RF-induced heating for helical stents under a 1.5T MRI system," *IEEE Trans. Electromagn. Compat.*, vol. 61, no. 1, pp. 57–64, Feb. 2019.
- [339] Q. Zeng et al., "Investigation of RF-induced heating near interventional catheters at 1.5 T MRI: A combined modeling and experimental study," *IEEE Trans. Electromagn. Compat.*, vol. 61, no. 5, pp. 1423–1431, Oct. 2019.
- [340] J. Zheng, X. Ji, W. Kainz, and J. Chen, "Study on search strategies for assessing the worst case RF-induced heating for multi-configuration implant system under MRI," *IEEE Trans. Electromagn. Compat.*, vol. 62, no. 1, pp. 43–51, Feb. 2020.
- [341] Y. Cho and H. Yoo, "Numerical analysis of RF-induced heating while wearing face mask at magnetic resonance imaging," *IEEE Access*, vol. 10, pp. 60946–60954, 2022.
- [342] B. R. Steensma, J. P. Tokaya, P. R. Stijnman, M. A. Erturk, C. A. van den Berg, and A. J. Raaijmakers, "Effect of transmit frequency on RF heating on metallic implants," in *Proc. ISMRM Annu. Meeting Exhib.*, 2021, Art. no. 0357.
- [343] M. K. Akter, R. Guo, M. Z. Islam, J. Zheng, and J. Chen, "Effects of strain relief loop on MRI RF-induced heating of active implantable medical devices," in *Proc. IEEE Texas Symp. Wireless Microw. Circuits Syst.*, 2022, pp. 1–5.
- [344] J. Wooldridge and D. Bownds, "The importance of sensor placement during the measurement of RF heating of implants in MRI," *IEEE J. Electromagn. RF Microw. Med. Biol.*, vol. 6, no. 3, pp. 399–405, Sep. 2022.
- [345] Z. Wang et al., "One-dimensional deep low-rank and sparse network for accelerated MRI," *IEEE Trans. Med. Imag.*, early access, Aug. 31, 2022, doi: [10.1109/TMI.2022.3203312](https://doi.org/10.1109/TMI.2022.3203312).
- [346] M. Yurt et al., "Semi-supervised learning of MRI synthesis without fully-sampled ground truths," *IEEE Trans. Med. Imag.*, *IEEE Trans. Med. Imag.*, vol. 41, no. 12, pp. 3895–3906, Dec. 2022.
- [347] C. Chen et al., "Synthesizing MR image contrast enhancement using 3D high-resolution convnets," *IEEE Trans. Biomed. Eng.*, early access, Jul. 19, 2022, doi: [10.1109/TBME.2022.3192309](https://doi.org/10.1109/TBME.2022.3192309).
- [348] D. S. Goolaub et al., "Volumetric fetal flow imaging with magnetic resonance imaging," *IEEE Trans. Med. Imag.*, vol. 41, no. 10, pp. 2941–2952, Oct. 2022.
- [349] F. Parveen and P. Wahid, "Microwave head imaging system for detection of blood clots inside the brain," in *Proc. IEEE Int. Symp. Antennas Propag. USNC-URSI Radio Sci. Meeting*, 2021, pp. 591–592.
- [350] D. Arava, M. Masarwy, S. Khawaled, and M. Freiman, "Deep-learning based motion correction for myocardial T1 mapping," in *Proc. IEEE Int. Conf. Microw. Antennas Commun. Electron. Syst.*, 2021, pp. 55–59.
- [351] M. Pastorino, *Microwave Imaging*. Hoboken, NJ, USA: Wiley, 2010.
- [352] E. C. Fear, "Microwave imaging of the breast," *Technol. Cancer Res. Treat.*, vol. 4, no. 1, pp. 69–82, 2005.
- [353] S. Kwon and S. Lee, "Recent advances in microwave imaging for breast cancer detection," *Int. J. Biomed. Imag.*, vol. 2016, Dec. 2016, Art. no. 5054912.
- [354] A. M. Hassan and M. El-Shenawee, "Review of electromagnetic techniques for breast cancer detection," *IEEE Rev. Biomed. Eng.*, vol. 4, pp. 103–118, 2011.
- [355] H. D. Nelson, K. Tyne, A. Naik, C. Bougatsos, B. K. Chan, and L. Humphrey, "Screening for breast cancer: An update for the U.S. preventive services task force," *Ann. Intern. Med.*, vol. 151, no. 10, pp. 727–737, 2009.
- [356] A. L. Siu and US Preventive Services Task Force, "Screening for breast cancer: US preventive services task force recommendation statement," *Ann. Intern. Med.*, vol. 164, no. 4, pp. 279–296, 2016.
- [357] L. L. Humphrey, M. Helfand, B. K. Chan, and S. H. Woolf, "Breast cancer screening: A summary of the evidence for the US preventive services task force," *Ann. Intern. Med.*, vol. 137, no. 5, pp. 347–360, 2002.

- [358] T. Huynh, A. M. Jarolimek, and S. Daye, "The false-negative mammogram," *Radiographics*, vol. 18, no. 5, pp. 1137–1154, 1998.
- [359] P. Shubik, "Vascularization of tumors: A review," *J. Cancer Res. Clin. Oncol.*, vol. 103, no. 3, pp. 211–226, 1982.
- [360] P. Auguste, S. Lemiere, F. Larrieu-Lahargue, and A. Bikfalvi, "Molecular mechanisms of tumor vascularization," *Crit. Rev. Oncol./Hematol.*, vol. 54, no. 1, pp. 53–61, 2005.
- [361] T. M. Buzug, S. Schumann, L. Pfaffmann, U. Reinhold, and J. Ruhlmann, "Functional infrared imaging for skin-cancer screening," in *Proc. IEEE Int. Conf. Eng. Med. Biol. Soc.*, 2006, pp. 2766–2769.
- [362] J. Gonzalez-Hernandez, A. N. Recinella, S. G. Kandlikar, D. Dabydeen, L. Medeiros, and P. Phatak, "Technology, application and potential of dynamic breast thermography for the detection of breast cancer," *Int. J. Heat Mass Transfer*, vol. 131, pp. 558–573, 2019.
- [363] K. L. Carr, "Microwave radiometry: Its importance to the detection of cancer," *IEEE Trans. Microw. Theory Techn.*, vol. 37, no. 12, pp. 1862–1869, Dec. 1989.
- [364] B. Bocquet et al., "Microwave radiometric imaging at 3 GHz for the exploration of breast tumors," *IEEE Trans. Microw. Theory Techn.*, vol. 38, no. 6, pp. 791–793, Jun. 1990.
- [365] K. L. Carr, P. Cevalco, P. Dunlea, and J. Shaeffer, "Radiometric sensing: An adjunct to mammography to determine breast biopsy," in *Proc. IEEE MTT-S Int. Microw. Symp.*, 2000, pp. 929–932.
- [366] J. W. Lee et al., "Experimental investigation of the mammary gland tumour phantom for multifrequency microwave radio-thermometers," *Med. Biol. Eng. Comput.*, vol. 42, no. 5, pp. 581–590, 2004.
- [367] S. Jacobsen and O. Klemetsen, "Improved detectability in medical microwave radio-thermometers as obtained by active antennas," *IEEE Trans. Biomed. Eng.*, vol. 55, no. 12, pp. 2778–2785, Dec. 2008.
- [368] S. Gabriel, R. W. Lau, and C. Gabriel, "The dielectric properties of biological tissues: III. Parametric models for the dielectric spectrum of tissues," *Phys. Med. Biol.*, vol. 41, no. 11, 1996, Art. no. 2271.
- [369] T. Joines, Y. Zhang, C. Li, and R. L. Jirtle, "The measured electrical properties of normal and malignant human tissues from 50 to 900 MHz," *Med. Phys.*, vol. 21, no. 4, pp. 547–550, 1994.
- [370] S. Chaudhary, R. K. Mishra, A. Swarup, and J. M. Thomas, "Dielectric properties of normal & malignant human breast tissues at radiowave & microwave frequencies," *Indian J. Biochem. Biophys.*, vol. 21, no. 1, pp. 76–79, 1984.
- [371] M. Lazebnik et al., "A large-scale study of the ultrawideband microwave dielectric properties of normal breast tissue obtained from reduction surgeries," *Phys. Med. Biol.*, vol. 52, no. 10, pp. 2637–2656, 2007.
- [372] M. Lazebnik et al., "A large-scale study of the ultrawideband microwave dielectric properties of normal, benign and malignant breast tissues obtained from cancer surgeries," *Phys. Med. Biol.*, vol. 52, no. 20, pp. 6093–6115, 2007.
- [373] Y. Cheng and M. Fu, "Dielectric properties for non-invasive detection of normal, benign, and malignant breast tissues using microwave theories," *Thoracic Cancer*, vol. 9, no. 4, pp. 459–465, 2018.
- [374] P. M. Meaney, K. D. Paulsen, A. Hartov, and R. K. Crane, "Microwave imaging for tissue assessment: Initial evaluation in multitarget tissue-equivalent phantoms," *IEEE Trans. Biomed. Eng.*, vol. 43, no. 9, pp. 878–890, Sep. 1996.
- [375] P. M. Meaney, K. D. Paulsen, A. Hartov, and R. K. Crane, "An active microwave imaging system for reconstruction of 2-D electrical property distributions," *IEEE Trans. Biomed. Eng.*, vol. 42, no. 10, pp. 1017–1026, Oct. 1995.
- [376] P. M. Meaney, M. W. Fanning, D. Li, S. P. Poplack, and K. D. Paulsen, "A clinical prototype for active microwave imaging of the breast," *IEEE Trans. Microw. Theory Techn.*, vol. 48, no. 11, pp. 1841–1853, Nov. 2000.
- [377] T. M. Grzegorzczak, P. M. Meaney, P. A. Kaufman, R. M. diFlorio-Alexander, and K. D. Paulsen, "Fast 3-D tomographic microwave imaging for breast cancer detection," *IEEE Trans. Med. Imag.*, vol. 31, no. 8, pp. 1584–1592, Aug. 2012.
- [378] P. M. Meaney et al., "Microwave imaging for neoadjuvant chemotherapy monitoring: Initial clinical experience," *Breast Cancer Res.*, vol. 15, no. 2, pp. 1–16, 2013.
- [379] N. A. Simonov, S. Jeon, S. Son, J. Lee, and H. Kim, "3D microwave breast imaging based on multistatic radar concept system," in *Proc. IEEE 3rd Int. Asia-Pacific Conf. Synthetic Aperture Radar*, 2011, pp. 1–4.
- [380] S. Ahsan, P. Kosmas, I. Sotiriou, G. Palikaras, and E. Kallos, "Balanced antipodal Vivaldi antenna array for microwave tomography," in *Proc. IEEE Conf. Antenna Meas. Appl.*, 2014, pp. 1–3.
- [381] Z. Q. Zhang and Q. H. Liu, "Three-dimensional nonlinear image reconstruction for microwave biomedical imaging," *IEEE Trans. Biomed. Eng.*, vol. 51, no. 3, pp. 544–548, Mar. 2004.
- [382] S. Semenov, "Microwave tomography: Review of the progress towards clinical applications," *Philos. Trans. Roy. Soc. A, Math. Phys. Eng. Sci.*, vol. 367, no. 1900, pp. 3021–3042, 2009.
- [383] A. Abubakar, P. M. Van den Berg, and S. Y. Semenov, "Two-and three-dimensional algorithms for microwave imaging and inverse scattering," *J. Electromagn. Waves Appl.*, vol. 17, no. 2, pp. 209–231, 2003.
- [384] M. Klemm, I. J. Craddock, J. A. Leendertz, A. Preece, and R. Benjamin, "Radar-based breast cancer detection using a hemispherical antenna array-Experimental results," *IEEE Trans. Antennas Propag.*, vol. 57, no. 6, pp. 1692–1704, Jun. 2009.
- [385] X. Li, E. J. Bond, B. D. Van Veen, and S. C. Hagness, "An overview of ultra-wideband microwave imaging via space-time beamforming for early-stage breast-cancer detection," *IEEE Antennas Propag. Mag.*, vol. 47, no. 1, pp. 19–34, Feb. 2005.
- [386] B. Guo, Y. Wang, J. Li, P. Stoica, and R. Wu, "Microwave imaging via adaptive beamforming methods for breast cancer detection," *J. Electromagn. Waves Appl.*, vol. 20, no. 1, pp. 53–63, 2006.
- [387] Y. Xie, B. Guo, L. Xu, J. Li, and P. Stoica, "Multistatic adaptive microwave imaging for early breast cancer detection," *IEEE Trans. Biomed. Eng.*, vol. 53, no. 8, pp. 1647–1657, Aug. 2006.
- [388] S. K. Davis, H. Tandrinatea, S. C. Hagness, and B. D. Van Veen, "Ultra-wideband microwave breast cancer detection: A detection-theoretic approach using the generalized likelihood ratio test," *IEEE Trans. Biomed. Eng.*, vol. 52, no. 7, pp. 1237–1250, Jul. 2005.
- [389] S. C. Hagness, A. Taflove, and J. E. Bridges, "Two-dimensional FDTD analysis of a pulsed microwave confocal system for breast cancer detection: Fixed-focus and antenna-array sensors," *IEEE Trans. Biomed. Eng.*, vol. 45, no. 12, pp. 1470–1479, Dec. 1998.
- [390] K. Davis, E. J. Bond, S. C. Hagness, and B. D. Van Veen, "Microwave imaging via space-time beamforming for early detection of breast cancer: Beamformer design in the frequency domain," *J. Electromagn. Waves Appl.*, vol. 17, no. 2, pp. 357–381, 2003.
- [391] X. Li, S. K. Davis, S. C. Hagness, D. W. Van der Weide, and B. D. Van Veen, "Microwave imaging via space-time beamforming: Experimental investigation of tumor detection in multilayer breast phantoms," *IEEE Trans. Microw. Theory Techn.*, vol. 52, no. 8, pp. 1856–1865, Aug. 2004.
- [392] E. C. Fear, S. C. Hagness, P. M. Meaney, M. Okoniewski, and M. A. Stuchly, "Enhancing breast tumor detection with near-field imaging," *IEEE Microw. Mag.*, vol. 3, no. 1, pp. 48–56, Mar. 2002.
- [393] E. C. Fear, X. Li, S. C. Hagness, and M. A. Stuchly, "Confocal microwave imaging for breast cancer detection: Localization of tumors in three dimensions," *IEEE Trans. Biomed. Eng.*, vol. 49, no. 8, pp. 812–822, Aug. 2002.
- [394] E. C. Fear, J. Sill, and M. A. Stuchly, "Experimental feasibility study of confocal microwave imaging for breast tumor detection," *IEEE Trans. Microw. Theory Techn.*, vol. 51, no. 3, pp. 887–892, Mar. 2003.
- [395] E. C. Fear, J. Bourqui, C. Curtis, D. Mew, B. Docktor, and C. Romano, "Microwave breast imaging with a monostatic radar-based system: A study of application to patients," *IEEE Trans. Microw. Theory Techn.*, vol. 61, no. 5, pp. 2119–2128, May 2013.
- [396] J. Bourqui, M. Okoniewski, and E. C. Fear, "Balanced antipodal Vivaldi antenna with dielectric director for near-field microwave imaging," *IEEE Trans. Antennas Propag.*, vol. 58, no. 7, pp. 2318–2326, Jul. 2010.
- [397] J. C. Lin, "Microwave thermoelastic tomography and imaging," in *Advances in Electromagnetic Fields in Living Systems*. New York, NY, USA: Springer, 2005, pp. 41–76.
- [398] J. C. Lin, "Microwave thermoacoustic tomographic (MTT) imaging," *Phys. Med. Biol.*, vol. 66, no. 10, 2021, Art. no. 10TR02.
- [399] Y. Cui, C. Yuan, and Z. Ji, "A review of microwave-induced thermoacoustic imaging: Excitation source, data acquisition system and biomedical applications," *J. Innov. Opt. Health Sci.*, vol. 10, no. 04, 2017, Art. no. 1730007.
- [400] S. Zhao et al., "Ultrashort-pulse-microwave excited whole-breast thermoacoustic imaging with uniform field of large size aperture antenna for tumor screening," *IEEE Trans. Biomed. Eng.*, vol. 69, no. 2, pp. 725–733, Feb. 2022.

- [401] H. Nan and A. Arbabian, "Peak-power-limited frequency-domain microwave-induced thermoacoustic imaging for handheld diagnostic and screening tools," *IEEE Trans. Microw. Theory Techn.*, vol. 65, no. 7, pp. 2607–2616, Jul. 2017.
- [402] D. O'Loughlin, M. O'Halloran, B. M. Moloney, M. Glavin, E. Jones, and M. A. Elahi, "Microwave breast imaging: Clinical advances and remaining challenges," *IEEE Trans. Biomed. Eng.*, vol. 65, no. 11, pp. 2580–2590, Nov. 2018.
- [403] M. A. Aldhaeabi, K. Alzoubi, T. S. Almoneef, S. M. Bamatraf, H. Attia, and O. M. Ramahi, "Review of microwaves techniques for breast cancer detection," *Sensors*, vol. 20, no. 8, 2020, Art. no. 2390.
- [404] C. Cao, L. Nie, C. Lou, and D. Xing, "The feasibility of using microwave-induced thermoacoustic tomography for detection and evaluation of renal calculi," *Phys. Med. Biol.*, vol. 55, no. 17, 2010, Art. no. 5203.
- [405] S. K. Patch, D. Hull, W. A. See, and G. W. Hanson, "Toward quantitative whole organ thermoacoustics with a clinical array plus one very low-frequency channel applied to prostate cancer imaging," *IEEE Trans. Ultrasonics Ferroelect. Freq. Control*, vol. 63, no. 2, pp. 245–255, Feb. 2016.
- [406] M. S. Aliroteh and A. Arbabian, "Microwave-induced thermoacoustic imaging of subcutaneous vasculature with near-field RF excitation," *IEEE Trans. Microw. Theory Techn.*, vol. 66, no. 1, pp. 577–588, Jan. 2018.
- [407] Z. Chi, Y. Zhao, J. Yang, T. Li, G. Zhang, and H. Jiang, "Thermoacoustic tomography of in vivo human finger joints," *IEEE Trans. Biomed. Eng.*, vol. 66, no. 6, pp. 1598–1608, Jun. 2019.
- [408] L. V. Wang, "Prospects of photoacoustic tomography," *Med. Phys.*, vol. 35, no. 12, pp. 5758–5767, 2008.
- [409] Y. Zhao, Z. Chi, L. Huang, Z. Zheng, J. Yang, and H. Jiang, "Thermoacoustic tomography of in vivo rat brain," *J. Innov. Opt. Health Sci.*, vol. 10, no. 4, 2017, Art. no. 1740001.
- [410] A. Yan, L. Lin, C. Liu, J. Shi, S. Na, and L. V. Wang, "Microwave-induced thermoacoustic tomography through an adult human skull," *Med. Phys.*, vol. 46, no. 4, pp. 1793–1797, 2019.
- [411] L. Olansky and L. Kennedy, "Finger-stick glucose monitoring: Issues of accuracy and specificity," *Diabetes Care*, vol. 33, no. 4, pp. 948–949, 2010.
- [412] M. S. Venkatesh and G. Raghavan, "An overview of dielectric properties measuring techniques," *Can. Biosyst. Eng.*, vol. 47, no. 7, pp. 15–30, 2005.
- [413] V. Sekar, W. J. Torke, S. Palermo, and K. Entesari, "A self-sustained microwave system for dielectric-constant measurement of lossy organic liquids," *IEEE Trans. Microw. Theory Techn.*, vol. 60, no. 5, pp. 1444–1455, May 2012.
- [414] R. A. Alahnomi et al., "Review of recent microwave planar resonator-based sensors: Techniques of complex permittivity extraction, applications, open challenges and future research directions," *Sensors*, vol. 21, no. 7, 2021, Art. no. 2267.
- [415] C. Gabriel, S. Gabriel, and Y. E. Corthout, "The dielectric properties of biological tissues: I. Literature survey," *Phys. Med. Biol.*, vol. 41, no. 11, 1996, Art. no. 2231.
- [416] J. Park, C. Kim, B. Choi, and K. Ham, "The correlation of the complex dielectric constant and blood glucose at low frequency," *Biosensors Bioelectron.*, vol. 19, no. 4, pp. 321–324, 2003.
- [417] T. Karacolak, E. C. Moreland, and E. Topsakal, "Cole-cole model for glucose-dependent dielectric properties of blood plasma for continuous glucose monitoring," *Microw. Opt. Technol. Lett.*, vol. 55, no. 5, pp. 1160–1164, 2013.
- [418] T. Yilmaz, R. Foster, and Y. Hao, "Radio-frequency and microwave techniques for non-invasive measurement of blood glucose levels," *Diagnostics*, vol. 9, no. 1, 2019, Art. no. 6.
- [419] P. F. Smulders, M. G. Buysse, and M. D. Huang, "Dielectric properties of glucose solutions in the 0.5–67 GHz range," *Microw. Opt. Technol. Lett.*, vol. 55, no. 8, pp. 1916–1917, 2013.
- [420] M. Hofmann, G. Fischer, R. Weigel, and D. Kissinger, "Microwave-based noninvasive concentration measurements for biomedical applications," *IEEE Trans. Microw. Theory Techn.*, vol. 61, no. 5, pp. 2195–2204, May 2013.
- [421] H. Chen et al., "Quantify glucose level in freshly diabetic's blood by terahertz time-domain spectroscopy," *J. Infrared Millimeter THz Waves*, vol. 39, no. 4, pp. 399–408, 2018.
- [422] C. G. Juan, B. Potelon, C. Quendo, and E. Bronchalo, "Microwave planar resonant solutions for glucose concentration sensing: A systematic review," *Appl. Sci.*, vol. 11, no. 15, 2021, Art. no. 7018.
- [423] A. E. Omer et al., "Multiple-cell microfluidic dielectric resonator for liquid sensing applications," *IEEE Sensors J.*, vol. 21, no. 5, pp. 6094–6104, Mar. 2021.
- [424] G. Govind and M. J. Akhtar, "Design of an ELC resonator-based reusable RF microfluidic sensor for blood glucose estimation," *Sci. Rep.*, vol. 10, no. 1, pp. 1–10, 2020.
- [425] T. Chretiennot, D. Dubuc, and K. Grenier, "Microwave-based microfluidic sensor for non-destructive and quantitative glucose monitoring in aqueous solution," *Sensors*, vol. 16, no. 10, 2016, Art. no. 1733.
- [426] Omkar, W. Yu, and S. Y. Huang, "T-shaped patterned microstrip line for noninvasive continuous glucose sensing," *IEEE Microw. Wireless Compon. Lett.*, vol. 28, no. 10, pp. 942–944, Oct. 2018.
- [427] C. G. Juan, E. Bronchalo, B. Potelon, C. Quendo, and J. M. Sabater-Navarro, "Glucose concentration measurement in human blood plasma solutions with microwave sensors," *Sensors*, vol. 19, no. 17, 2019, Art. no. 3779.
- [428] C. G. Juan, B. Potelon, C. Quendo, E. Bronchalo, and J. M. Sabater-Navarro, "Highly-sensitive glucose concentration sensor exploiting inter-resonators couplings," in *Proc. IEEE 49th Eur. Microw. Conf.*, 2019, pp. 662–665.
- [429] U. Scherthoeffer, R. Weigel, and D. Kissinger, "A highly sensitive glucose biosensor based on a microstrip ring resonator," in *Proc. IEEE MTT-S Int. Microw. Workshop Ser. RF Wireless Technol. for Biomed. Healthcare Appl.*, 2013, pp. 1–3.
- [430] J. A. Byford, K. Y. Park, and P. Chahal, "Metamaterial inspired periodic structure used for microfluidic sensing," in *Proc. IEEE 65th Electron. Compon. Technol. Conf.*, 2015, pp. 1997–2002.
- [431] N. Y. Kim, R. Dhakal, K. K. Adhikari, E. S. Kim, and C. Wang, "A reusable robust radio frequency biosensor using microwave resonator by integrated passive device technology for quantitative detection of glucose level," *Biosensors Bioelectron.*, vol. 67, pp. 687–693, 2015.
- [432] L. Heinemann, "Finger pricking and pain: A never ending story," *J. Diabetes Sci. Technol.*, vol. 2, no. 5, pp. 919–921, 2008.
- [433] S. K. Vashist, D. Zheng, K. Al-Rubeaan, J. H. Luong, and F. Sheu, "Technology behind commercial devices for blood glucose monitoring in diabetes management: A review," *Analytica Chimica Acta*, vol. 703, no. 2, pp. 124–136, 2011.
- [434] D. Bruen, C. Delaney, L. Florea, and D. Diamond, "Glucose sensing for diabetes monitoring: Recent developments," *Sensors*, vol. 17, no. 8, 2017, Art. no. 1866.
- [435] Z. Peng et al., "Blood glucose sensors and recent advances: A review," *J. Innov. Opt. Health Sci.*, vol. 15, no. 2, 2022, Art. no. 2230003.
- [436] G. Cappon, M. Vettoretti, G. Sparacino, and A. Facchinetti, "Continuous glucose monitoring sensors for diabetes management: A review of technologies and applications," *Diabetes Metab. J.*, vol. 43, no. 4, pp. 383–397, 2019.
- [437] H. Lee, Y. J. Hong, S. Baik, T. Hyeon, and D. Kim, "Enzyme-based glucose sensor: From invasive to wearable device," *Adv. Healthcare Mater.*, vol. 7, no. 8, 2018, Art. no. 1701150.
- [438] Y. Jing, S. J. Chang, C. Chen, and J. Liu, "Review-glucose monitoring sensors: History, principle, and challenges," *J. Electrochem. Soc.*, vol. 169, no. 5, 2022, Art. no. 057514.
- [439] V. Gonzales, A. T. Mobashsher, and A. Abbosh, "The progress of glucose monitoring—A review of invasive to minimally and non-invasive techniques, devices and sensors," *Sensors*, vol. 19, no. 4, 2019, Art. no. 800.
- [440] L. Tang, S. J. Chang, C. Chen, and J. Liu, "Non-invasive blood glucose monitoring technology: A review," *Sensors*, vol. 20, no. 23, 2020, Art. no. 6925.
- [441] R. Zhang et al., "Noninvasive electromagnetic wave sensing of glucose," *Sensors*, vol. 19, no. 5, 2019, Art. no. 1151.
- [442] V. Turgul and I. Kale, "Permittivity extraction of glucose solutions through artificial neural networks and non-invasive microwave glucose sensing," *Sensors Actuators A, Phys.*, vol. 277, pp. 65–72, 2018.
- [443] H. Choi et al., "Design and in vitro interference test of microwave noninvasive blood glucose monitoring sensor," *IEEE Trans. Microw. Theory Techn.*, vol. 63, no. 10, pp. 3016–3025, Oct. 2015.
- [444] H. Choi, S. Luzio, J. Beutler, and A. Porch, "Microwave noninvasive blood glucose monitoring sensor: Human clinical trial results," in *Proc. IEEE MTT-S Int. Microw. Symp.*, 2017, pp. 876–879.

- [445] Y. Nikawa and T. Michiyama, "Non-invasive measurement of blood-sugar level by reflection of millimeter-waves," in *Proc. IEEE Asia-Pacific Microw. Conf.*, 2006, pp. 47–50.
- [446] Y. Nikawa and T. Michiyama, "Blood-sugar monitoring by reflection of millimeter wave," in *Proc. IEEE Asia-Pacific Microw. Conf.*, 2007, pp. 1–4.
- [447] P. H. Siegel, Y. Lee, and V. Pikov, "Millimeter-wave non-invasive monitoring of glucose in anesthetized rats," in *Proc. IEEE 39th Int. Conf. Infrared Millimeter THz Waves*, 2014, pp. 1–2.
- [448] P. H. Siegel, W. Dai, R. A. Kloner, M. Csete, and V. Pikov, "First millimeter-wave animal in vivo measurements of L-glucose and D-glucose: Further steps towards a non-invasive glucometer," in *Proc. IEEE 41st Int. Conf. Infrared Millimeter THz Waves*, 2016, pp. 1–3.
- [449] H. Cano-Garcia, S. Saha, I. Sotiriou, P. Kosmas, I. Gouzouasis, and E. Kallos, "Millimeter-wave sensing of diabetes-relevant glucose concentration changes in pigs," *J. Infrared Millimeter THz Waves*, vol. 39, no. 8, pp. 761–772, 2018.
- [450] D. B. Keenan, J. J. Mastrototaro, S. A. Weinzimer, and G. M. Steil, "Interstitial fluid glucose time-lag correction for real-time continuous glucose monitoring," *Biomed. Signal Process. Control*, vol. 8, no. 1, pp. 81–89, 2013.
- [451] S. Saha et al., "A glucose sensing system based on transmission measurements at millimetre waves using micro strip patch antennas," *Sci. Rep.*, vol. 7, no. 1, pp. 1–11, 2017.
- [452] J. W. Hodges and M. E. Rippen, "Apparatus for in vivo dielectric spectroscopy," U.S. Patent 20200217809A1, Jul. 09, 2020.
- [453] V. Balasubramanian, S. Baskerville, R. Bailey, K. McCarthy, M. Rippen, and J. Burd, "Noninvasive continuous blood glucose monitoring by dielectric spectroscopy," *Curr. Res. Diabetes Obesity J.*, vol. 14, no. 5, Jun. 2021, Art. no. 555897.
- [454] L. A. Buehler et al., "Noninvasive glucose monitor using dielectric spectroscopy," *Endocr. Pract.*, vol. 28, no. 2, pp. 142–147, 2022.
- [455] E. Pickwell and V. P. Wallace, "Biomedical applications of terahertz technology," *J. Phys. D, Appl. Phys.*, vol. 39, no. 17, 2006, Art. no. R301.
- [456] A. A. Angeluts et al., "Characteristic responses of biological and nanoscale systems in the terahertz frequency range," *Quantum Electron.*, vol. 44, no. 7, pp. 614, 2014, Art. no. 614.
- [457] A. Angeluts et al., "Study of terahertz-radiation-induced DNA damage in human blood leukocytes," *Quantum Electron.*, vol. 44, no. 3, 2014, Art. no. 247.
- [458] E. Pickwell, B. E. Cole, A. J. Fitzgerald, M. Pepper, and V. P. Wallace, "In vivo study of human skin using pulsed terahertz radiation," *Phys. Med. Biol.*, vol. 49, no. 9, 2004, Art. no. 1595.
- [459] K. I. Zaytsev, A. A. Gavadush, N. V. Chernomyrdin, and S. O. Yurchenko, "Highly accurate in vivo terahertz spectroscopy of healthy skin: Variation of refractive index and absorption coefficient along the human body," *IEEE Trans. THz Sci. Technol.*, vol. 5, no. 5, pp. 817–827, Sep. 2015.
- [460] K. I. Zaytsev, K. G. Kudrin, V. E. Karasik, I. V. Reshetov, and S. O. Yurchenko, "In vivo terahertz spectroscopy of pigmented skin nevi: Pilot study of non-invasive early diagnosis of dysplasia," *Appl. Phys. Lett.*, vol. 106, no. 5, 2015, Art. no. 053702.
- [461] A. J. Fitzgerald et al., "Terahertz pulsed imaging of human breast tumors," *Radiology*, vol. 239, no. 2, pp. 533–540, 2006.
- [462] E. P. J. Parrott, Y. Sun, and E. Pickwell-MacPherson, "Terahertz spectroscopy: Its future role in medical diagnoses," *J. Mol. Struct.*, vol. 1006, no. 1–3, pp. 66–76, 2011.
- [463] O. P. Cherkasova, M. M. Nazarov, A. A. Angeluts, and A. P. Shkurinov, "Analysis of blood plasma at terahertz frequencies," *Opt. Spectrosc.*, vol. 120, no. 1, pp. 50–57, 2016.
- [464] O. Cherkasova, M. Nazarov, and A. Shkurinov, "Noninvasive blood glucose monitoring in the terahertz frequency range," *Opt. Quantum Electron.*, vol. 48, no. 3, pp. 1–12, 2016.
- [465] F. B. Nerbass, R. Pecoits-Filho, W. F. Clark, J. M. Sontrop, C. W. McIntyre, and L. Moist, "Occupational heat stress and kidney health: From farms to factories," *Kidney Int. Rep.*, vol. 2, no. 6, pp. 998–1008, 2017.
- [466] J. Xiang, P. Bi, D. Pisanelli, and A. Hansen, "Health impacts of workplace heat exposure: An epidemiological review," *Ind. Health*, vol. 52, no. 2, pp. 91–101, 2014.
- [467] J. Edmonds, E. Foglia, P. Booth, C. H. Fu, and M. Gardner, "Dehydration in older people: A systematic review of the effects of dehydration on health outcomes, healthcare costs and cognitive performance," *Arch. Gerontol. Geriatrics*, vol. 95, 2021, Art. no. 104380.
- [468] M. H. Gorelick, K. N. Shaw, and K. O. Murphy, "Validity and reliability of clinical signs in the diagnosis of dehydration in children," *Pediatrics*, vol. 99, no. 5, 1997, Art. no. e6.
- [469] A. Cataldo et al., "Portable microwave reflectometry system for skin sensing," *IEEE Trans. Instrum. Meas.*, vol. 71, 2022, Art. no. 4003308.
- [470] R. Eldamak and E. C. Fear, "Conformal and disposable antenna-based sensor for non-invasive sweat monitoring," *Sensors*, vol. 18, no. 12, 2018, Art. no. 4088.
- [471] I. Butterworth, J. Serallés, C. S. Mendoza, L. Giancardo, and L. Daniel, "A wearable physiological hydration monitoring wristband through multi-path non-contact dielectric spectroscopy in the microwave range," in *Proc. IEEE MTT-S Int. Microw. Workshop Ser. RF Wireless Technol. Biomed. Healthcare Appl.*, 2015, pp. 60–61.
- [472] D. C. Garrett and E. C. Fear, "Feasibility study of hydration monitoring using microwaves—Part 1: A model of microwave property changes with dehydration," *IEEE J. Electromagn. RF Microw. Med. Biol.*, vol. 3, no. 4, pp. 292–299, Dec. 2019.
- [473] D. C. Garrett, J. R. Fletcher, D. B. Hogan, T. S. Fung, and E. C. Fear, "Feasibility study of hydration monitoring using microwaves—Part 2: Measurements of athletes," *IEEE J. Electromagn. RF Microw. Med. Biol.*, vol. 3, no. 4, pp. 300–307, Dec. 2019.
- [474] C. Besler and E. C. Fear, "Microwave hydration monitoring: System assessment using fasting volunteers," *Sensors*, vol. 21, no. 21, 2021, Art. no. 6949.
- [475] R. Brendtke, M. Wiehl, F. Groeber, T. Schwarz, H. Walles, and J. Hansmann, "Feasibility study on a microwave-based sensor for measuring hydration level using human skin models," *PLoS One*, vol. 11, no. 4, 2016, Art. no. e0153145.
- [476] S. Bing, K. Chawang, and J. C. Chiao, "A radio-frequency planar resonant loop for noninvasive monitoring of water content," in *Proc. IEEE Sensors Conf.*, 2022, pp. 1–4.
- [477] S. Bing, K. Chawang, and J. C. Chiao, "A flexible tuned radio-frequency planar resonant loop for noninvasive hydration sensing," *IEEE J. Microwaves*, vol. 3, no. 1, Jan. 2023, doi: [10.1109/JMW.2022.3224087](https://doi.org/10.1109/JMW.2022.3224087).
- [478] W. Y. Shi and J. C. Chiao, "A double-resonant sensor for identifying biological tissues," in *Proc. IEEE SENSORS Conf.*, 2018, pp. 1–4.
- [479] J. Kilpijärvi, J. Tolvanen, J. Juuti, N. Halonen, and J. Hannu, "A non-invasive method for hydration status measurement with a microwave sensor using skin phantoms," *IEEE Sensors J.*, vol. 20, no. 2, pp. 1095–1104, Jan. 2020.
- [480] Z. Wang and C. Wang, "Is breath acetone a biomarker of diabetes? A historical review on breath acetone measurements," *J. Breath Res.*, vol. 7, no. 3, 2013, Art. no. 037109.
- [481] M. H. Zarifi, A. Sohrabi, P. M. Shaibani, M. Daneshmand, and T. Thundat, "Detection of volatile organic compounds using microwave sensors," *IEEE Sensors J.*, vol. 15, no. 1, pp. 248–254, Jan. 2015.
- [482] S. Chopra, A. Pham, J. Gaillard, A. Parker, and A. M. Rao, "Carbon-nanotube-based resonant-circuit sensor for ammonia," *Appl. Phys. Lett.*, vol. 80, no. 24, pp. 4632–4634, 2002.
- [483] M. H. Zarifi, M. Fayaz, J. Goldthorp, M. Abdolrazzaghi, Z. Hashisho, and M. Daneshmand, "Microbead-assisted high resolution microwave planar ring resonator for organic-vapor sensing," *Appl. Phys. Lett.*, vol. 106, no. 6, 2015, Art. no. 062903.
- [484] J. Rossignol et al., "Microwave-based gas sensor with phthalocyanine film at room temperature," *Sensors Actuators B, Chem.*, vol. 189, pp. 213–216, 2013.
- [485] M. H. Zarifi, S. Farsinezhad, M. Abdolrazzaghi, M. Daneshmand, and K. Shankar, "Selective microwave sensors exploiting the interaction of analytes with trap states in TiO₂ nanotube arrays," *Nanoscale*, vol. 8, no. 14, pp. 7466–7473, 2016.
- [486] A. Rydosz, E. Maciak, K. Wincza, and S. Gruszczynski, "Microwave-based sensors with phthalocyanine films for acetone, ethanol and methanol detection," *Sensors Actuators B, Chem.*, vol. 237, pp. 876–886, 2016.
- [487] Y. H. Kim, S. Yoon, S. Park, D. Lim, H. Jung, and Y. Kim, "A simple and direct biomolecule detection scheme based on a microwave resonator," *Sensors Actuators B, Chem.*, vol. 130, no. 2, pp. 823–828, 2008.
- [488] M. Fok, M. Bashir, H. Fraser, N. Strouther, and A. Mason, "A novel microwave sensor to detect specific biomarkers in human cerebrospinal fluid and their relationship to cellular ischemia during thoracoabdominal aortic aneurysm repair," *J. Med. Syst.*, vol. 39, no. 4, pp. 1–5, 2015.

- [489] A. Rydosz, E. Brzozowska, S. Górka, K. Wincza, A. Gamian, and S. Gruszczynski, "A broadband capacitive sensing method for label-free bacterial LPS detection," *Biosensors Bioelectron.*, vol. 75, pp. 328–336, 2016.
- [490] H. Lee et al., "A planar split-ring resonator-based microwave biosensor for label-free detection of biomolecules," *Sensors Actuators B, Chem.*, vol. 169, pp. 26–31, 2012.
- [491] L. Wei, L. Yu, H. Jiaoqi, H. Guorong, Z. Yang, and F. Weiling, "Application of terahertz spectroscopy in biomolecule detection," *Front. Lab. Med.*, vol. 2, no. 4, pp. 127–133, 2018.
- [492] M. Amin, O. Siddiqui, H. Abutarboush, M. Farhat, and R. Ramzan, "A THz graphene metasurface for polarization selective virus sensing," *Carbon*, vol. 176, pp. 580–591, 2021.
- [493] Y. Bian, X. Zhang, Z. Zhu, X. Wu, X. Li, and B. Yang, "Investigation of the correlations between amino acids, amino acid mixtures and dipeptides by terahertz spectroscopy," *J. Infrared Millimeter THz Waves*, vol. 42, no. 1, pp. 64–75, 2021.
- [494] S. Pal and A. Chattopadhyay, "Hydration dynamics in biological membranes: Emerging applications of terahertz spectroscopy," *J. Phys. Chem. Lett.*, vol. 12, no. 39, pp. 9697–9709, 2021.
- [495] T. Liu, F. Yan, J. Zhang, and B. Jin, "Application of terahertz spectroscopy in the detection of carbohydrate isomers," in *Advances in Precision Instruments and Optical Engineering*. Berlin/Heidelberg, Germany: Springer, 2022, pp. 345–352.
- [496] M. Konnikova et al., "Terahertz and infrared spectroscopy of SARS-CoV-2 spike protein," in *Proc. IEEE 46th Int. Conf. Infrared Millimeter THz Waves*, 2021, pp. 1–2.
- [497] C. P. Hancock et al., "A new wave in electrosurgery: A review of existing and introduction to new radio-frequency and microwave therapeutic systems," *IEEE Microw. Mag.*, vol. 16, no. 2, pp. 14–30, Mar. 2015.
- [498] A. Rosen, H. D. Rosen, and S. D. Edwards, "Microwave surgery," in *New Frontiers for RF/Microwaves in Therapeutic Medicine*. Boca Raton, FL, USA: CRC Press, 2000, ch. 18, pp. 1–25.
- [499] G. Hannon, F. L. Tansi, I. Hilger, and A. Prina-Mello, "The effects of localized heat on the hallmarks of cancer," *Adv. Therapeutics*, vol. 4, no. 7, 2021, Art. no. 2000267.
- [500] C. Rappaport, "Cardiac tissue ablation with catheter-based microwave heating," *Int. J. Hyperthermia*, vol. 20, no. 7, pp. 769–780, 2004.
- [501] P. Walinsky, A. Rosen, and A. J. Greenspon, "Method and apparatus for high frequency catheter ablation," U.S. Patent 4,641,649 A, Feb. 10, 1987.
- [502] H. D. Rosen and A. Rosen, "RF/microwaves [medical applications]," *IEEE Potentials*, vol. 18, no. 3, pp. 33–37, Aug./Sep. 1999.
- [503] P. C. Qian et al., "Irrigated microwave catheter ablation can create deep ventricular lesions through epicardial fat with relative sparing of adjacent coronary arteries," *Circulation, Arrhythmia Electrophysiol.*, vol. 13, no. 5, 2020, Art. no. e008251.
- [504] R. E. Kass and C. E. Clancy, *Basis and Treatment of Cardiac Arrhythmias*. New York, NY, USA: Springer, 2005.
- [505] H. V. Huikuri, A. Castellanos, and R. J. Myerburg, "Sudden death due to cardiac arrhythmias," *New England J. Med.*, vol. 345, no. 20, pp. 1473–1482, 2001.
- [506] M. D. Morady, "Radio-frequency ablation as treatment for cardiac arrhythmias," *New England J. Med.*, vol. 340, no. 7, pp. 534–544, 1999.
- [507] J. C. Lin, "Microwave surgery inside the heart," *IEEE Microw. Mag.*, vol. 7, no. 3, pp. 32–36, Jun. 2006.
- [508] J. C. Lin, Y. Wang, and R. J. Hariman, "Comparison of power deposition patterns produced by microwave and radio frequency cardiac ablation catheters," *Electron. Lett.*, vol. 30, no. 12, pp. 922–923, 1994.
- [509] G. Keane, "New catheter ablation techniques for the treatment of cardiac arrhythmias," *Cardiac Electrophysiol. Rev.*, vol. 6, no. 4, pp. 341–348, 2002.
- [510] J. G. Whayne, S. Nath, and D. E. Haines, "Microwave catheter ablation of myocardium in vitro. Assessment of the characteristics of tissue heating and injury," *Circulation*, vol. 89, no. 5, pp. 2390–2395, 1994.
- [511] H. Fallahi and P. Prakash, "Antenna designs for microwave tissue ablation," *Crit. Rev. Biomed. Eng.*, vol. 46, no. 6, pp. 495–521, 2018.
- [512] B. A. VanderBrink et al., "Microwave ablation using a spiral antenna design in a porcine thigh muscle preparation: In vivo assessment of temperature profile and lesion geometry," *J. Cardiovasc. Electrophysiol.*, vol. 11, no. 2, pp. 193–198, 2000.
- [513] Z. Gu, C. M. Rappaport, P. J. Wang, and W. Zhu, "A conformal microwave antenna applicator for circumferential ablation," in *Proc. IEEE MTT-S Int. Microw. Symp.*, 2003, pp. 391–394.
- [514] H. Luyen, S. C. Hagness, and N. Behdad, "Tissue ablation at 10 GHz vs. 1.9 GHz: Ex vivo experiments demonstrate comparable ablation zones," in *Proc. IEEE Antennas Propag. Soc. Int. Symp.*, 2013, pp. 2042–2043.
- [515] J. C. Lin, "Catheter microwave ablation therapy for cardiac arrhythmias," *Bioelectromagnetics*, vol. 20, no. S4, pp. 120–132, 1999.
- [516] H. Chiu, A. S. Mohan, A. R. Weily, D. J. Guy, and D. L. Ross, "Analysis of a novel expanded tip wire (ETW) antenna for microwave ablation of cardiac arrhythmias," *IEEE Trans. Biomed. Eng.*, vol. 50, no. 7, pp. 890–899, Jul. 2003.
- [517] H. M. Chiu, A. S. Mohan, D. Guy, S. P. Thomas, and D. L. Ross, "Miniaturized antennas for microwave ablation of cardiac arrhythmias," in *Proc. IEEE Asia-Pacific Microw. Conf.*, 2000, pp. 50–53.
- [518] D. Keane, J. Ruskin, N. Norris, P. Chapelon, and D. Bérubé, "In vitro and in vivo evaluation of the thermal patterns and lesions of catheter ablation with a microwave monopole antenna," *J. Interventional Cardiac Electrophysiol.*, vol. 10, no. 2, pp. 111–119, 2004.
- [519] S. Labonte, H. O. Ali, and L. Roy, "Monopoles for microwave catheter ablation of heart tissue," in *Proc. IEEE MTT-S Int. Microw. Symp.*, 1995, pp. 303–306.
- [520] H. Luyen, S. C. Hagness, and N. Behdad, "A balun-free helical antenna for minimally invasive microwave ablation," *IEEE Trans. Antennas Propag.*, vol. 63, no. 3, pp. 959–965, Mar. 2015.
- [521] H. Chiu, A. M. Sanagavarapu, G. Duncan, and D. L. Ross, "Novel parallel loop antenna for circumferential microwave ablation of the pulmonary veins," in *Proc. IEEE Int. Symp. Antennas Propag.*, 2002, pp. 331–334.
- [522] J. M. Bertram, D. Yang, M. C. Converse, J. G. Webster, and D. M. Mahvi, "Antenna design for microwave hepatic ablation using an axisymmetric electromagnetic model," *Biomed. Eng. Online*, vol. 5, no. 1, pp. 1–9, 2006.
- [523] Z. Wen, X. Q. Lin, C. Li, J. Guo, and Y. L. Fan, "A microwave ablation antenna based on substrate-integrated coaxial line," *IEEE Antennas Wireless Propag. Lett.*, vol. 20, no. 5, pp. 713–717, May 2021.
- [524] J. M. Bertram, D. Yang, M. C. Converse, J. G. Webster, and D. M. Mahvi, "A review of coaxial-based interstitial antennas for hepatic microwave ablation," *Crit. Rev. Biomed. Eng.*, vol. 34, no. 3, pp. 187–213, 2006.
- [525] S. Kikuchi, K. Saito, M. Takahashi, and K. Ito, "Control of heating pattern for interstitial microwave hyperthermia by a coaxial-dipole antenna—Aiming at treatment of brain tumor," *Electron. Commun. Jpn. (Part I: Commun.)*, vol. 90, no. 12, pp. 31–38, 2007.
- [526] J. Ji, *Radiofrequency and Microwave Ablation for Pancreatic Cancer*. Amsterdam, The Netherlands: Elsevier, 2021, ch. 13, pp. 347–354.
- [527] J. Wolf, D. J. Grand, J. T. Machan, T. A. DiPetrillo, W. W. Mayo-Smith, and D. E. Dupuy, "Microwave ablation of lung malignancies: Effectiveness, CT findings, and safety in 50 patients," *Radiology*, vol. 247, no. 3, pp. 871–879, 2008.
- [528] P. Song, L. Sheng, Y. Sun, Y. An, Y. Guo, and Y. Zhang, "The clinical utility and outcomes of microwave ablation for colorectal cancer liver metastases," *Oncotarget*, vol. 8, no. 31, 2017, Art. no. 51792.
- [529] A. E. Spiliotis, G. Gäbelein, S. Holländer, P. Scherber, M. Glanemann, and B. Patel, "Microwave ablation compared with radiofrequency ablation for the treatment of liver cancer: A systematic review and meta-analysis," *Radiol. Oncol.*, vol. 55, no. 3, pp. 247–258, 2021.
- [530] P. Liang and Y. Wang, "Microwave ablation of hepatocellular carcinoma," *Oncology*, vol. 72, no. Suppl. 1, pp. 124–131, 2007.
- [531] X. Wu, B. Liu, and B. Xu, "Theoretical evaluation of high frequency microwave ablation applied in cancer therapy," *Appl. Thermal Eng.*, vol. 107, pp. 501–507, 2016.
- [532] J. Hardenburger, P. Prakash, T. R. Angeli, and L. K. Cheng, "Microwave ablation: A potential minimally invasive solution for gastric motility disorders," in *Proc. ASME Front. Biomed. Devices*, 2019, Art. no. V001T06A010.
- [533] C. P. Hancock, S. Chaudhry, P. Wall, and A. M. Goodman, "Proof of concept percutaneous treatment system to enable fast and finely controlled ablation of biological tissue," *Med. Biol. Eng. Comput.*, vol. 45, no. 6, pp. 531–540, 2007.
- [534] M. Ahmed et al., "Radiofrequency ablation: Effect of surrounding tissue composition on coagulation necrosis in a canine tumor model," *Radiology*, vol. 230, no. 3, pp. 761–767, 2004.
- [535] S. C. P. Miet and C. P. H. Smiee, "14.5 GHz circular waveguide applicator for the treatment of skin cancer," in *Proc. IEEE Asia-Pacific Microw. Conf.*, 2018, pp. 1399–1401.

- [536] C. P. Hancock and P. Sibbons, "14.5 GHz energy for dermatological applications-initial in-vivo data with histology," in *Proc. IEEE MTT-S Int. Microw. Symp.*, 2016, pp. 1–4.
- [537] P. Cresson, C. Ricard, N. Bernardin, L. Dubois, and J. Pribetich, "Design and modeling of a specific microwave applicator for the treatment of snoring," *IEEE Trans. Microw. Theory Techn.*, vol. 54, no. 1, pp. 302–308, Jan. 2006.
- [538] P. J. Strollo Jr. and R. M. Rogers, "Obstructive sleep apnea," *New England J. Med.*, vol. 334, no. 2, pp. 99–104, 1996.
- [539] M. L. Ho and S. D. Brass, "Obstructive sleep apnea," *Neurol. Int.*, vol. 3, no. 3, 2011, Art. no. e15.
- [540] N. B. Powell, R. W. Riley, R. J. Troell, K. Li, M. B. Blumen, and C. Guillemineault, "Radiofrequency volumetric tissue reduction of the palate in subjects with sleep-disordered breathing," *Chest*, vol. 113, no. 5, pp. 1163–1174, 1998.
- [541] L. A. Turner, P. B. Burn, J. E. Coad, and C. P. Hancock, "A novel miniature tissue resection device with moveable jaws that combines 400 kHz and 5.8 GHz energy for cutting and coagulation," in *Proc. IEEE Int. Microw. Biomed. Conf.*, 2018, pp. 148–150.
- [542] C. T. Dotter, A. R. Grüntzig, W. Schoop, and E. Zeitler, *Percutaneous Transluminal Angioplasty: Technique, Early and Late Results*. Berlin, Germany: Springer, 1983, pp. 1–90.
- [543] F. J. Benetti, C. Ballester, G. Sani, P. Doonstra, and J. Grandjean, "Video assisted coronary bypass surgery," *J. Cardiac Surg.*, vol. 10, no. 6, pp. 620–625, 1995.
- [544] A. Rosen et al., "Microwave balloon angioplasty," in *Proc. IEEE 19th Eur. Microw. Conf.*, 1989, pp. 913–917.
- [545] A. Rosen and P. Walinsky, "Percutaneous transluminal microwave catheter angioplasty," U.S. Patent 4,643,186 A, Feb. 17, 1987.
- [546] P. Walinsky, A. Rosen, D. Smith, D. Nardone, A. Martinez-Hernandez, and Z. Kosman, "Microwave balloon angioplasty," in *Proc. IEEE MTT-S Int. Microw. Symp.*, 1991, pp. 797–800.
- [547] Z. Gu, M. Rappaport, P. J. Wang, and B. A. VanderBrink, "Development and experimental verification of the wide-aperture catheter-based microwave cardiac ablation antenna," *IEEE Trans. Microw. Theory Techn.*, vol. 48, no. 11, pp. 1892–1900, Nov. 2000.
- [548] I. Landau, J. W. Currier, C. C. Haudenschild, A. C. Minihan, D. Heymann, and D. P. Faxon, "Microwave balloon angioplasty effectively seals arterial dissections in an atherosclerotic rabbit model," *J. Amer. College Cardiol.*, vol. 23, no. 7, pp. 1700–1707, 1994.
- [549] C. P. Gyawali and R. Fass, "Management of gastroesophageal reflux disease," *Gastroenterology*, vol. 154, no. 2, pp. 302–318, 2018.
- [550] R. Badillo and D. Francis, "Diagnosis and treatment of gastroesophageal reflux disease," *World J. Gastrointestinal Pharmacol. Therapeutics*, vol. 5, no. 3, pp. 105–112, 2014.
- [551] T. A. Zikos and J. O. Clarke, "Non-acid reflux: When it matters and approach to management," *Curr. Gastroenterol. Rep.*, vol. 22, no. 9, pp. 1–10, 2020.
- [552] T. Hershovici, H. Mashimo, and R. Fass, "The lower esophageal sphincter," *Neurogastroenterol. Motility*, vol. 23, no. 9, pp. 819–830, 2011.
- [553] H. J. Stein, A. P. Barlow, T. R. DeMeester, and R. A. Hinder, "Complications of gastroesophageal reflux disease. role of the lower esophageal sphincter, esophageal acid and acid/alkaline exposure, and duodenogastric reflux," *Ann. Surg.*, vol. 216, no. 1, pp. 35–43, 1992.
- [554] G. Triadafilopoulos, "Stretta: A valuable endoscopic treatment modality for gastroesophageal reflux disease," *World J. Gastroenterol.*, vol. 20, no. 24, pp. 7730–7738, 2014.
- [555] K. A. Perry, A. Banerjee, and W. S. Melvin, "Radiofrequency energy delivery to the lower esophageal sphincter reduces esophageal acid exposure and improves GERD symptoms: A systematic review and meta-analysis," *Surg. Laparoscopy Endoscopy Percutaneous Techn.*, vol. 22, no. 4, pp. 283–288, 2012.
- [556] C. Hancock, N. Dharmasiri, C. I. Duff, and M. White, "New microwave antenna structures for treating gastro-oesophageal reflux disease (GERD)," *IEEE Trans. Microw. Theory Techn.*, vol. 61, no. 5, pp. 2242–2252, May 2013.
- [557] C. P. Hancock, N. Dharmasiri, M. White, and A. M. Goodman, "The design and development of an integrated multi-functional microwave antenna structure for biological applications," *IEEE Trans. Microw. Theory Techn.*, vol. 61, pp. 2230–2241, May 2013.
- [558] F. Sterzer, "Apparatus and method for hyperthermia treatment," U.S. Patent 4,190,053 A, Feb. 26, 1980.
- [559] P. R. Stauffer, D. B. Rodrigues, D. Haemmerich, and C. Chou, "Thermal therapy applications of electromagnetic energy," *Biological and Medical Aspects of Electromagnetic Fields*. Boca Raton, FL, USA: CRC Press, 2018, pp. 305–343.
- [560] M. Hurwitz and P. Stauffer, "Hyperthermia, radiation and chemotherapy: The role of heat in multidisciplinary cancer care," *Seminars Oncol.*, vol. 41, no. 6, pp. 714–729, Dec. 2014.
- [561] I. O. Olweny, S. L. Jow, and W. W. Jow, "Prolieve transurethral thermodilatation for treatment of symptomatic benign prostatic hyperplasia: 5-year results from a prospective multicenter trial," *J. Endourol.*, vol. 36, no. 1, pp. 117–123, 2022.
- [562] A. Rosen and F. Sterzer, "Applications of microwave heating in medicine," in *Proc. IEEE MTT-S Int. Microw. Symp.*, 1994, pp. 1615–1618.
- [563] G. Zhou, J. He, G. Huang, L. Ren, W. Zhuge, and W. Wang, "Efficacy and safety of transurethral columnar balloon dilation of the prostate for the treatment of benign prostatic hyperplasia: A multicenter trial," *Comput. Math. Methods Med.*, vol. 2022, 2022, Art. no. 7881247.
- [564] A. Thorpe and D. Neal, "Benign prostatic hyperplasia," *Lancet*, vol. 361, no. 9366, pp. 1359–1367, 2003.
- [565] C. G. Roehrborn, "Benign prostatic hyperplasia: An overview," *Rev. Urol.*, vol. 7, no. Suppl 9, pp. S3–S14, 2005.
- [566] B. Chughtai et al., "Benign prostatic hyperplasia," *Nature Rev. Dis. Primers*, vol. 2, no. 1, pp. 1–15, 2016.
- [567] I. Pearce, "Prostatic hyperthermia," in *Imaging and Technology in Urology*. New York, NY, USA: Springer, 2012, pp. 319–322.
- [568] S. Gravas, "Microwave therapy," in *Smith's Textbook of Endourology*. Hoboken, NJ, USA: Wiley, 2012, ch. 124, pp. 1490–1502.
- [569] R. J. Ziętek and Z. M. Ziętek, "Transurethral microwave thermotherapy (TUMT) in the treatment of benign prostatic hyperplasia: A preliminary report," *Med. Sci. Monitor; Int. Med. J. Exp. Clin. Res.*, vol. 27, 2021, Art. no. e931597.
- [570] I. Wren, "Evaluation of three temperature measurement methods used during microwave thermotherapy of prostatic enlargement," *Int. J. Hyperthermia*, vol. 20, no. 3, pp. 300–316, 2004.
- [571] T. Eliasson and J. Damber, "Temperature controlled high energy transurethral microwave thermotherapy for benign prostatic hyperplasia using a heat shock strategy," *J. Urol.*, vol. 160, no. 3, pp. 777–782, 1998.
- [572] S. Jandang, P. Phasukkit, and S. Tungjitkusolmun, "Validation of urinary tract expansion using balloon-type microwave thermotherapy," in *Proc. IEEE 10th Biomed. Eng. Int. Conf.*, 2017, pp. 1–4.
- [573] R. Bartoletti et al., "Transperineal microwave thermoablation in patients with obstructive benign prostatic hyperplasia: A phase I clinical study with a new mini-choked microwave applicator," *J. Endourol.*, vol. 22, no. 7, pp. 1509–1518, 2008.
- [574] B. W. Henderson and T. J. Dougherty, "How does photodynamic therapy work?," *Photochemistry Photobiol.*, vol. 55, no. 1, pp. 145–157, 1992.
- [575] G. Happawana, A. Premasiri, and A. Rosen, "Tumor modeling and microwave heating for increasing oxygen in tumors during photodynamic therapy," *J. Bioeng. Technol.*, vol. 1, Jul. 2021, Art. no. 1.
- [576] R. F. Saidi and N. E. Marcon, "Nonthermal ablation of malignant esophageal strictures: Photodynamic therapy, endoscopic intratumoral injections, and novel modalities," *Gastrointestinal Endoscopy Clin. North Amer.*, vol. 8, no. 2, pp. 465–491, 1998.
- [577] B. J. Qumseya, W. David, and H. C. Wolfsen, "Photodynamic therapy for Barrett's esophagus and esophageal carcinoma," *Clin. Endoscopy*, vol. 46, no. 1, pp. 30–37, 2013.
- [578] B. F. Overholt, M. Panjehpour, and J. M. Haydek, "Photodynamic therapy for barrett's esophagus: Follow-up in 100 patients," *Gastrointestinal Endoscopy*, vol. 49, no. 1, pp. 1–7, 1999.
- [579] B. F. Overholt et al., "Five-year efficacy and safety of photodynamic therapy with photofrin in Barrett's high-grade dysplasia," *Gastrointestinal Endoscopy*, vol. 66, no. 3, pp. 460–468, 2007.
- [580] H. Rosen, A. Rosen, and P. Walinsky, "Microwave balloon systems in medicine," *IEEE Pulse*, vol. 1, no. 2, pp. 8–15, Sep./Oct. 2010.
- [581] A. Premasiri, G. Happawana, G. Evans, and A. Rosen, "Design of a high yielding photonic light delivery system to be used in photodynamic therapy for esophageal cancer, with microwave antenna imprinted balloon catheter for oxygen enhancement," in *Proc. ASME Front. Biomed. Devices*, 2006, pp. 29–30.
- [582] B. Jacob, "Treatment of hyperhidrosis with microwave technology," *Seminars Cutan. Med. Surg.*, vol. 32, no. 1, pp. 2–8, Mar. 2013.

- [583] C. R. Stratton, J. W. Kowalski, D. A. Glaser, and P. E. Stang, "U.S. prevalence of hyperhidrosis and impact on individuals with axillary hyperhidrosis: Results from a national survey," *J. Amer. Acad. Dermatol.*, vol. 51, no. 2, pp. 241–248, 2004.
- [584] E. Sammons and A. Khachemoune, "Axillary hyperhidrosis: A focused review," *J. Dermatological Treat.*, vol. 28, no. 7, pp. 582–590, 2017.
- [585] E. Johnson, K. F. O'Shaughnessy, and S. Kim, "Microwave thermolysis of sweat glands," *Lasers Surg. Med.*, vol. 44, no. 1, pp. 20–25, 2012.
- [586] A. A. Glaser et al., "A randomized, blinded clinical evaluation of a novel microwave device for treating axillary hyperhidrosis: The dermatologic reduction in underarm perspiration study," *Dermatologic Surg.*, vol. 38, no. 2, pp. 185–191, 2012.
- [587] C.-H. Hong, M. Lupin, and K. F. O'Shaughnessy, "Clinical evaluation of a microwave device for treating axillary hyperhidrosis," *Dermatologic Surg.*, vol. 38, no. 5, pp. 728–735, 2012.
- [588] C. K. Chang et al., "Brachial plexus injury after microwave-based treatment for axillary hyperhidrosis and osmidrosis," *J. Cosmetic Laser Ther.*, vol. 19, no. 7, pp. 439–441, 2017.
- [589] V. Vorst, A. Rosen, and Y. Kotsuka, *RF/Microwave Interaction With Biological Tissues*. Hoboken, NJ, USA: Wiley, 2006.
- [590] M. Tofghi and C. T. Huynh, "A microwave system for blood perfusion measurements of tissue; a preliminary study," in *Proc. IEEE Topical Conf. Biomed. Wireless Technol. Netw. Sens. Syst.*, 2013, pp. 49–51.
- [591] A. Rosen and W. P. Santamore, "Method of measuring blood perfusion," U.S. Patent 4,228,805 A, Oct. 21, 1980.
- [592] M. Tofghi, J. R. Pardeshi, and B. A. Maicke, "Microwave system and methods for combined heating and radiometric sensing for blood perfusion measurement of tissue," in *Proc. IEEE MTT-S Int. Microw. Symp.*, 2016, pp. 1–4.
- [593] A. Rosen, D. Rosen, G. A. Tuma, and L. P. Bucky, "RF/microwave-aided tumescent liposuction," *IEEE Trans. Microw. Theory Techn.*, vol. 48, no. 11, pp. 1879–1884, Nov. 2000.
- [594] J. Hwang et al., "A study on non-invasive hyperthermic lipolysis using microwave," in *Proc. IEEE Int. Symp. Antennas Propag.*, 2011, pp. 3313–3316.
- [595] J. C. Lin and J. Salinger, "Microwave measurement of respiration," in *Proc. IEEE-MTT-S Int. Microw. Symp.*, 1975, pp. 285–287.
- [596] J. C. Chiao, *IEEE Journal of Electromagnetics, RF and Microwaves in Medicine and Biology | About Journal*. [Online]. Available: <https://iee-jerm.org/home/>



J.-C. CHIAO (Fellow, IEEE) received the B.S. degree from the Department of Electrical Engineering, National Taiwan University, New Taipei, Taiwan, and the M.S. and Ph.D. degrees in electrical engineering from the California Institute of Technology, Pasadena, CA, USA. He was a Research Scientist with the Optical Networking Systems and Testbeds Group, Bell Communications Research; an Assistant Professor of electrical engineering with the University of Hawaii, Honolulu, HI, USA; and a Product Line Manager and Senior Technol-

ogy Advisor with Chorum Technologies. From 2002 to 2018, he was Janet and Mike Greene endowed Professor and Jenkins Garrett Professor of electrical engineering with the University of Texas-Arlington, Arlington, TX, USA. He is currently Mary and Richard Templeton Centennial Chair Professor of electrical and computer engineering with Southern Methodist University, Dallas, TX. He has authored or coauthored and edited numerous peer-reviewed technical journal and conference papers, book chapters, proceedings, and books, and holds 20 U.S. patents. Dr. Chiao has been the Chair and Technical Program Chair of several international conferences, including the 2018 IEEE International Microwave Biomedical Conference (IMBioC) Chair and 2022 IEEE Sensors Conference Chair. He was the Chair of the IEEE MTT-S Technical Committee Biological Effect and Medical Applications of RF and Microwave, and an Associate Editor for IEEE TRANSACTIONS ON MICROWAVE THEORY AND TECHNIQUES. He was the founding Editor-in-Chief of IEEE JOURNAL OF ELECTROMAGNETICS, RF, AND MICROWAVES IN MEDICINE AND BIOLOGY. He is on the Editorial Board of IEEE ACCESS and Topic Editor of IEEE JOURNAL OF MICROWAVES. He was the recipient of Lockheed

Martin Aeronautics Company Excellence in Engineering Teaching Award, Tech Titans Technology Innovator Award, Research in Medicine Award in the Heroes of Healthcare, IEEE Region 5 Outstanding Engineering Educator Award, IEEE Region 5 Excellent Performance Award, 2012–2014 IEEE MTT Distinguished Microwave Lecturer, 2017–2019 IEEE Sensors Council Distinguished Lecturer, 2022 Pan Wen-Yuan Foundation Excellence in Research Award, and 2011 Edith and Peter O'Donnell Award in Engineering by The Academy of Medicine, Engineering and Science of Texas. He is also a Fellow of IET, SPIE, and AIMBE.



CHANGZHI LI (Senior Member, IEEE) received the B.S. degree in electrical engineering from Zhejiang University, Hangzhou, China, in 2004, and the Ph.D. degree in electrical engineering from the University of Florida, Gainesville, FL, USA, in 2009. He is currently a Professor with Texas Tech University, Lubbock, TX, USA. His research interests include microwave/millimeter-wave sensing for health-care, security, energy efficiency, structural monitoring, and human-machine interface. Dr. Li is an IEEE Microwave Theory and Techniques Society (MTT-S) Distinguished Microwave Lecturer with the Tatsuo Itoh Class of 2022–2024. He was the recipient of the IEEE MTT-S Outstanding Young Engineer Award, IEEE Sensors Council Early Career Technical Achievement Award, ASEE Frederick Emmons Terman Award, IEEE-HKN Outstanding Young Professional Award, NSF Faculty Early CAREER Award, and IEEE MTT-S Graduate Fellowship Award. He is an Associate Editor for IEEE TRANSACTIONS ON MICROWAVE THEORY AND TECHNIQUES and IEEE JOURNAL OF ELECTROMAGNETICS, RF AND MICROWAVES IN MEDICINE AND BIOLOGY.



JENSHAN LIN (Fellow, IEEE) received the Ph.D. degree in electrical engineering from the University of California at Los Angeles (UCLA), Los Angeles, CA, USA, in 1994. From 1994 to 2001, he was with Bell Labs, Murray Hill, NJ, USA. From 2001 to 2003, he was with Agere Systems, Holmdel, NJ. In 2003, he joined the University of Florida (UF), Gainesville, FL, USA, where he retired in January 2022 and became a Professor Emeritus. After his retirement from UF, he was the Program Director of the Division of Electrical, Communications and Cyber Systems, U.S. National Science Foundation (NSF), where he was the Rotator Program Director from 2016 to 2020. At NSF, he managed the Communications, Circuits, and Sensing Systems Program and several other cross-cutting programs involving wireless, spectrum, semiconductor, sensing, security, and machine learning. He has authored or coauthored more than 300 technical publications in refereed journals and conference proceedings. He holds 24 U.S. patents. Dr. Lin was the recipient of the 1994 UCLA Outstanding Ph.D. Award, 1997 Eta Kappa Nu Outstanding Young Electrical Engineer Honorable Mention Award, 2007 IEEE Microwave Theory and Techniques Society N. Walter Cox Award, 2015 IEEE Wireless Power Transfer Conference Best Paper Award, 2016 Distinguished Alumnus Award from National Chiao Tung University, Hsinchu, Taiwan, and 2016 IEEE RFIC Symposium Tina Quach Outstanding Service Award. He was the General Chair of the 2008 RFIC Symposium, Technical Program Chair of the 2009 Radio and Wireless Symposium, General Co-Chair of the 2012 Asia-Pacific Microwave Conference, TPC Co-Chair of 2021 International Microwave Symposium, and Chair of the 2021 IEEE Wireless Power Transfer Conference. From 2014 to 2016, he was the Editor-in-Chief of IEEE TRANSACTIONS ON MICROWAVE THEORY AND TECHNIQUES. He was the Chair of MTT-S Tatsuo Itoh Prize Award Committee during 2019–2021, and Chair of MTT-S Fellow Evaluating Committee during 2021–2022.



ROBERT H. CAVERLY (Life Fellow, IEEE) was born in Cincinnati, OH, USA, in 1954. He received the B.S.E.E. and M.S.E.E. degrees from North Carolina State University, Raleigh, NC, USA, in 1978 and 1976, respectively, and the Ph.D. degree in electrical engineering from Johns Hopkins University, Baltimore, MD, USA, in 1983. Since 1997, he has been a Faculty Member with the Department of Electrical and Computer Engineering, Villanova University, Villanova, PA, USA, where he is currently a Full Professor. He was with the University

of Massachusetts Dartmouth (formerly Southeastern Massachusetts University), Dartmouth, MA, USA, for more than 14 years. He has authored or coauthored more than 100 journal and conference papers and two books *Microwave and RF Control Device Modeling* (Norwood, MA, USA: Artech House, 2016) and *CMOS RFIC Design Principles* (Norwood, MA, USA: Artech House, 2007). His research interests include the characterization and modeling of semiconductor devices, such as PIN diodes and FETs in the microwave and RF control environment. He is currently the Editor-in-Chief of *IEEE Microwave Magazine*, Track Editor of IEEE JOURNAL OF MICROWAVES, and a member of the Administrative Committee of the IEEE Microwave Theory and Technology Society (MTT-S). From 2014 to 2016, he was a Distinguished Microwave Lecturer (DML) representing the MTT-S. He is also an Emeritus DML.



JAMES C. M. HWANG (Life Fellow, IEEE) received the B.S. degree in physics from National Taiwan University, Taipei, Taiwan, and the M.S. and Ph.D. degrees in materials science and engineering from Cornell University, Ithaca, NY, USA. He is currently a Professor with the Department of Materials Science and Engineering, Cornell University. Prior to that, he spent most of his academic career with Lehigh University, Bethlehem, PA, USA, after years of industrial experience with IBM, Yorktown Hts., NY; Bell Labs, Murray Hill,

NJ, USA; GE, Syracuse, NY; and GAIN, Somerville, NJ. He cofounded GAIN and QED, Bethlehem, PA, USA, which later became a Public Company (IQE). He was the Program Officer for GHz-THz Electronics with the Air Force Office of Scientific Research, Arlington, VA, USA. He is an IEEE Distinguished Microwave Lecturer and a Track Editor of IEEE TRANSACTIONS ON MICROWAVE THEORY AND TECHNIQUES. He has worked on microwave materials, devices, and circuits for four decades.



HAREL ROSEN received the bachelor's degree (*cum laude*) in biochemistry from the Cook College of Rutgers University, Piscataway, NJ, USA, and his medical school training from Jefferson Medical College, Philadelphia, PA, USA. He trained in pediatrics with the Medical Center of Delaware, Newark, DE, USA, and completed his training as a Neonatologist with the University of Medicine and Dentistry of New Jersey, Newark, NJ, and Robert Wood Johnson Medical School, New Brunswick, NJ. Since 1995, he has been practicing neonatology, and is currently a Neonatologist with Onsite Neonatal Partners, Inc. Voorhees, NJ. He has been a Research Associate Professor with the Drexel University School of Biomedical Engineering Science and Health Systems, and a Volunteer Clinical Associate Professor with the Rowan University School of Osteopathic Medicine. He has coauthored numerous papers in the field of neonatal applications of biomedical technologies, contributed to several textbooks on medical device technology, and also holds several medical and engineering patents.



ARYE ROSEN (Life Fellow, IEEE) received the B.S. degree in electrical engineering from Howard University, Washington, DC, USA, the Masters of Science degree in engineering from Johns Hopkins University, Baltimore, MD, USA, the M.Sc. degree in physiology from Thomas Jefferson University, Philadelphia, PA, USA, and the Ph.D. degree in electrical engineering from Drexel University, Philadelphia, PA, USA. During the B.S. degree, he was with the Embassy of Israel, Office of the Scientific Counselor. From 1967 to 2003, he

was with RCA/David Sarnoff Research Center, rising to the highest technical rank of Distinguished Member of Technical Staff, where he was involved in research and development of microwave and millimeter wave/THz devices and circuits, microwave optical interaction, and high power semiconductor lasers. He has also been engaged in medical research and consulting in the utilization of energies for applications in therapeutic medicine for the past 50 years. He has held an appointment with the School of Biomedical Engineering, Science and Health Systems, Drexel University, Philadelphia, PA, as an Academy Professor of biomedical and electrical engineering, and Associate Vice Provost for Strategic Initiatives until June 2014. In October 2014, he was appointed the Associate Vice President of Biomedical Research Partnerships, Rowan University, Glassboro, NJ, USA. He has authored more than 250 technical papers, coedited two books: *High Power Optically Activated Solid-State Switches* (Norwood, MA, USA: Artech House, 1993) and *New Frontiers in Medical Device Technology* (New York, NY, USA: Wiley, 1995), and coauthored a textbook titled *RF/Microwave Interaction with Biological Tissue* (New York, NY, USA: Wiley, 2006/2007). He holds more than 60 U.S. patents in the fields of engineering and medicine. A patent issued in 2019 is assigned to Medtronic Ardian Luxembourg S.A.R.L, titled: Microwave Catheter Apparatuses, Systems, and Methods for Renal Neuromodulation. He is/was a member of the National Academies and National Academy of Engineering (NAE). Dr. Rosen was elected a NAE member in 2002 for contributions to microwave and laser technologies and the medical applications of these technologies. He was involved in the early research of the utilization of ultrasound imaging for the detection and diagnosis of heart dysfunction (echocardiography), use of light emitting diodes/lasers for functional near infrared spectroscopy, and photodynamic therapy) in cancer treatment. He was elected as an IEEE Fellow in 1992 for innovation in semiconductor devices and circuits for use in microwave systems and for microwave applications to medicine. He is a Fellow of the American Institute for Medical and Biological Engineering, Fellow of the National Academy of Inventors, and a retired member of the Association of Professional Engineers of the Province of British Columbia, Canada. He was an IEEE Distinguished Microwave Lecturer from 1997 to 2000, during which time he has presented his and others' work in the United States, Japan, Europe, and the Middle East. He has consulted to several medical technology companies worldwide, and to investment trust corporations interested in funding innovative biomedical research. He was the recipient of numerous awards, including the IEEE MTT-S Microwave Career Award in May 2010, IEEE Third Millennium Medal in January 2000, and IEEE Microwave Application Award in June 2000. He was honored with a Special IMS 2003 Session Honoring Kiyoo Tomiyasu, Martin Schneider, and Arye Rosen (*IEEE Microwave Magazine*, March 2004). He was also the recipient of the 1989 IEEE Region One Award, and 1997 Drexel University College of Engineering, Electrical and Computer Engineering Department Distinguished Alumni Award.